Simulation Analysis of the Ground-Water Flow System in the Portland Basin, Oregon and Washington

United States Geological Survey Water-Supply Paper 2470–B

Prepared in cooperation with Oregon Water Resources Department, City of Portland Bureau of Water Works, and Intergovernmental Resource Center

AVAILABILITY OF BOOKS AND MAPS OF THE U.S. GEOLOGICAL SURVEY

Instructions on ordering publications of the U.S. Geological Survey, along with prices of the last offerings, are given in the current-year issues of the monthly catalog "New Publications of the U.S. Geological Survey." Prices of available U.S. Geological Survey publications released prior to the current year are listed in the most recent annual "Price and Availability List." Publications that may be listed in various U.S. Geological Survey catalogs (**see back inside cover**) but not listed in the most recent annual "Price and Availability List" may be no longer available.

Order U.S. Geological Survey publications **by mail** or **over the counter** from the offices given below.

BY MAIL

Books

Professional Papers, Bulletins, Water-Supply Papers, Techniques of Water-Resources Investigations, Circulars, publications of general interest (such as leaflets, pamphlets, booklets), single copies of Preliminary Determination of Epicenters, and some miscellaneous reports, including some of the foregoing series that have gone out of print at the Superintendent of Documents, are obtainable by mail from

U.S. Geological Survey, Information Services
Box 25286, Federal Center, Denver, CO 80225

Subscriptions to Preliminary Determination of Epicenters can be obtained ONLY from the

Superintendent of Documents
Government Printing Office
Washington, DC 20402

(Check or money order must be payable to Superintendent of Documents.)

Maps

For maps, address mail orders to

U.S. Geological Survey, Information Services
Box 25286, Federal Center, Denver, CO 80225

OVER THE COUNTER

Books and Maps

Books and maps of the U.S. Geological Survey are available over the counter at the following U.S. Geological Survey Earth Science Information Centers (ESIC's), all of which are authorized agents of the Superintendent of Documents:

- **ANCHORAGE, Alaska**—Rm. 101, 4230 University Dr.
- **LAKEWOOD, Colorado**—Federal Center, Bldg. 810
- **MENLO PARK, California**—Bldg. 3, Rm. 3128, 345 Middlefield Rd.
- **RESTON, Virginia**—USGS National Center, Rm. 1C402, 12201 Sunrise Valley Dr.
- **SALT LAKE CITY, Utah**—Federal Bldg., Rm. 8105, 125 South State St.
- **SPOKANE, Washington**—U.S. Post Office Bldg., Rm. 135, West 904 Riverside Ave.
- **WASHINGTON, D.C.**—Main Interior Bldg., Rm. 2650, 18th and C Sts., NW.

Maps Only

Maps may be purchased over the counter at the following U.S. Geological Survey office:

- **ROLLA, Missouri**—1400 Independence Rd.

Simulation Analysis of the Ground-Water Flow System in the Portland Basin, Oregon and Washington

By DAVID S. MORGAN and WILLIAM D. MCFARLAND

Prepared in cooperation with
Oregon Water Resources Department,
City of Portland Bureau of Water Works, and
Intergovernmental Resource Center

U.S. GEOLOGICAL SURVEY WATER-SUPPLY PAPER 2470–B

U.S. DEPARTMENT OF THE INTERIOR
BRUCE BABBITT, Secretary

U.S. GEOLOGICAL SURVEY
Gordon P. Eaton, Director

For sale by the
U.S. Geological Survey
Branch of Information Services
Box 25286
Federal Center
Denver, CO 80225

Library of Congress Cataloging in Publication Data

Morgan, David S.
Simulation analysis of the ground-water flow system in the Portland Basin, Oregon and Washington / by David S. Morgan and William D. McFarland.
p. 83 cm. — (U.S. Geological Survey water-supply paper ; 2470–B
"Prepared in cooperation with the Oregon Water Resources Department, City of Portland Bureau of Water Works, and Intergovernmental Resource Center [of Clark County, Wash]."
Includes bibliographical references.
Supt. of Docs. no. : I 19.13:2470–B
1. Groundwater flow — Oregon —Portland Region — Simulation Methods.
I. McFarland, William D. II. Oregon. Water Resources Dept.III. Portland (Or.). Water Bureau IV. Intergovernmental Resource Center of Clark County (Wash.) V. Title.
VI. Series.
GB1197.7.M67 1996 96–52463
551.49´09795´49—dc21CIP

ISBN 0-607-87040-0

CONTENTS

PLATES

[Plates are in pocket]

FIGURES

TABLES

CONVERSION FACTORS AND VERTICAL DATUM

Multiply	By	To obtain
	Length	
inch (in)	25.4	millimeter
foot (ft)	0.3048	meter
mile (mi)	1.609	kilometer
	Area	
acre	4,047	square meter
acre	0.407	hectare
square mile (mi^2)	259.0	hectare
square mile (mi^2)	2.590	square kilometer
	Volume	
cubic foot (ft^3)	0.02832	cubic meter
	Flow	
cubic feet per second (ft^3/s)	0.02832	cubic meter per second
gallons per minute (gal/min)	0.06308	liter per second
gallons per minute (gal/min)	0.002228	cubic foot per second

Sea level: In this report "sea level" refers to the National Geodetic Vertical Datum of 1929 (NGVD of 1929)—a geodetic datum derived from a general adjustment of the first-order level nets of both the United States and Canada, formerly called Sea Level Datum of 1929.

Simulation Analysis of the Ground-Water Flow System in the Portland Basin, Oregon and Washington

By David S. Morgan *and* William D. McFarland

Abstract

A numerical model of the ground-water flow system in the Portland Basin, Oregon and Washington, was used to (1) test and refine the conceptual understanding of the flow system, (2) estimate the effects of past and future human-caused changes to ground-water recharge and discharge on ground-water levels and stream-flow, and (3) determine priorities for ground-water monitoring and data collection that would facilitate improvements in the utility and accuracy of the model. The model covered an area of 981 square miles that includes most of Multnomah County, Oregon, and Clark County, Washington, as well as parts of Clackamas, Washington, and Columbia Counties in Oregon, and Skamania County in Washington.

Model results were most sensitive to the horizontal hydraulic conductivity of the Troutdale gravel aquifer and the Troutdale sandstone aquifer and to the vertical hydraulic conductivity of the confining units and undifferentiated fine-grained sediments. The model was insensitive to the hydraulic characteristics of the unconsolidated sedimentary aquifer because of the strong control that streams and rivers have on water levels in the unit.

The model was calibrated using time-averaged data for 1987–88. Horizontal hydraulic conductivity, vertical hydraulic conductivity, and streambed and riverbed conductances were adjusted until a reasonable fit was obtained between simulated and observed water levels and seepage to streams. Final horizontal hydraulic conductivities had median values ranging from 11 to 110 ft/d (feet per day) in the four aquifer units and from 1 to 8 ft/d in finer grained units. Horizontal to vertical anisotropy ratios ranged from 100:1 in the aquifer units to 1,000:1 in the finer grained units. Approximately 410 observed water levels were available for comparison with simulated water levels in the four aquifer units. The root-mean-squared error ranged from 54 feet in the unconsolidated sedimentary aquifer to 74 feet in the Troutdale sandstone aquifer. Simulated seepage to streams agreed closely with observed seepage at 67 measurement sites.

Recharge to the basin in 1987–88 consisted primarily of 1,440 ft^3/s (cubic feet per second) from direct infiltration of precipitation, but was augmented in unsewered urban areas by 62 ft^3/s from runoff to drywells and 27 ft^3/s from on-site waste-disposal systems. Forty-nine percent of the recharge in the basin enters the system through the Troutdale gravel aquifer and 22 percent enters through the unconsolidated sedimentary aquifer. Simulated discharge in 1987–88 was chiefly by seepage to small rivers and streams (971 ft^3/s), followed by seepage to the Columbia and Willamette Rivers and other large water bodies (457 ft^3/s) and by pumpage (166 ft^3/s). The unconsolidated sedimentary aquifer and Troutdale gravel aquifer supplied 85 percent of 1987–88 pumpage. Most of the ground-water flux through the aquifer system occurred within these two units with 75 percent of total recharge to the system entering through them and 80 percent of total discharge leaving through them in 1987–88.

Recharge under predevelopment conditions was 180 ft^3/s (12 percent) more than in 1987–88 due to the absence of impervious surfaces associated with urbanization. Simulation of the

effects of the increased recharge and no well discharge indicates that water levels may have declined as much as 50 feet in the Troutdale gravel aquifer in southern Clark County in response to municipal pumping. Declines similar in magnitude were simulated in the gravel aquifer in the Troutdale gravel aquifer and Troutdale sandstone aquifer in the vicinity of Sandy, Oregon, in response to pumping for irrigation. Since predevelopment conditions, the combination of reduced recharge and increased pumpage may have reduced discharge to large rivers by 25 percent and reduced discharge to small rivers and streams by 16 percent.

One hypothetical condition for future ground-water development was simulated to test the effects of additional pumping stress on the ground-water system. Pumpage estimates in this condition were based on projected municipal supply demands in Clark County through the year 2010 and on limited use of the city of Portland Columbia South Shore well field. The resulting pumpage was 55 percent (92 ft^3/s) greater than 1987–88 pumpage. Equilibrium water-level declines were as much as 20–40 ft within the Troutdale gravel aquifer in Clark County and in the Troutdale sandstone aquifer underlying the Columbia South Shore well field. At equilibrium, much of the additional pumpage was supplied by capture of discharge to the Columbia River (14 ft^3/s) and by additional recharge induced from the Columbia River (26 ft^3/s).

Further data collection through ground-water-level monitoring and periodic updating of well discharge and recharge from on-site waste-disposal systems and drywells would facilitate future improvements in the model developed in this study.

INTRODUCTION

The Portland Basin study area is located in northwestern Oregon and southwestern Washington (fig. 1). The study area, referred to in this report as the "Portland Basin," is defined by geologic, hydrologic, and political boundaries that encompass an area of about 1,310 mi^2 (square miles). It is referred to as a basin because most of the area is underlain by a sediment-filled structural basin and the related streams and rivers all flow to the Columbia River. Population of the basin is approximately 1 million (1991), of which about 238,000 reside in Clark County, Washington. A large part of the population lives within the city of Portland (440,000) and about 46,000 people live within the neighboring city of Vancouver.

Historically, most of the industrial and municipal water needs of Portland and surrounding Oregon communities have been met by surface-water supplies from the Bull Run watershed, located approximately 25 miles southeast of downtown Portland, on the western flank of the Cascade Range (see fig. 1). In the late 1970's, ground water was identified as the source that would supply Portland's emergency and peak water needs; therefore, a 100 million gallon per day (155 ft^3/s [cubic feet per second]) capacity well field was developed on the south shore of the Columbia River, east of the city of Portland (Willis, 1977; Willis, 1978). Ground water is used extensively in rural and agricultural areas to supply domestic and agricultural water needs.

In Clark County, ground water is the primary source for municipal and industrial uses and is an important source for agricultural use. Also, a large percentage of rural Clark County residents rely on individual private wells for their domestic water needs.

Adequacy of ground-water supplies in the basin has not been a major issue in the past; however, an increasing reliance on ground water has emphasized the need for an improved quantitative understanding of the resource. Ground-water-level declines that have occurred in response to ground-water withdrawals have become a problem in some areas and are anticipated to be a continuing problem as more ground-water supplies are developed to accommodate future growth in the basin. Contamination of ground water in the basin also has reinforced the need for a quantitative description of the rate and direction of ground-water movement in the basin.

In 1987, the U.S. Geological Survey began a cooperative study with the Oregon Water Resources Department, the city of Portland Bureau of Water Works, and the Intergovernmental Resource Center located in Clark County, Washington, with the objective of describing and quantifying the ground-water resource in the basin. This report is the seventh and final report resulting from this cooperative study. Previous reports are described in the following sections of this report.

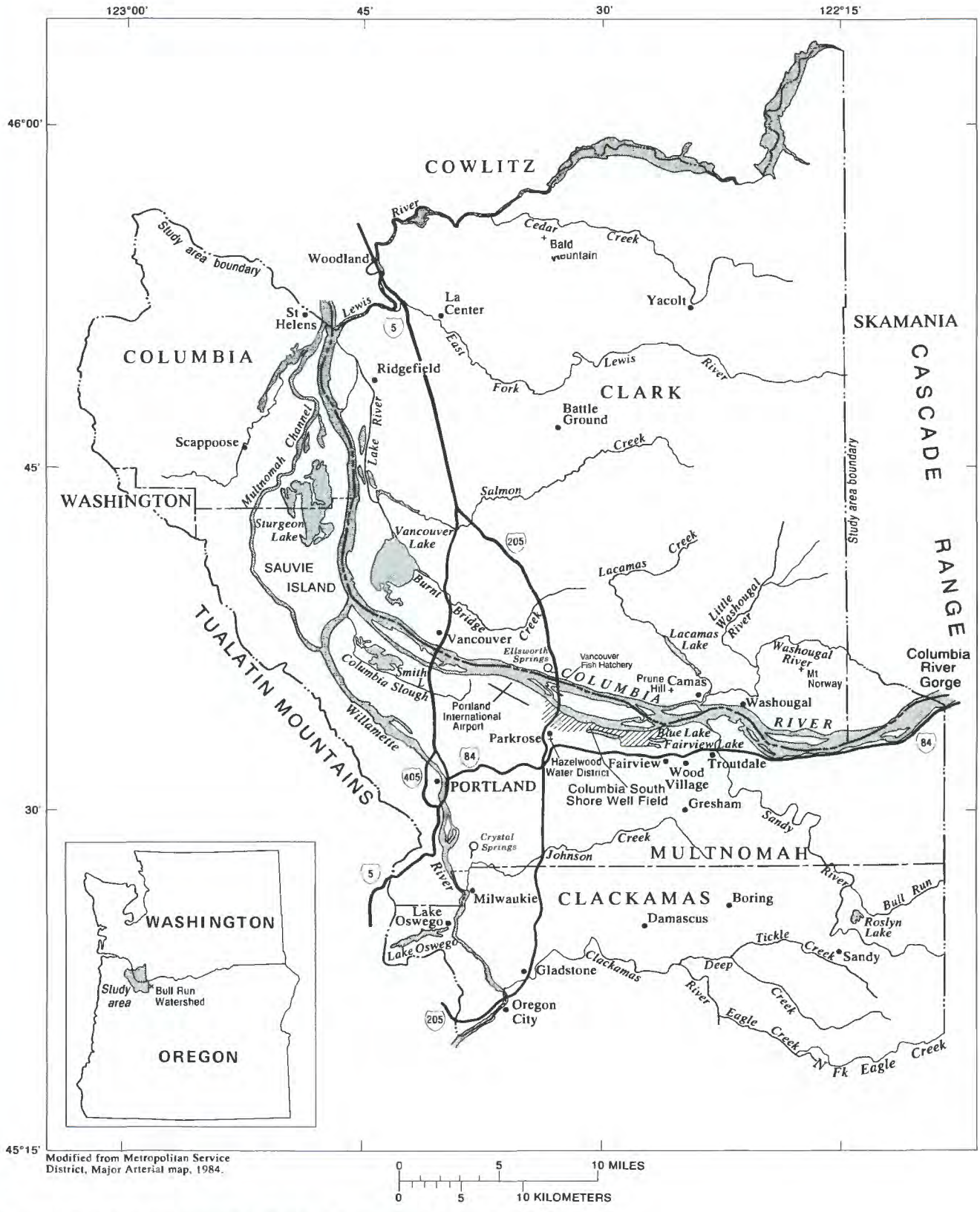

Figure 1. Location and general features of the Portland Basin study area.

Purpose and Scope

The purpose of this report is to describe the results of a numerical model analysis of the regional ground-water flow system of the Portland Basin.

A numerical model of the ground-water flow system in the Portland Basin, Oregon and Washington, was used to (1) test and refine the conceptual understanding of the flow system, (2) estimate the effects of past and future manmade changes to ground-water recharge and discharge on ground-water levels and streamflow, and (3) determine priorities for ground-water monitoring and data collection that would facilitate improvements in the utility and accuracy of the model.

The numerical model described in this report was constructed using data and information published in several other reports produced during the study; these reports are referenced frequently within this report and are summarized briefly below. Basic ground-water data used in the study are listed by McCarthy and Anderson (1990) and include (1) information on the location, ownership, construction, and yield of 1,586 field-located wells; (2) hydrographs for selected wells; and (3) information on the location, ownership, and discharge of 41 springs. A software interface for data exchange between the Geographic Information System and the ground-water flow model used in the study was documented by Orzol and McGrath (1992). The thickness and extent of hydrogeologic units defined in this study were described by Swanson and others (1993). Estimated ground-water withdrawals for municipal, industrial, and agricultural uses during 1987–88 were listed by Collins and Broad (1993). Recharge to the ground-water system from infiltration of precipitation, on-site waste-disposal systems, and urban runoff to drywells were described by Snyder and others (1994). Finally, the ground-water flow model used in the numerical model analysis described in this report is based on the conceptual model of the ground-water flow system presented by McFarland and Morgan (1996).

This report describes (1) the assumptions made to represent the conceptual model of the ground-water flow system within the framework of the mathematical model, including justification of the boundary conditions; (2) the hydraulic characteristics of the ground-water flow system; (3) the model calibration procedure and results; and (4) the results of simulations of predevelopment steady-state conditions and of a hypothetical future pumping condition.

Description of the Study Area

The study area is in the Willamette-Puget Trough, a north-south structural basin between the Coast Range on the west and the Cascade Range on the east. The study area encompasses 1,310 mi^2 and is located in the lower Columbia River Basin at the confluence of the Columbia and Willamette Rivers (fig. 1). In this report, the study area is referred to as the "Portland Basin" and is bounded approximately by the Lewis River on the north, the Clackamas River on the south, the western Cascade Range on the east, and the Tualatin Mountains on the west. The study area includes all or part of six counties in two States: Multnomah, Clackamas, Washington, and Columbia Counties in Oregon; and Clark and Skamania Counties in Washington (fig. 1). The model described in this report covers all of the study area except for the eastern and northeastern parts of Clark County, which are underlain by low-permeability volcanic rocks, and small areas in the extreme northwestern and southwestern parts of the study area (fig. 2). The total area covered by the model was 981 mi^2.

Land-surface altitude in the basin ranges from about 10 ft (feet) at the Columbia River to more than 3,000 ft in the western Cascade Range. The basin floor is elongated southeast to northwest in accordance with the structural configuration of the bedrock. In Clark County, a series of nearly flat, step-like plains and benches rise to the north and east from the Columbia River, finally giving way to the steeper western slopes of the Cascade Range. South of the Columbia River, smooth alluvial plains near the river contrast with the hilly topography formed by volcanic buttes such as Mount Scott and Powell Butte.

The climate of the basin is temperate, with moderately warm, dry summers and mild, wet winters. Precipitation ranges from 36 in/yr (inches per year) near Portland to more than 80 in/yr in the western Cascade Range.

The Columbia River occupies the lowest part of the basin and is the ultimate sink for all water entering the basin that is not lost to evapotranspiration. With a drainage area of nearly 240,000 mi^2 upstream of the study area and a mean annual discharge of about 195,000 ft^3/s (period of record, 1878–1958) (Mundorff, 1964), the river directly or indirectly controls all surface- and ground-water movement in the basin. The other major rivers in the basin are the Lewis, East Fork Lewis, and Washougal Rivers in Washington, and the Willamette, Sandy, and Clackamas Rivers in Oregon.

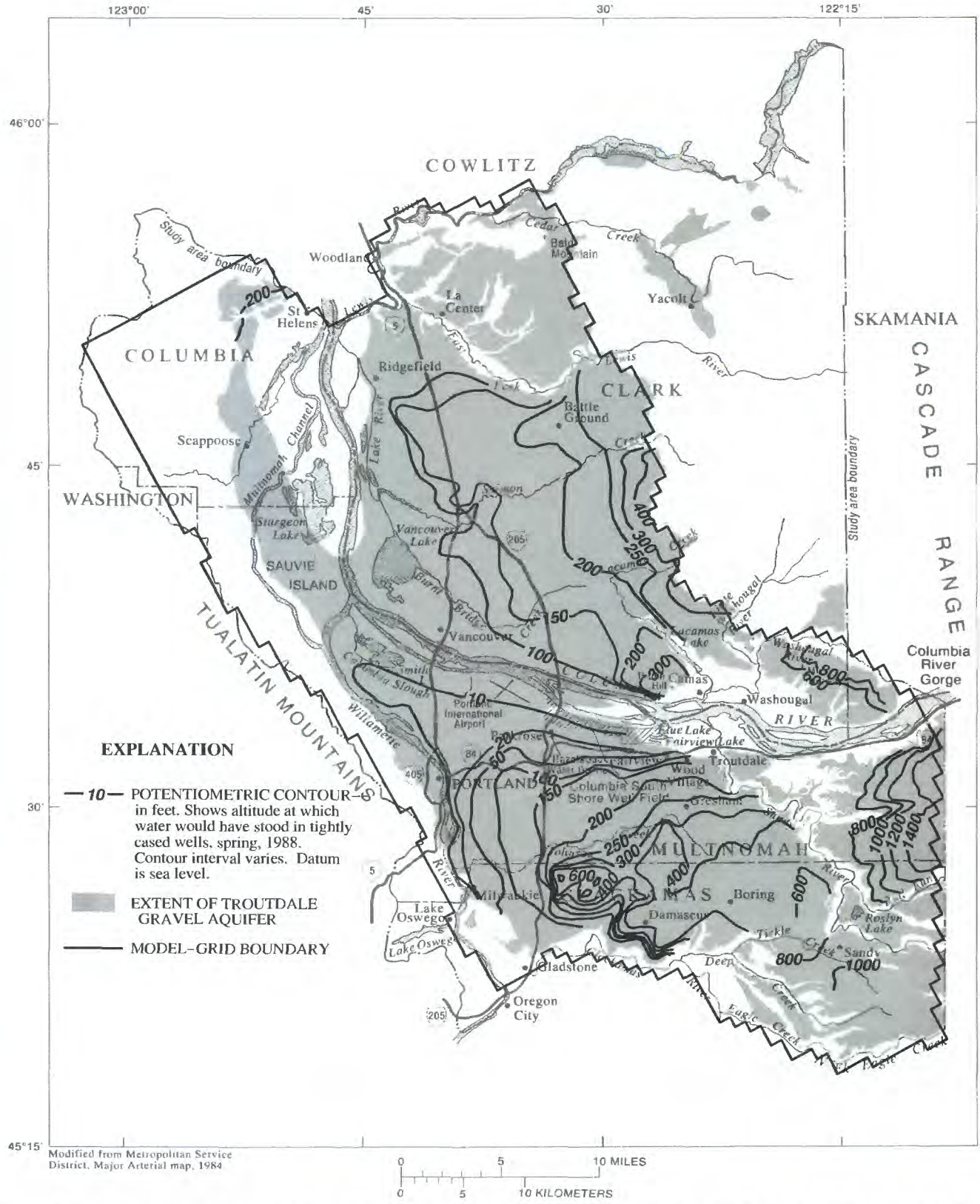

Figure 2. Potentiometric surface in the Troutdale gravel aquifer, spring 1988 (modified from McFarland and Morgan, plate 3, 1996).

Principal streams include Cedar, Salmon, Burnt Bridge, and Lacamas Creeks in Washington and Johnson and Deep Creeks in Oregon (fig. 1).

Acknowledgments

The authors extend their appreciation to the many staff members from cooperating agencies who provided valuable data and consultation throughout the study. In particular, we would like to thank Rodney Swanson (formerly of the Intergovernmental Resource Center located in Clark County, Washington); Jeffery Leighton (city of Portland Bureau of Water Works); Ken Lite (Oregon Water Resources Department); and Terry McClure and Patrick Easley (city of Vancouver).

Special acknowledgment is made to Daniel T. Snyder, U.S. Geological Survey, Portland, Oregon, for his efforts in the preparation of model input data and in making runs and compiling results during the sensitivity analysis of the model. David G. Weatherby, formerly of the U.S. Geological Survey, Eugene, Oregon, deserves special credit for compiling extensive statistical and graphical summaries of model results. Finally, Timothy McGrath, formerly of the U.S. Geological Survey, Eugene, Oregon, is gratefully acknowledged for his outstanding contributions to the project through development of many useful geographic-information software tools that facilitated construction and calibration of the model.

HYDROGEOLOGY

The overviews of the geology and hydrology of the Portland Basin in the following sections summarize more detailed descriptions in reports by (1) Swanson and others (1993), who discussed the thickness, extent and lithology of hydrogeologic units in the basin; and (2) McFarland and Morgan (1996), who describe the ground-water flow system of the basin, including its boundaries, hydraulic characteristics, and components of recharge and discharge.

Geologic Setting

The Portland Basin was formed by structural deformation of the underlying Eocene and Miocene volcanic and marine sedimentary rocks. As much as 1,800 ft of fluvial and lacustrine sediment has accumulated in the basin. The youngest deposits in the basin are primarily unconsolidated Pleistocene sediments brought into the basin during catastrophic flooding of the Columbia River. These sediment fill the center of the basin (pl. 1) and tend to be coarsest and thickest near the channels of the Columbia and Willamette Rivers. Most ground water developed in the basin is extracted from these deposits. The most extensive sedimentary geologic unit in the basin is the Troutdale Formation (Trimble, 1963), which, where it is not exposed, directly underlies the Pleistocene sediments. The Sandy River Mudstone (Trimble, 1963) underlies and is interleaved with the Troutdale Formation (Swanson and others, 1993). The Sandy River Mudstone is composed primarily of fine-grained sediments that overlie the volcanic and marine sedimentary bedrock throughout most of the basin. Mundorff (1964) referred to the Troutdale Formation as the Upper Troutdale Formation and to the Sandy River Mudstone as the Lower Troutdale Formation.

Hydrogeologic Units

Hydrogeologic units, as defined in this report, may comprise one or more geologic units; if a hydrogeologic unit contains more than one geologic unit, the geologic units must be adjacent to each other and have similar hydraulic characteristics so as to form a hydraulically connected continuum of similar materials. These hydrogeologic units can function as aquifers, or confining beds, or, where heterogeneous, both.

The nine hydrogeologic units delineated within the basin were the:

(1) unconsolidated sedimentary aquifer (US);
(2) Troutdale gravel aquifer (TG);
(3) confining unit 1 (C1);
(4) Troutdale sandstone aquifer (TS);
(5) confining unit 2 (C2);
(6) sand and gravel aquifer, upper coarse-grained subunit (SC);
(7) sand and gravel aquifer, lower fine-grained subunit (SF);
(8) undifferentiated fine-grained sediments (UF); and
(9) older rocks (OR).

The lithologic characteristics of these units, along with the geologic formations each unit comprises, are listed in plate 1.

In a detailed study of the hydrogeology of the city of Portland's Columbia South Shore well field in east Multnomah County (fig. 1), Hartford and McFarland (1989) defined the thickness and nature of several hydrogeologic units in the immediate vicinity of the well field. Swanson and others (1993) mapped the regional thickness and extent of these hydrogeologic units by using field mapping, well logs, and geophysical data. These units are described briefly in the following paragraphs; for more complete descriptions of the thickness, nature and extent of these units the reader is referred to Swanson and others (1993) and McFarland and Morgan (1996). The surface exposure of the units and representative sections are shown on plate 1.

Swanson and others (1993) grouped the hydrogeologic units into three subsystems on the basis of regionally continuous contacts between units with distinctly different lithologic and hydrogeologic characteristics: the upper sedimentary subsystem, lower sedimentary subsystem, and older rocks (pl. 1).

The unconsolidated sedimentary aquifer (US), a member of the upper sedimentary subsystem, contains Pleistocene catastrophic flood deposits, Holocene Columbia River alluvium, and to a lesser extent, flood-plain and terrace deposits along major tributaries and glacial outwash deposits in small basins in northern Clark County (McFarland and Morgan, 1996). The average thickness of the saturated part of the aquifer is about 75 ft; however, local accumulations of catastrophic-flood deposits are as much as 240 ft thick. Some parts of the unit are saturated only during the winter and spring or during prolonged periods of normal or above-normal recharge. The thickness and extent of the saturated part of the unconsolidated sedimentary aquifer is shown in Appendix A, figure A–1.

The Troutdale gravel aquifer (TG) is also a part of the upper sedimentary subsystem and includes sandy and cemented conglomerates, Boring Lava and Cascade lavas, and mantling soil horizons (McFarland and Morgan, 1996). Conglomerates within the unit extend basinwide and include the upper part of the Troutdale Formation of Trimble (1963) and Mundorff (1964), Cascade Range volcaniclastics of the Springwater and Gresham Formations (Trimble, 1963), and the informal upper member of the Troutdale Formation (Mundorff, 1964). Boring Lava and vent rocks are included in the Troutdale gravel aquifer. These rocks form many of the isolated hills in the southern part of the study area, including Kelly Butte, Mount Tabor, and the Boring Hills; occurrences in Clark County include Mount Norway and Prune Hill. Throughout much of the basin, the Boring Lava lies above the regional water table (Hogenson and Foxworthy, 1965), and ground water contained within them is perched above old soil zones and dense, low-permeability flow centers. In the southeastern parts of the study area and east of the Sandy River, the unit is composed of a thickening sheet of Cascade lavas (McFarland and Morgan, 1996). The unit has a maximum saturated thickness of approximately 900 ft and thins to zero at the margins of the basin and where it has been eroded by the Columbia, Sandy, Clackamas, and East Fork Lewis Rivers (Appendix A, fig. A–2); average thickness of the saturated part of the unit is 180 ft.

Confining unit 1 (C1) is the uppermost member of the lower sedimentary subsystem and consists of silt, clay, and discontinuous beds of medium- to fine-grained sand. Some low-discharge wells develop water from the interbedded sands, but overall the unit is not an important source of supply. The unit is overlain by the Troutdale gravel aquifer and underlain by the Troutdale sandstone aquifer. Confining unit 1 has a maximum thickness of nearly 300 ft in T.3N., R.2E. and in T.1N., R.2E. (Appendix A, fig. A–3); the average thickness of the saturated part of the unit is 110 ft.

The Troutdale sandstone aquifer (TS) underlies confining unit 1, except in the area east of the Sandy River and Lacamas Creek where the unit directly underlies the Troutdale gravel aquifer. The unit consists of two distinctive lithologic subunits: an upper, vitric sandstone and a lower, basaltic conglomerate (McFarland and Morgan, 1996). Both are highly productive. Thickness of the unit ranges from zero where it interfingers with the undifferentiated fine-grained sediments or has been eroded by the Columbia River to 320 ft in the eastern part of the basin (Appendix A, fig. A–4); the average thickness of the saturated part of the unit is 120 ft.

Confining unit 2 (C2) underlies the Troutdale sandstone aquifer and overlies either the upper, coarse-grained subunit of the sand and gravel aquifer or older rocks. The principal lithology of the unit is clay and silt with some lenses of silt and fine- to medium-grained sand (McFarland and Morgan, 1996). The extent of confining unit 2 is defined by the extent of the Troutdale sandstone aquifer. Where the Troutdale sandstone aquifer is absent, confining beds 1 and 2 are indistinguishable and are mapped as the

undifferentiated fine-grained sediments. This definition results in large variations in the thickness of the unit, as shown in Appendix A, figure A–5. The maximum thickness of the unit, 1,100 ft, occurs in Clark County, where the sand and gravel aquifer is absent and confining unit 2 directly overlies older rocks. The unit thins to 50 ft where it overlies the upper, coarse-grained subunit of the sand and gravel aquifer; the average thickness of the saturated part of the unit is 450 ft.

The sand and gravel aquifer was mapped as a single hydrogeologic unit by Hartford and McFarland (1989) and Swanson and others (1993). McFarland and Morgan (1996) noted that the unit contained two distinct lithologic subunits: a relatively coarse upper subunit composed mostly of sandy gravel, and a predominantly fine-grained lower subunit composed of silty sand, clay, and fine sand. The coarse-grained subunit is an important aquifer, being tapped by several public-supply systems on the south shore of the Columbia River and being actively explored for development in southern Clark County (McFarland and Morgan, 1996). The fine-grained subunit is not used as an aquifer. To permit a more accurate simulation of the contrast of their hydraulic properties, the sand and gravel aquifer was subdivided in the model into an upper, coarse-grained subunit (SC) and a lower, fine-grained subunit (SF). Well logs show that the upper subunit has an average thickness of about 100–150 ft. Where the sand and gravel aquifer was more than 125 ft thick, the upper subunit was assigned a constant thickness of 125 ft (Appendix A, fig. A–6) and the lower subunit was assigned the remaining thickness of the unit. Where the thickness of the sand and gravel unit was less than 125 ft, the entire thickness was assigned to the upper subunit (Appendix A, fig. A–7). The average thickness of the saturated part of the lower subunit is 500 ft.

The undifferentiated fine-grained sediments (UF) occur where the Troutdale sandstone aquifer is missing and confining units 1 and 2 cannot be differentiated. Throughout most of the basin, undifferentiated fine-grained sediments underlie the Troutdale gravel aquifer and overlie the older rocks. Regionally, the undifferentiated fine-grained sediments are not a good aquifer; however, coarse facies within the unit are an important source of ground water in central and northern Clark County. Thickness of the undifferentiated fine-grained sediments ranges from zero at the margins of the basin to 1,400 ft near Vancouver (Appendix A, fig. A–8). The average thickness of the saturated part of the undifferentiated fine-grained sediments is 580 ft.

The older rock subsystem (OR) includes Miocene and older volcanic and marine sedimentary rocks that underlie and, to a large extent, form a low-permeability boundary to the basin-fill sediments. The lower permeability members of this subsystem include the dense, altered basalts of the Skamania Volcanics, Goble Volcanics, basalts of Waverly Heights, and fine-grained marine sedimentary rocks such as the Scappoose Formation. The Columbia River Basalt Group is a member of the older rock subsystem and can have high permeability interflow zones that yield large quantities of water to wells (McFarland and Morgan, 1996). The thickness of older rocks in the basin is not well defined; however, on the basis of well-log data, they are known to extend to at least 2,000 ft below sea level (Swanson and others, 1993). The thickness of the older rocks above this altitude is shown in Appendix A, figure A–9.

Occurrence and Movement of Ground Water

The ground-water system in the basin is recharged primarily by direct infiltration of precipitation, but recharge from urban runoff shunted to drywells and from on-site waste-disposal systems also are significant sources in densely populated, unsewered, urban areas (Snyder and others,1994). The distribution of infiltration of precipitation is closely related to annual precipitation, altitude, and the percentage of the area covered by impervious surfaces. Infiltration from precipitation ranges from zero in highly developed urban areas to nearly 50 in/yr in the upland forested areas of the basin (Snyder and others, 1994). Streams may constitute locally important sources of seasonal recharge during periods of high flow; however, much of this recharge is lost to base flow during stream recession. High discharge wells near the Columbia River also can induce recharge from the river to the shallow alluvial aquifers (Mundorff, 1964).

Movement and discharge of ground water is controlled primarily by the topography of the basin. Regional, intermediate, and local ground-water flow systems exist in the basin. The Willamette, Lewis, Clackamas, and Columbia Rivers represent the discharge areas for the regional ground-water flow system. Most of the ground water discharging to them enters the system in upland recharge areas, moves downward through hundreds of feet of sediment, moves horizontally, and finally moves upward to

discharge to the rivers. The East Fork Lewis River, Salmon Creek, and the Sandy River are examples of discharge areas for intermediate ground-water flow systems. The general directions of ground-water flow in the Troutdale gravel aquifer are shown in figure 2. Local ground-water flow systems are much smaller and ground water within them has much shorter residence times; commonly, recharge and discharge points are within hundreds of feet of each other. Discharge can occur as direct seepage to a stream, hillslope seepage, or as evapotranspiration by riparian vegetation. All the conditions discussed above are based on the assumption of natural flow conditions. Manmade changes, such as the addition of wells, drywells, on-site waste-disposal systems, and paved surfaces in the basin, disrupt these natural flow paths. One of the goals of this study was to develop a quantitative understanding of the influence of manmade changes on the natural flow system.

SIMULATION ANALYSIS OF THE GROUND-WATER FLOW SYSTEM

A steady-state numerical model of the ground-water system was constructed and calibrated to time-averaged data for the period April 1987 through March 1988. Time-averaged data for the 1987–88 period were used in the calibration because data needed to define long-term historical changes in ground-water levels, pumpage, and recharge within the basin were not available. The April 1987 through March 1988 period was used because this was the time during which most of the water-level and water-use data were collected in the study.

Estimates of all model-parameter values, fluxes, and boundary conditions were made to construct the initial model. A systematic sensitivity analysis of model response to changes in each parameter value and boundary conditions was then made. Calibration of the model consisted of making changes to parameters and boundary conditions, focusing on the most sensitive parameters, until the best fit between model simulated and measured ground-water levels and fluxes was obtained.

The model was then used to simulate past and future changes to the ground-water system. First, historical changes that have occurred due to the loss of pervious surfaces in urban areas, ground-water pumpage, and diversion of surface runoff were simulated. Second, the future changes that may occur due to increased ground-water pumpage under one hypothetical condition were simulated.

General Features of the Model

A three-dimensional, steady-state, finite-difference, ground-water flow model of the Portland Basin was constructed using the McDonald and Harbaugh (1988) modular code (MODFLOW). Since MODFLOW was published, several additional modules, or packages, have been developed that facilitate the simulation of more complex hydrologic systems. One example (Prudic, 1989) is a streamflow-routing package that was used in this study to simulate stream-aquifer relations in the basin. Another package, written by Orzol and McGrath (1992) for use in this study, allows MODFLOW to read and write data directly from and to the ARC/INFO geographic information system file format.

The data manipulation and analysis tasks related to construction, calibration, and use of the ground-water model were enormous. The complex and varied sedimentary environment of the Portland Basin presented significant challenges when trying to represent that structure within the framework of a numerical model. The use of a geographic information system to store and manage spatial data and the software interface to MODFLOW by Orzol and McGrath (1992) made it possible to include a great deal of that complexity in the model and facilitated graphical presentation of simulation results.

MODFLOW simulates ground-water flow through three-dimensional, heterogeneous, anisotropic aquifer systems by iteratively solving a finite-difference approximation of the partial differential equation for ground-water flow (McDonald and Harbaugh, 1988). The flow equation may be solved using one of several iterative techniques; the strongly implicit procedure (SIP) was used for the Portland Basin model.

The general equation for three-dimensional ground-water flow through porous material is:

$$\frac{\partial}{\partial x}\left(K_{xx}\frac{\partial h}{\partial x}\right)+\frac{\partial}{\partial y}\left(K_{yy}\frac{\partial h}{\partial y}\right)+\frac{\partial h}{\partial z}\left(K_{zz}\frac{\partial h}{\partial z}\right)-W=S_s\frac{\partial h}{\partial t}\ , \qquad (1)$$

where

K_{xx}, K_{yy}, K_{zz} are values of hydraulic conductivity along the x, y, and z axes (LT^{-1});

h is the potentiometric head (L);

W is a volumetric flux per unit volume and represents sources and or sinks of water (T^{-1});

S_s is the specific storage of the porous material (L^{-1}); and

t is time (T).

Equation (1) can be used to simulate either transient or steady-state ground-water flow systems. In transient analyses, the storage term on the right-hand side of equation (1) represents the rate of change in storage in the system; for steady-state simulations, the rate of change in storage is zero. The general flow equation may also be time averaged (Prych, 1983) by integrating over time and dividing by the time interval, resulting in the following equation:

$$\frac{\partial}{\partial x}\left(K_{xx}\frac{\partial \bar{h}}{\partial x}\right)+\frac{\partial}{\partial y}\left(K_{yy}\frac{\partial \bar{h}}{\partial y}\right)+\frac{\partial \bar{h}}{\partial z}$$

$$\left(K_{zz}\frac{\partial \bar{h}}{\partial z}\right)-\bar{W}=S_s\frac{\left(h_{t_2}-h_{t_1}\right)}{t_2-t_1}, \qquad (2)$$

where

$\bar{h}$ is average potentiometric head for the time interval, t_2-t_1 (L);

$\bar{W}$ is the average volumetric flux per unit volume for the time interval, t_2-t_1 (T^{-1}); and

t_1, t_2 are times at the beginning and end of the time interval, respectively (t).

Time averaging is a method of converting certain transient flow problems into steady-state flow problems. If the heads in the system at times t_1 and t_2 are the same, then the storage term on the right hand side of equation (2) is zero. However, if there is a change in head and thus a change in storage between times t_1 and t_2, then the storage term represents the average rate of change in storage during the time interval. The time-averaged flow equation (2) was used to model the Portland Basin for the calibration period of April 1987 through March 1988; the rationale for this approach is described in the section, "Calibration of the Model".

The finite-difference grid used to subdivide the ground-water flow system in the Portland Basin consisted of 91 rows and 50 columns. This grid formed 4,550 cells, 3,040 of which were "active" in each of the 8 model layers. The dimensions of each cell were 3,000 ft per side, but the thicknesses were variable (fig. 3).

The complex history of deposition and erosion in the basin has created hydrogeologic units that are discontinuous and that vary greatly in thickness. A hydrogeologic section illustrating the stratigraphic complexity of the basin is shown in figure 4. Discontinuous hydrogeologic units present special problems to the construction of ground-water models. These problems stem from the inability of most models (including MODFLOW) to allow vertical flow across inactive model cells that must separate nonadjacent layers; thus, if a hydrogeologic unit has been truncated or has pinched out, vertical flow cannot be simulated between the overlying and underlying units. This problem has historically been addressed by either leaving "pseudo-cells" in missing layers with very large vertical conductances and very low horizontal hydraulic conductivity (Morgan and Dettinger, 1994) or by modifying the model to allow vertical flow between nonadjacent layers (Hansen, 1993).

The primary goal in construction of the Portland Basin model was to maintain as much of the stratigraphic complexity of the real ground-water flow system as possible and yet avoid making changes to the basic MODFLOW code or incorporating "pseudo-cells" into the system. The approach used to meet these goals was a "unit-code" method in which hydrogeologic units are not restricted to a single model layer, but may span multiple layers. Hydraulic characteristics and thicknesses vary within model layers to reflect the character and thickness of the unit represented by individual cells within the layer.

Although nine hydrogeologic units were defined in the basin, the maximum number of units that were found to occur in any vertical section was eight; thus, eight model layers were used to simulate the ground-water flow system. A vertical column of model cells could simulate from one to eight hydrogeologic units. If eight units were present in the section, each would be simulated by one of the cells in the column. Where the section consisted of only one unit, all eight cells in the column were used to represent the unit. The vertical subdivision of the hydrogeologic section with the model section is shown in figure 4.

For cases in which sections contained more than one but fewer than eight hydrogeologic units, hydrogeologic units were allocated to the eight cells on the basis of stratigraphic relations between units (table 1).

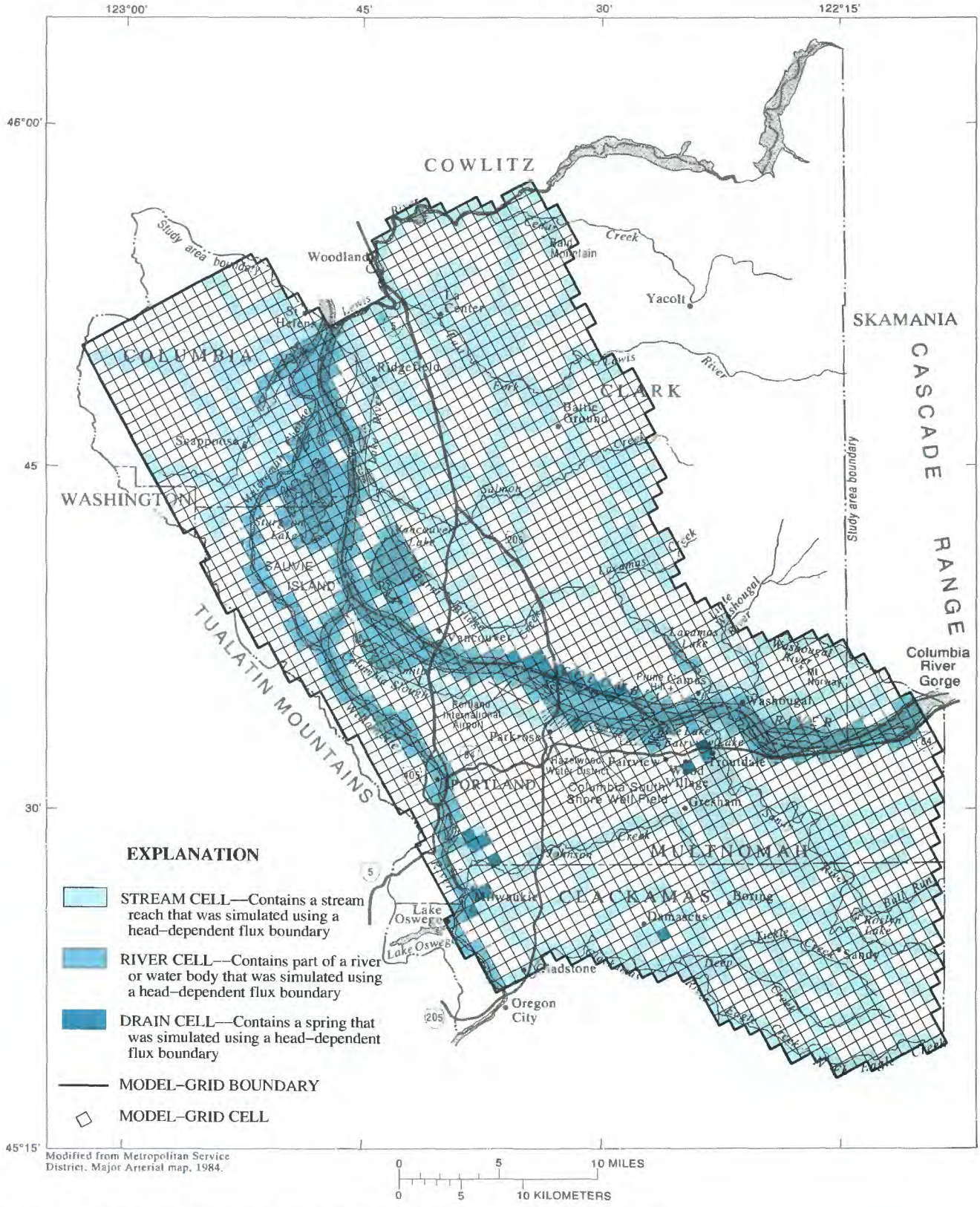

Figure 3. Boundary conditions and extent of grid used in the ground-water flow model.

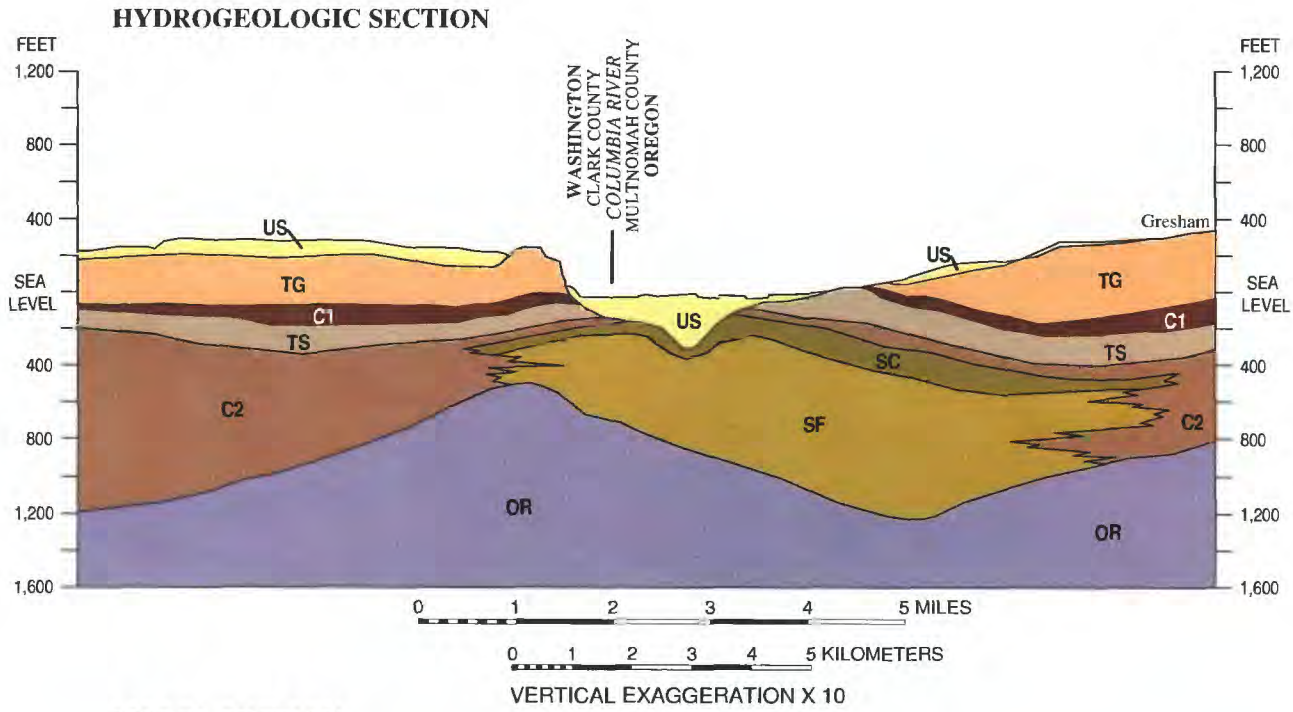

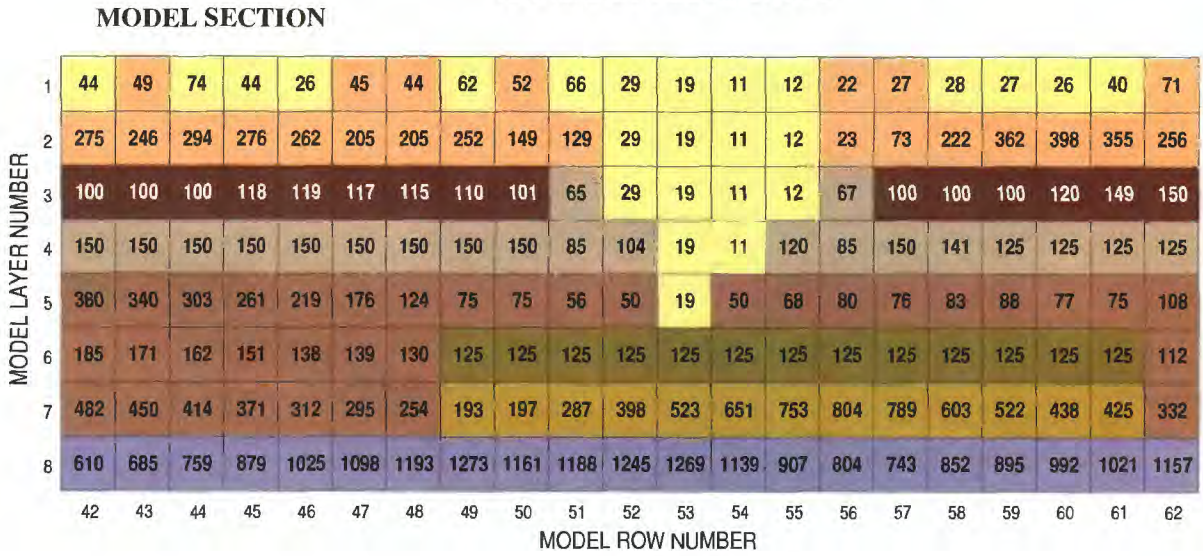

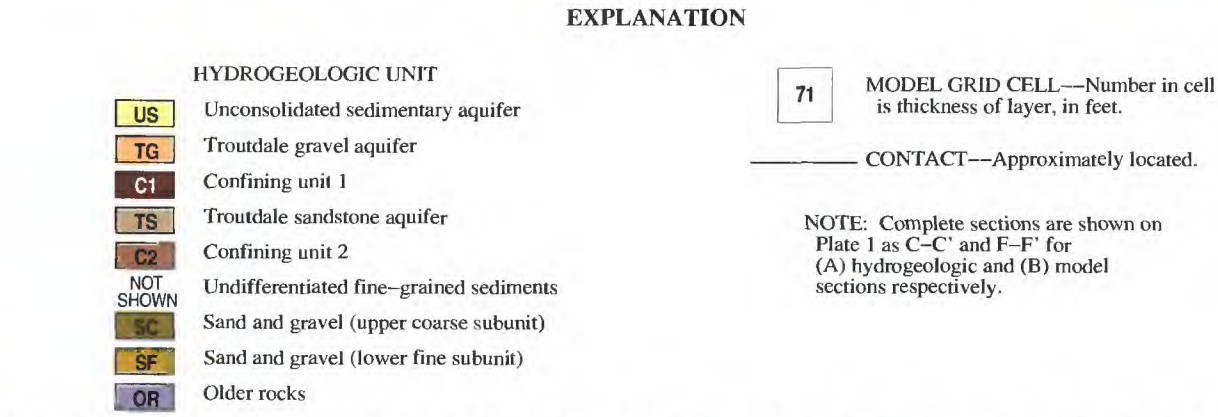

Figure 4. Hydrogeologic and model sections showing correlation of model layers with hydrogeologic units along column 28 of model. (Location of sections do not match exactly and hydrogeologic section shows total thickness [saturated and unsaturated]; model section shows saturated thickness only.)

Table 1. Assignment of hydrogeologic units to model layers

[US, unconsolidated sedimentary aquifer; TG, Troutdale gravel aquifer; C1, confining unit 1; TS, Troutdale sandstone aquifer; C2, confining unit 2; SC, sand and gravel aquifer, upper coarse-grained subunit; SF, sand and gravel aquifer, lower fine-grained subunit; UF, undifferentiated fine-grained sediments; OR, older rocks; ●, unit occurs most frequently in layer; 0, unit occurs in layer; --, unit does not occur in layer]

	Hydrogeologic unit								
	Upper sedimentary subsystem		Lower sedimentary subsystem					Older rock subsystem	
	Unit code								
	1	2	3	4	5	7	8	6	9
	Unit name								
Model layer	US	TG	C1	TS	C2	SC	SF	UF	OR
1	●	0	0	0	0	0	--	0	0
2	0	●	0	0	0	0	--	0	0
3	0	--	●	0	0	0	--	0	0
4	0	--	--	●	0	0	--	0	0
5	0	--	--	--	●	0	--	0	0
6	0	--	--	--	0	●	--	0	0
7	--	--	--	--	0	0	●	0	0
8	--	--	--	--	--	--	--	--	●

If a unit was represented by only one layer, the entire saturated thickness of the unit was assigned to that layer. If multiple layers were assigned to the unit, the unit's thickness was apportioned among the layers to minimize the changes in thickness between adjacent cells in the same layer. A computer program was written to automate the allocation of model layers to units and calculation of unit thickness in each model cell. The assignment of units to model layers is summarized in table 1.

Data arrays, containing integer unit codes to indicate the hydrogeologic unit represented by each cell, were constructed for each model layer. Input arrays for hydraulic characteristics were prepared for each model layer from arrays for each hydrogeologic unit and the unit-code arrays that link the layer arrays to the units arrays. The unit code files were used to prepare the input data files for several of the model packages.

Boundary Conditions

The boundaries of the model were selected to coincide with either geologic or hydrologic boundaries of the ground-water flow system. Three types of boundary conditions were used to represent the individual hydrogeologic conditions: no-flow, specified flux, and head-dependent flux (fig. 3).

No-Flow Boundaries

The model grid was extended horizontally to boundaries that were assumed to allow very little or no ground-water flow across them into or out of the basin. These boundaries coincide with the edge of the model grid (fig. 3). The following description of no-flow boundaries applies to each layer of the model. This type of boundary condition was used to represent three types of physical boundaries:

(1) nearly impermeable rocks,

(2) ground-water flow divides, and

(3) streams that function as sinks to the regional ground-water system.

The northern boundary of the model is formed by the Lewis River from Lake Merwin to the Columbia River. Because older rocks that underlie the Lewis River have very low hydraulic conductivity and because the river acts as a regional ground-water sink, the outer edge of cells underlying the river was designated a no-flow boundary. The uppermost layer of cells containing the Lewis River were designated head-dependent flux cells to allow flux between the river and the ground-water system.

The eastern boundary of the model, from the Lewis River south to the Columbia River, follows the contact between the basin-fill sediments and the older rocks. The older rocks in this area are basalts of low hydraulic conductivity and were designated a no-flow boundary to the model. The no-flow boundary extends southward from the Columbia River across the western flank of the Cascade Range to the North Fork of Eagle Creek, a tributary of the Clackamas River. The Troutdale gravel aquifer underlying this part of the no-flow boundary is composed of low-permeability Cascade lavas and volcaniclastic conglomerates (McFarland and Morgan, 1996).

The southern boundary of the model is coincident with North Fork Eagle Creek to its confluence with the Clackamas River and with the Clackamas River to its confluence with the Willamette River. The channels of Eagle Creek and the Clackamas River have been cut down into the lower-permeability older rocks or fine-grained sediments throughout most of their length. There is no evidence to indicate that ground-water flow occurs beneath the rivers, and they were assumed to function as regional sinks that intercept all ground-water flow.

The western boundary of the model follows several faults in the older rocks from the confluence of the Clackamas and Willamette Rivers northwest to the axis of the Tualatin Mountains anticline (pl. 1). The anticlinal axis coincides with the drainage divide for the Portland Basin and the boundary follows the divide northward to Scappoose Creek, where the boundary of the model grid coincides approximately with the drainage divide of the creek. The western boundary of the model was assumed to be a no-flow boundary because of the structural barrier to flow created by the anticline and because a ground-water divide probably exists that coincides with the surface-water divide.

The no-flow boundaries shown in figure 3 extend through all eight model layers. The lower boundary of the model is also a no-flow boundary, and it is located at an altitude of 2,000 ft below sea level throughout the model. This altitude was selected so that older, less permeable rocks would form the basal unit of the model throughout the area and have a minimum thickness of about 400 ft. Where the unit has been used as an aquifer, or is likely to be, its top is generally at or above sea level. At least the uppermost 2,000 ft of the unit is simulated wherever it might be subjected to pumping stress that would induce upward vertical flow and large changes in storage.

Specified Flux Boundaries

Specified flux boundaries were used to simulate recharge and discharge processes that are not a function of head. Two types of flux specified in the model were discharge by wells and recharge. During calibration of the model to time averaged conditions for 1987–88, a third type of flux was specified to account for changes in ground-water storage during the calibration period; this flux is described in the section, "Calibration of the Model." Rates of recharge and change in storage were specified using the "RECHARGE" package of MODFLOW; well-discharge rates were specified using the "WELL" package.

Recharge

The annual recharge to the ground-water system is principally derived from three sources: (1) infiltration of precipitation, (2) runoff to drywells, and (3) on-site waste-disposal systems (Snyder and others, 1994).

Snyder and others (1994) used a deep percolation model to estimate recharge from direct infiltration of precipitation in three small drainages within the basin. Regression analysis of the results revealed that recharge from direct infiltration of precipitation is most dependent on mean annual rainfall, altitude, and the percentage of impervious area. They found that the regression equation:

$$R = -4.79 + 0.482\,P - 0.354\,I + 0.0097\,E, \quad (3)$$

where

R = mean annual recharge, in/yr;

P = mean annual precipitation, in/yr;

I = impervious area, in percent; and

E = altitude of land surface, in feet;

has an r-squared value of 0.91. The recharge rates estimated by Snyder and others (1994) are average rates for land areas within each cell. The mean annual rate for the study area is about 21 in/yr. The recharge rate for model cells containing substantial areas of surface water was adjusted by multiplying by the ratio of land area to the total area of the cell. For example, a model cell with a recharge rate of 10 in/yr, with one-half of its area covered by surface water, would have a recharge rate of 5 in/yr in the model.

Application of the regression equation resulted in estimated recharge rates that range from 0 to 49 in/yr within the model area. The mean annual rate for the

basin is about 21 in/yr. Recharge rates generally are greatest in the higher altitudes of the Tualatin Mountains and the western Cascade Range. Recharge rates are least in the most urbanized parts of the basin, where impervious surfaces, such as streets and parking lots, intercept water that would otherwise infiltrate to the ground-water system. In some urban areas, however, runoff from impervious areas is routed to the subsurface through drywells, making them a locally important source of recharge, with areally averaged rates within model cells of from 1 to 26 in/yr. Effluent from on-site waste-disposal systems also is an important source of recharge in densely populated, unsewered areas. In east Multnomah County where densities are highest, Snyder and others (1994) estimated areally averaged recharge rates within model cells of as much as 26 in/yr from on-site waste-disposal systems. The areal distribution of total mean annual recharge is shown on plate 2.

Well Discharge

Average well-discharge rates in the model were based on data published by Collins and Broad (1993). Discharge rates for 1988 were used for calibration of the model because they were more representative of average conditions during the 1987–88 calibration period. The discharge rates for 1987 were unusually high due to operation of wells in the city of Portland's Columbia South Shore well field from August through October of that year.

In 1988, the average rate of well discharge for the basin was 166 ft^3/s; 40 percent (66 ft^3/s) of this total was used for public supply, 50 percent (83 ft^3/s) for industrial process water, and 10 percent (17 ft^3/s) for irrigation (Collins and Broad, 1993). The distribution of well discharge, by model cell, is shown in figure 5. Fifty-eight percent of 1988 well discharge was from the unconsolidated sedimentary aquifer, 27 percent from the Troutdale gravel aquifer, and 7 percent from the Troutdale sandstone aquifer. The areal distributions of well discharge from these units are shown in Appendix B. The remaining 8 percent of well discharge was from the undifferentiated fine-grained sediments (3 percent), the upper, coarse-grained subunit of the sand and gravel aquifer (3 percent), and the older rocks (2 percent).

Head-Dependent Flux Boundaries

Ground-water interaction with surface-water bodies was simulated using three separate packages in MODFLOW. Lakes and large rivers were simulated using the RIVER package. Streams and medium-sized rivers were simulated using the STREAM package (Prudic, 1989). Springs were simulated using the DRAIN package.

Lakes and Large Rivers

The Willamette and Columbia Rivers, Multnomah Channel, Vancouver and Sturgeon Lakes, and other low-lying water bodies are regional discharge points for ground-water flow and were simulated in the model as head-dependent flux boundaries using the RIVER package of MODFLOW (fig. 3). The rates of ground-water discharge to, or recharge from RIVER cells are simulated as a piecewise linear function of the hydraulic conductance of the riverbed and the difference between river stage and the ground-water level in the cell. The mean annual stage at RIVER cells on the Willamette and Columbia Rivers was estimated by extrapolation of data from the gaging stations at Portland and Vancouver. The mean altitude of the riverbed in each RIVER cell was estimated from 7.5-minute USGS topographic maps. The 434 model cells designated as RIVER boundaries are shown in figure 3.

Streams and Small Rivers

All other rivers and major streams were designated as head-dependent flux boundaries in the model using the STREAM package developed by Prudic (1989) for use with MODFLOW (fig. 3). The STREAM package calculates leakage between the stream and the aquifer in a manner identical to that used in the RIVER package, and it also calculates flow into and out of each reach of the stream.

Use of the STREAM package requires that streams in the model be divided into segments and reaches (Prudic, 1989). A segment is a length of stream that has no tributaries or diversions; a reach is a part of a segment that lies within one model cell. A segment can be made up of one or more reaches. Segment and reach numbers are assigned in downstream order to facilitate the flow accounting by the model. A second input file defines the tributary and diversion relations between segments. In the Portland Basin model, 1,253 stream reaches were specified in 150 segments. Model cells containing STREAM boundaries are shown in figure 3.

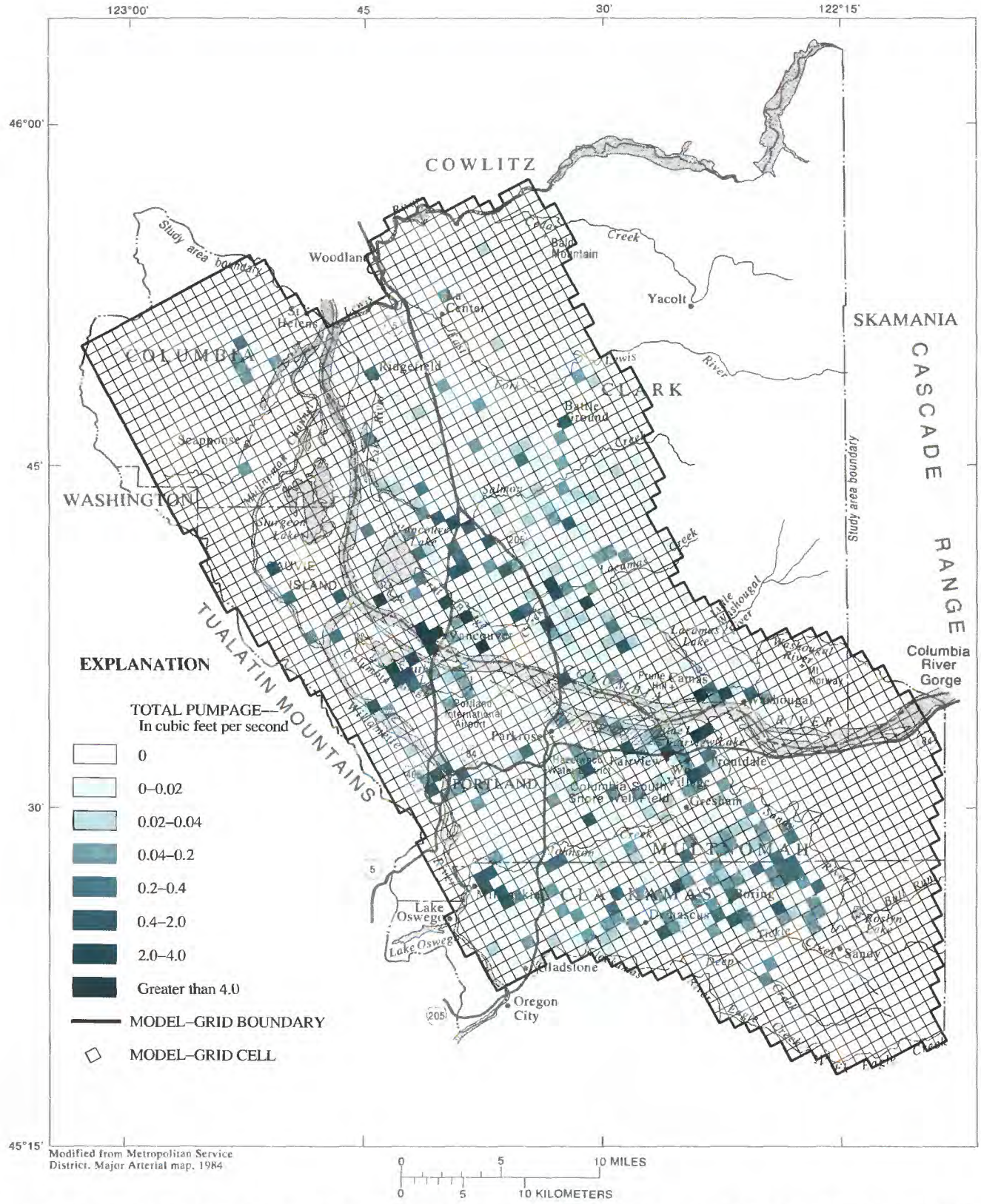

Figure 5. Estimated rates and distribution of ground-water discharge by wells, 1988 (modified from Collins and Broad, 1993).

The mean streambed altitude of each reach was determined from 7.5-minute USGS topographic maps. The mean stream stage in each reach was assumed to be 2 ft above the streambed, and the streambed thickness was assumed to be 2 ft.

Springs

All major springs in the basin were represented as head-dependent flux boundaries in the model using the DRAIN package of MODFLOW. In contrast to the STREAM and RIVER packages, the DRAIN package allows only discharge from the system. Thus, when the calculated head in the drain cell is above the altitude of the spring, the discharge rate of the spring is calculated as a piecewise linear function of the hydraulic conductance of the spring and the difference between the spring altitude and the head in the cell. The 23 model cells containing springs simulated with the DRAIN package are shown in figure 3.

Hydraulic Characteristics

The hydraulic characteristics of the rocks and sediment that form aquifers and confining beds of the ground-water system are major controlling factors on the direction and velocity of ground-water movement within the system.

Horizontal Hydraulic Conductivity

Estimates of horizontal hydraulic conductivity were made by McFarland and Morgan (1996) from approximately 500 single-well specific-capacity tests and 55 multiple-well aquifer tests. These estimates were used to delineate the distributions of hydraulic conductivity for the unconsolidated sedimentary aquifer, Troutdale gravel aquifer, Troutdale sandstone aquifer, and the upper, coarse-grained subunit of the sand and gravel aquifer. These distributions were used as initial values that were subsequently modified during calibration of the numerical model. The statistical distributions of the precalibration and postcalibration hydraulic conductivity estimates are compared for each hydrogeologic unit in figure 6.

Few wells in the basin have openings adjacent to fine-grained units; therefore, specific-capacity or aquifer-test data were insufficient to directly estimate the areal distribution of hydraulic conductivity in these units. There are, however, many wells that penetrate the confining units (1 and 2) and the undifferentiated fine-grained sediments. This made it possible to delineate variations in the lithology of the fine-grained units that might be related to variations in the hydraulic characteristics of the units. Lithologic logs from drillers' reports on these wells were used to construct a map of the average percentage of fine-grained sediments within the units. For wells with specific- capacity tests, the percentage of fine-grained sediments was compared with the estimated hydraulic conductivity, but no relation was found. The reasons for this lack of correlation are probably twofold. First, differences in the fraction of the hydrogeologic unit penetrated by the wells or well-screen placement probably bias the estimated hydraulic conductivities toward high values, because wells typically are selectively completed in coarser-grained sediments. Second, the percentage of fine-grained sediments at each well was estimated on the basis of subjective interpretation of drillers' descriptions of lithology.

The percentage of fine-grained sediments nonetheless was considered an indicator of the hydraulic conductivity of the fine-grained units. A simplistic, but reasonable, relation between the percentage of fine-grained sediments and the hydraulic conductivity of the fine-grained units was derived using the distribution of hydraulic-conductivity estimates for the undifferentiated fine-grained sediments. It was assumed that the maximum hydraulic conductivity of 37 ft/d (feet per day) would occur where there were no fine-grained sediments in the unit, and the minimum (0.1 ft/d) would occur where the unit was composed entirely of fine-grained sediments. Assuming a linear relation between percentage of fine-grained sediments and hydraulic conductivity, the following relation was used to estimate the distribution of hydraulic conductivity in the fine-grained units:

$$Kh = 37.0 - 0.369\,Pf, \qquad (4)$$

where

Kh is horizontal hydraulic conductivity (LT^{-1}),

and

Pf is percentage of fine-grained sediments (dimensionless).

Not enough wells penetrated the fine-grained units to map the percentage of fine-grained sediments for each unit. A composite map of the percentage of fine-grained sediments was constructed using data from all of the wells that penetrated fine-grained units.

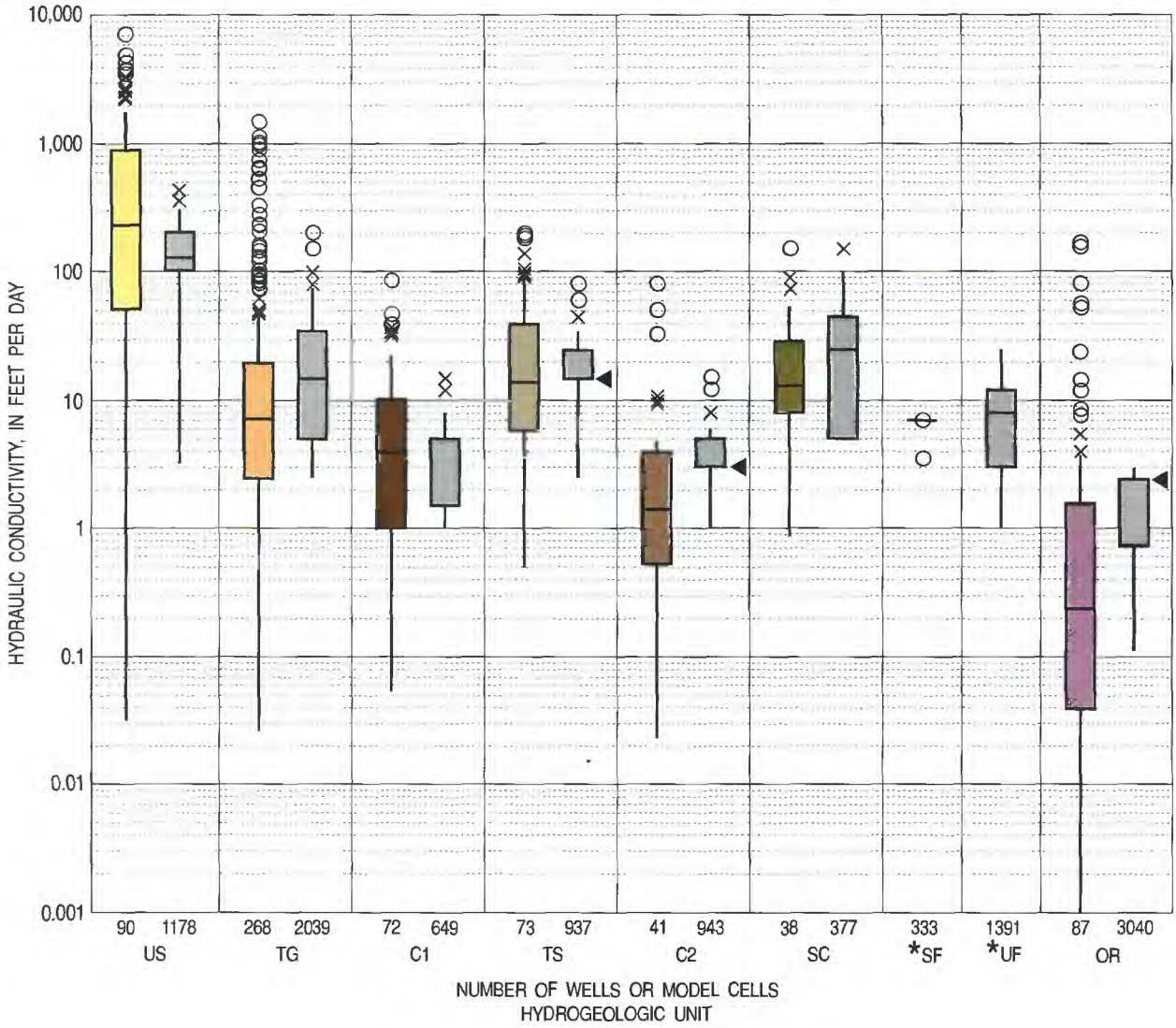

EXPLANATION

Interquartile range equals the value of the 75th percentile minus the value of the 25th percentile.

- More than 3 times the interquartile range from the 75th percentile value
- 1.5 to 3 times the interquartile range from the 75th percentile value
- Less than 1.5 times the interquartile range from the 75th percentile value
- 75th percentile value
- Median value
- 25th percentile value
- Less than 1.5 times the interquartile range from the 25th percentile value

Data from wells

Data from model calibration

HYDROGEOLOGIC UNIT

US	Unconsolidated sedimentary aquifer
TG	Troutdale gravel aquifer
C1	Confining unit 1
TS	Troutdale sandstone aquifer
C2	Confining unit 2
SC	Sand and gravel aquifer (upper subunit)
SF	Sand and gravel aquifer (lower subunit)
UF	Undifferentiated fine-grained sediments
OR	Older rocks

* Note: Data from model calibration only

Figure 6. Distributions of hydraulic conductivity for hydrogeologic units. (Data are from specific-capacity and aquifer tests on wells and from model calibration.)

Therefore, the initial areal distribution of hydraulic conductivity, derived by determining the percentage of fine-grained sediments at each model cell and applying the above relation, was the same for each of the fine-grained units (confining units 1 and 2, the lower sub-unit of the sand and gravel aquifer, and the undifferentiated fine-grained sediments).

Hydraulic conductivity of the older rocks also was estimated from specific-capacity data; however, the areal distribution of data was insufficient to allow contouring of hydraulic conductivity. A subsurface geologic map of the older rocks subsystem (McFarland and Morgan, 1996) was used to delineate zones of differing hydraulic conductivity within the older rocks. First, the mean hydraulic conductivity of each geologic unit composing the older rocks subsystem was computed from available specific-capacity and aquifer-test data. Geologic units included within the older rocks subsystem are the Columbia River Basalt Group, Rhododendron Formation, Skamania Volcanics, Goble Volcanics, and the basalts of Waverly Heights (McFarland and Morgan, 1996). Second, the predominant geologic unit within each model cell was determined. Finally, each cell was assigned the mean hydraulic conductivity of the predominant geologic unit in the cell.

Estimates of hydraulic conductivity for some units were modified during the calibration process to achieve a best fit between simulated and observed data. The postcalibration distributions of hydraulic conductivity for all units are shown on plates 3–8.

Vertical Hydraulic Conductivity

In an aquifer system, the hydraulic conductivity varies with direction. In sedimentary aquifer systems, the horizontal and vertical hydraulic conductivity can differ by orders of magnitude. Hydraulic conductivity is typically greatest in the horizontal direction because that is the usual orientation of sediment particles and layers during deposition.

Field measurement of vertical hydraulic conductivity is difficult and expensive, requiring carefully designed multiple-well aquifer tests using observation wells completed at multiple depths. This type of test was not within the scope of this study, and no other test data were found to allow this type of analysis. Laboratory measurement of vertical hydraulic conductivity can be made on core samples; however, the potential for sample disturbance and the very small part of the sediment represented severely limit the utility of these data. Because of these problems, vertical hydraulic conductivity generally is estimated through the model calibration process.

The hydraulic characteristic required by MODFLOW to define the capability of adjacent hydrogeologic units to transmit ground water vertically is called the vertical conductance (*VCONT*). Vertical conductance values must be specified between all adjacent model layers and typically are calculated as:

$$VCONT_{k,k+1} = \frac{2\left(\frac{Kh_k}{An_k}\right)\left(\frac{Kh_{k+1}}{An_{k+1}}\right)}{b_{k+1}\left(\frac{Kh_k}{An_k}\right) + b_k\left(\frac{Kh_{k+1}}{An_{k+1}}\right)}, \quad (5)$$

where

$VCONT$ = vertical conductance T^{-1};

Kh = horizontal hydraulic conductivity (LT^{-1});

An = vertical anisotropy ratio, horizontal to vertical (dimensionless);

b = thickness (L); and

k = model layer number.

In the model constructed for this study, vertical anisotropy ratios of hydraulic conductivities (horizontal to vertical) were estimated for each hydrogeologic unit from published values for similar classes of sediments. These ratios were modified during calibration. The initial ratios were 100:1 for all sediments and 1,000:1 for older rocks. Vertical anisotropy ratios were assumed to be constant within a unit; however, vertical conductance values varied because of variations in thickness and horizontal hydraulic conductivity within each unit.

Conductances of Head-Dependent Flux Boundaries

Ground-water flux across each of the head-dependent boundaries (rivers, streams, and drains) is calculated as a piecewise linear function of the difference between the water level in the aquifer and the water level at the boundary, and the conductance of that boundary. The conductance represents the ease with which ground water can flow across riverbeds, streambeds, or seepage faces (springs) (McDonald and Harbaugh, 1988).

Head-dependent boundary conductances are analogous to the vertical conductance between model layers described above; however, boundary conductances are adjusted external to the model to account for the area of a cell that is covered by the boundary, whereas vertical conductances are adjusted internally. The generalized boundary conductance equation is:

$$COND = \frac{KA}{b}, \quad (6)$$

where

$COND$ = boundary conductance (T^{-1});

K = hydraulic conductivity of the boundary normal to the direction of flow (LT^{-1});

b = length of the flow path (thickness) (L); and

A = area of boundary normal to the flow path within the cell (L^2).

Initial values of riverbed and streambed conductance were determined by assuming that the beds had the same hydraulic conductivity (K) as the underlying hydrogeologic units. The area (A) of each river or stream cell that was covered by water was estimated from 7.5-minute USGS topographic maps. Riverbed and streambed sediments were assumed to have thickness (b) of 5 ft and 2 ft, respectively, throughout the model.

Initial values of drain conductance also were determined by assuming that drains had the same hydraulic conductivity as the hydrogeologic units within the cells. The area (A) of the boundary normal to the flow path was estimated to be 3,000 ft (one cell width) wide by one-half the saturated thickness of the cell high. The length of the flow path was assumed to be 1,500 ft (one-half cell width). Initial estimates of boundary conductance were modified during calibration.

Calibration of the Model

Procedure

The first step in the calibration process was to analyze model sensitivity to changes in parameters and boundary conditions. The purpose of the analysis was to gain an understanding of the effects of uncertainty in hydraulic characteristics and boundary conditions on the heads and fluxes simulated by the model.

Using results of the sensitivity analysis as a guide, the model was calibrated to time-averaged conditions for the period April 1987 through March 1988. Time-averaged data were used for the calibration because there were no data available for any period in which the ground-water system was in a true steady state. Calibration to transient conditions was ruled out because of the lack of information on long-term or seasonal changes in stresses such as pumpage and recharge and the problem of specifying initial conditions.

When using the time-averaged, ground-water-flow equation (equation 2), if changes in storage occur in the ground-water flow system during the time-averaging interval, the rate of change in storage must be added to the right-hand side of the equation. Changes in ground-water storage occurred in some areas of the basin during the 1987–88 calibration period, as evidenced by changes in water levels mapped by McFarland and Morgan (1996, pl. 7). Water-level changes in unconfined aquifers can cause large changes in ground-water storage because water is lost from or taken into storage at a rate proportionate to the specific yield of the aquifer. Specific-yield values are similar in magnitude to porosity and generally range between 0.1 and 0.3. Thus, for a 5 ft/yr (feet per year) decline in ground-water level in an unconfined aquifer with a specific yield of 0.2, the rate of storage depletion would be 1 ft/yr, or about 0.3 ft^3/s within the area of a model cell. This rate is similar in magnitude to estimated recharge rates in the basin (pl. 2).

The rate of change in storage in the unconfined aquifers of the basin was estimated for the calibration period by determining the mean water-level change at each model cell by using maps of changes in the unconsolidated sedimentary aquifer and the Troutdale gravel aquifer compiled by McFarland and Morgan (1996, pl. 7). Estimates of specific yield for lithologies similar to those of the unconsolidated sedimentary aquifer and Troutdale gravel aquifer were taken from Johnson (1967). A value of 0.2 was selected for the unconsolidated sedimentary aquifer for sediments ranging from gravel and sand to silty sand and sandy silt. A value of 0.1 was selected for the Troutdale gravel aquifer due to the abundance of cemented sands and gravels in the unit. Ground-water storage was depleted by 12,000 acre-feet within the areas where water levels declined and was replenished by 50,000 acre-feet within areas where water levels increased. The net volume of change in storage was a gain of 38,000 acre-feet, which amounts to only 3 percent of total recharge to the modeled area.

Storage change estimates could be made only for the areas of the basin where water-level changes were mapped by McFarland and Morgan (1996). The areas mapped included approximately 80 percent of the modeled region and all of the areas where ground-water levels would be most affected by pumping. The estimated rates of change in storage in the unconfined parts of the aquifer system are shown in figure 7; these rates were specified fluxes during model calibration. Errors in the estimated water-level changes or in the specific yield of the aquifers would contribute to errors in estimated rates of storage change. These errors could be large if insufficient water-level data were available to define changes or if specific yields varied greatly from estimated values.

Storage changes in confined parts of the aquifer system were negligible because the storage coefficients of confined aquifers are at least two orders of magnitude less than the specific yield of unconfined aquifers. For example, in a confined aquifer with a storage coefficient of 0.001, a water-level decline of 5 ft/yr would result in a rate of storage depletion of only 0.005 ft/yr, or about 0.001 ft^3/s within the area of a model cell. This rate is insignificant compared with typical recharge rates of 1.5 ft/yr (0.428 ft^3/s) or typical well-discharge rates of 200 gallons per minute (0.446 ft^3/s).

Model calibration also includes the process of adjusting the hydraulic characteristics and boundary conditions of the model until the head and flux conditions simulated by the model agree, within acceptable limits, with observations in the real system. Parameter adjustment is an iterative process that can be accomplished either manually, by using a trial-and-error procedure, or automatically, by using regression techniques (Cooley and Naff, 1990). Parameters in the model constructed for this study were adjusted manually by systematically adjusting parameters, making simulations, and comparing simulated with observed ground-water levels and flow conditions. Approximately 70 model simulations were made in which horizontal hydraulic conductivity and vertical anisotropy ratios were modified from the original estimates. Streambed, riverbed, and drain-conductance values also were recomputed whenever values of horizontal and vertical hydraulic conductivity were modified. Recharge, rates of storage change, and well pumping rates were not modified during the calibration process.

Transmissivity, the product of horizontal hydraulic conductivity and saturated thickness, was read directly by MODFLOW after being computed externally. Only horizontal hydraulic conductivity values were varied during the calibration process; saturated thickness was held constant. Transmissivity also was assumed to remain constant within each simulation and did not change as a function of saturated thickness.

Parameter Sensitivity

A sensitivity analysis of the model was made in order to determine the relative sensitivity of model simulated heads and fluxes to uncertainty in hydraulic characteristics and boundary conditions. The relative sensitivities of these parameters were used as a guide to calibration of the model and later to help determine which types of data would be most useful to improve the ability of the model to simulate the ground-water flow system and thus should have priority for future collection.

The analysis was performed on the uncalibrated model with initial estimates of hydraulic characteristics and initial boundary conditions as a base condition. Individual parameters were changed and effects of the changes on model results were calculated after each simulation. The parameters that were changed included horizontal hydraulic conductivity (*Kh*), vertical hydraulic conductivity (*Kv*), streambed and riverbed conductance, recharge, and boundary conditions.

Although the eastern edge of the modeled area is a no-flow boundary in the calibrated model, this boundary was simulated as a specified-head boundary during the initial stages of model development and during the sensitivity analysis. Most of this boundary coincides with the surface contact between low-permeability older rocks (Skamania Volcanics) and basin-fill sediments; the remaining part follows the eastern extent of the more permeable part of the Troutdale gravel aquifer. Later in the calibration process, this boundary condition was changed to the no-flow condition described in the section on boundary conditions. The justification supporting this change is discussed later in the report.

The sensitivity of the model to parameter changes was measured by using the root-mean square (RMS) of the difference in simulated heads. RMS values were calculated for the entire model and for each hydrogeologic unit so that the relative sensitivities of units could be compared.

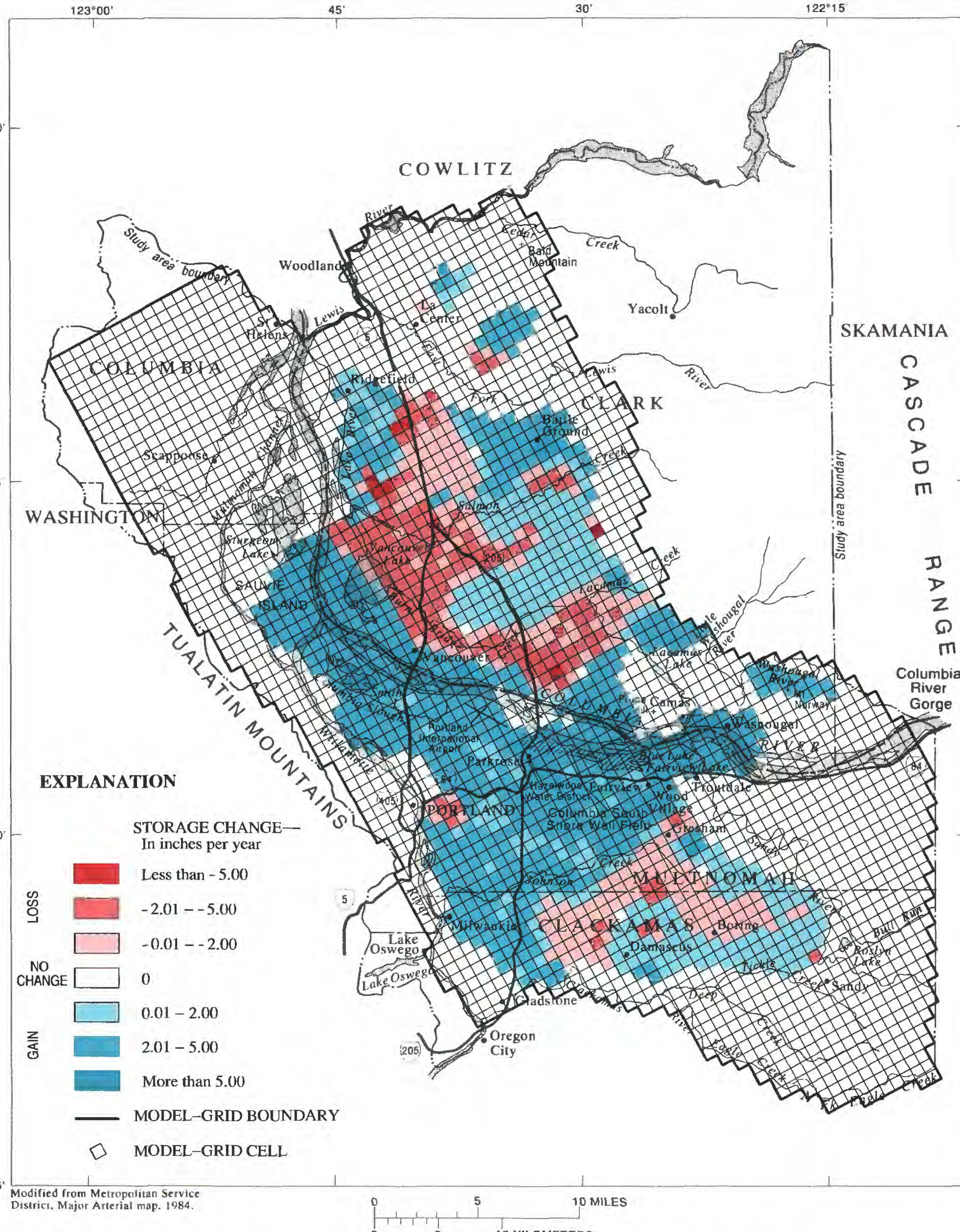

Figure 7. Estimated change in storage in unconfined parts of the ground-water flow system, 1987–88.

Horizontal Hydraulic Conductivity

Sixteen simulations were made, using four multipliers (0.01, 0.1, 10, and 100) to modify the horizontal hydraulic conductivity values in the four primary aquifer units (unconsolidated sedimentary aquifer, Troutdale gravel aquifer, Troutdale sandstone aquifer, and upper subunit of the sand and gravel aquifer). The results of these simulations, showing the sensitivity of simulated water levels to changes in horizontal hydraulic conductivity of the primary aquifer units, are shown in figure 8. The term "cumulative RMS," which is used to compare the sensitivities of units in the following discussion, is the sum of the RMS values for each of the four simulations for an individual unit.

The sensitivity of simulated water levels to changes in the horizontal hydraulic conductivity of the unconsolidated sedimentary aquifer was low (cumulative RMS values less than 100) to moderate (cumulative RMS values of 100 to 200) (fig. 8). Increases to the already high values of horizontal hydraulic conductivity in the unit had less effect on water levels than did decreases, and units at depth were less affected than shallow units. Increasing hydraulic conductivity by a factor of 100 resulted in physically unreasonable values in some areas, and the model was unable to reach a solution. The low sensitivity of simulated water levels in other units to changes in the horizontal hydraulic conductivity of the unconsolidated sedimentary aquifer and the low sensitivity of simulated water levels in the unconsolidated sedimentary aquifer to changes in the horizontal hydraulic conductivity of other units (fig. 8) are explained by the high hydraulic conductivity of the unit and the control on water levels imposed by surface-water features (stream and river boundaries) within the unit.

Changes to the horizontal hydraulic conductivity of the Troutdale gravel aquifer produced the most significant and widespread effects of any of the variations in this parameter. Simulated water levels in most units had moderate, high (cumulative RMS values of 200–300), and very high (cumulative RMS values greater than 300) sensitivity to changes in the horizontal hydraulic conductivity of the Troutdale gravel aquifer; the exception being the unconsolidated sedimentary aquifer, which had low sensitivity (fig. 8). Decreasing the horizontal hydraulic conductivity of the unit by a factor of 0.01 produced some of the largest RMS values in the entire analysis, both within the Troutdale gravel aquifer itself and in the underlying undifferentiated fine-grained sediments. The dominant control that horizontal hydraulic conductivity of the Troutdale gravel aquifer has on ground-water flow in the basin is due to the unit's broad areal distribution and exposure to recharge, and to its high permeability.

The horizontal hydraulic conductivity of the Troutdale sandstone aquifer also exerts important controls on ground-water movement in the basin as evidenced by the high sensitivity of simulated water levels in the Troutdale gravel aquifer, confining unit 1, Troutdale sandstone aquifer, and confining unit 2 (fig. 8). Simulated water levels were also disproportionately more sensitive to increases in the horizontal hydraulic conductivity in the Troutdale sandstone aquifer than they were to decreases.

The sensitivity of simulated water levels to changes in hydraulic conductivity of the upper, coarse-grained subunit of the sand and gravel aquifer was low in all units except the underlying fine-grained subunit of the sand and gravel aquifer, which had moderate sensitivity, and the coarse-grained subunit itself, which had high sensitivity (fig. 8). The depth and limited areal extent of the unit restrict the influence that changes to horizontal hydraulic conductivity have on the overall flow system.

Vertical Hydraulic Conductivity

The vertical anisotropy ratio (*Kh*/*Kv*) was varied to determine the sensitivity of the model to vertical hydraulic conductivity. Initial estimates of vertical anisotropy ratio for the uncalibrated model were 1,000:1 for the older rocks and 100:1 for all other units. The multipliers used to change vertical anisotropy ratios were 0.1, 0.5, 5, and 10, yielding ratios ranging from 100:1 to 10,000:1 in the older rocks and from 10:1 to 1,000:1 in all other units. The sensitivity of simulated water levels was calculated for all of the hydrogeologic units; however, the vertical hydraulic conductivities of confining units 1 and 2 and the undifferentiated fine-grained sediments were varied together, whereas vertical hydraulic conductivities were varied separately for each of the other units. The results of these simulations are shown for the Troutdale gravel aquifer, Troutdale sandstone aquifer, confining units and undifferentiated sediments, and the lower, fine-grained subunit of the sand and gravel aquifer in figure 9.

Within the ranges tested, the sensitivities of simulated heads to changes in vertical hydraulic conductivity were low (cumulative RMS values rarely exceeding 50) compared with those calculated for changes in horizontal hydraulic conductivity.

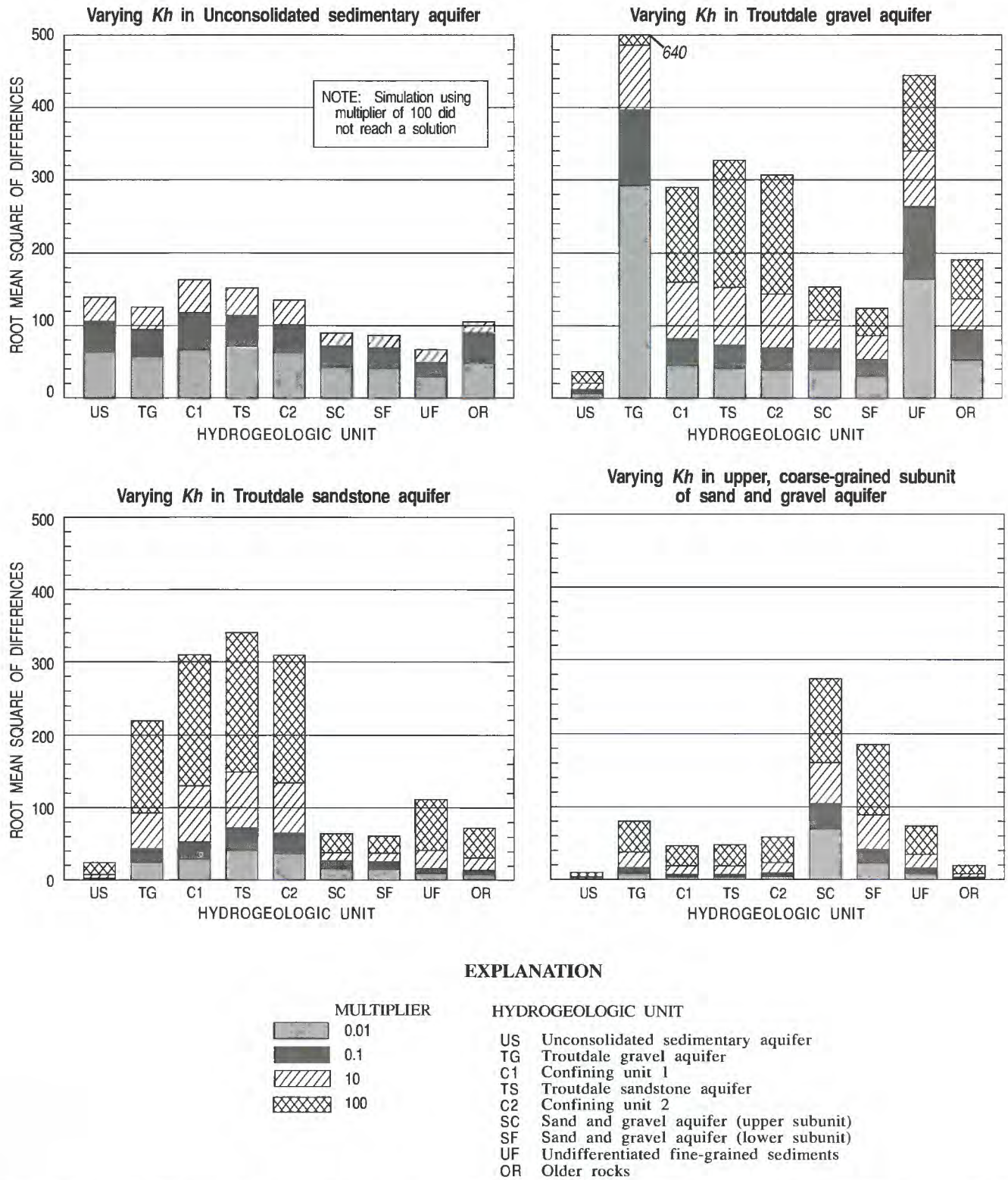

Figure 8. Sensitivity of simulated heads in different hydrogeologic units to variation in horizontal hydraulic conductivity in the unconsolidated sedimentary aquifer; Troutdale gravel aquifer; Troutdale sandstone aquifer; and upper, coarse-grained subunit of the sand and gravel aquifer.

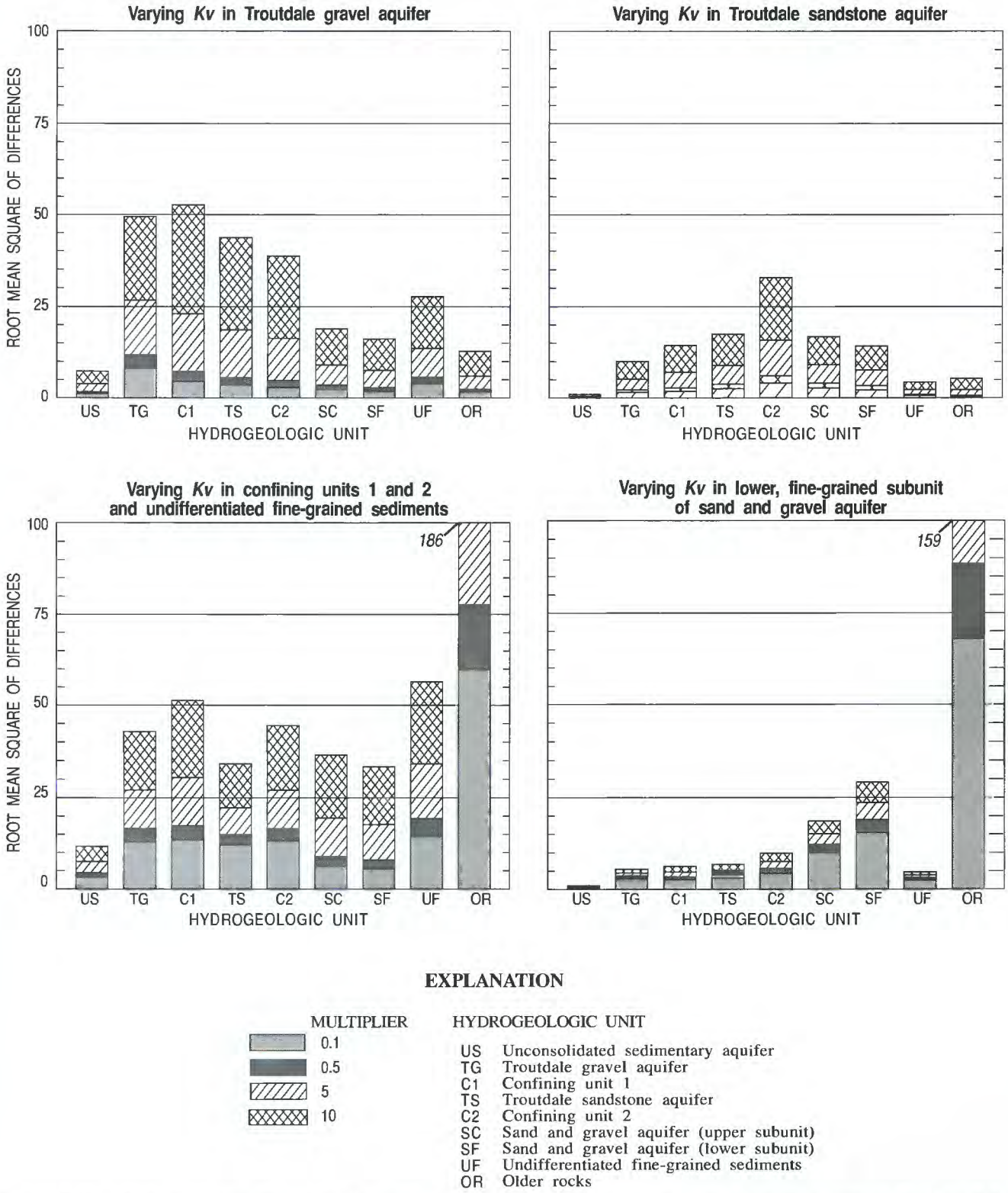

Figure 9. Sensitivity of simulated heads in different hydrogeologic units to variation in vertical anisotropy ratios in the Troutdale gravel aquifer; Troutdale sandstone aquifer; confining units 1 and 2 and undifferentiated fine-grained sediments; and lower, fine-grained subunit of the sand and gravel aquifer.

In the following discussion, the terms low, moderate, and high are used to describe the relative sensitivity of simulated water levels to changes in vertical hydraulic conductivity and correspond to cumulative RMS values of 0 to 25, 25 to 50, and greater than 50, respectively.

The sensitivity of simulated water levels to changes in the vertical hydraulic conductivity of the Troutdale gravel aquifer was high in the unit itself and in the underlying confining unit 1 (fig. 9). Moderate sensitivities were calculated for the Troutdale sandstone aquifer and undifferentiated fine-grained sediments, which also directly underlie the Troutdale gravel aquifer in some places, and confining unit 2, which underlies the Troutdale sandstone aquifer. Low sensitivity was calculated for the unconsolidated sedimentary aquifer due to the strong controls on water level imposed by surface-water features.

Decreasing the vertical hydraulic conductivity of the Troutdale sandstone aquifer had the greatest effect on simulated heads in confining unit 2 (fig. 9); this indicates that restricting the vertical conductance between the Troutdale sandstone and confining unit 2 requires much larger vertical head gradients between the two units in order to maintain the same net vertical flux. Nonetheless, sensitivity to changes in this parameter were comparatively low and showed a tendency to attenuate with vertical distance from the unit.

The vertical hydraulic conductivities of confining units 1 and 2 and the undifferentiated fine-grained sediments strongly influence water levels in nearly all units (fig. 9). Calculated sensitivities were moderate to high in all units except the unconsolidated sedimentary aquifer. This result can be attributed to the wide extent of these units and their relatively low vertical hydraulic conductivities. The extremely high cumulative RMS of the older rocks (186) resulted because that unit receives large quantities of recharge where it is exposed in the higher altitudes of the basin, and discharges by upward leakage in the lower parts of the basin, where it is overlain by the undifferentiated fine-grained sediments. Changes to the vertical hydraulic conductivity of the overlying unit in a discharge area greatly influence the water-level gradient required to maintain the same flux.

The effects of changes in the vertical hydraulic conductivity of the lower, fine-grained subunit of the sand and gravel aquifer were less pronounced for most units (fig. 9) because of the limited extent of the unit (Appendix A, fig. A–7). However, effects on water levels in the older rocks were again large (RMS of 159) and support the idea that water levels within discharge areas of the model are very sensitive to changes in vertical hydraulic conductivity within discharge areas.

Recharge

The sensitivity of simulated heads to changes in recharge rate was determined by multiplying each of the three components of total recharge (infiltration of precipitation, runoff into drywells, and on-site waste-disposal systems) by a constant for each sensitivity simulation. The RMS differences for the drywell and on-site waste-disposal system recharge simulations were relatively low (less than 5 ft) because these are important sources in only a small part of the modeled area. This makes it difficult to compare the sensitivity of these parameters with the sensitivities of regionally distributed parameters. Snyder and others (1994) determined that drywells and on-site waste-disposal systems contribute a large part of the recharge to the ground-water system in highly urbanized, unsewered areas. In those areas, simulated heads were more sensitive to variations in recharge from these sources.

Recharge from infiltration of precipitation occurs over nearly the entire modeled area, and thus variation of this parameter provides a measure of model sensitivity that can be compared with sensitivities related to aquifer properties. In three simulations, recharge was decreased by 50 percent and increased by 50 and 100 percent, respectively. Changes in recharge of this magnitude had significant effects on simulated heads in all units except the unconsolidated sedimentary aquifer (fig. 10). These effects were notably greater in the shallower units through which most of the recharge moves before being discharged and in the lower permeability units where heads are more sensitive to flux.

Streambed and Riverbed Conductance

Streambed and riverbed conductance values were changed together because each was estimated using the assumption that the conductance of the bed was a function of the vertical hydraulic conductivity of the underlying hydrogeologic unit. Increases in conductance values had little effect on simulated heads (fig. 10), indicating that initial values were high enough to not limit the flux across these boundaries.

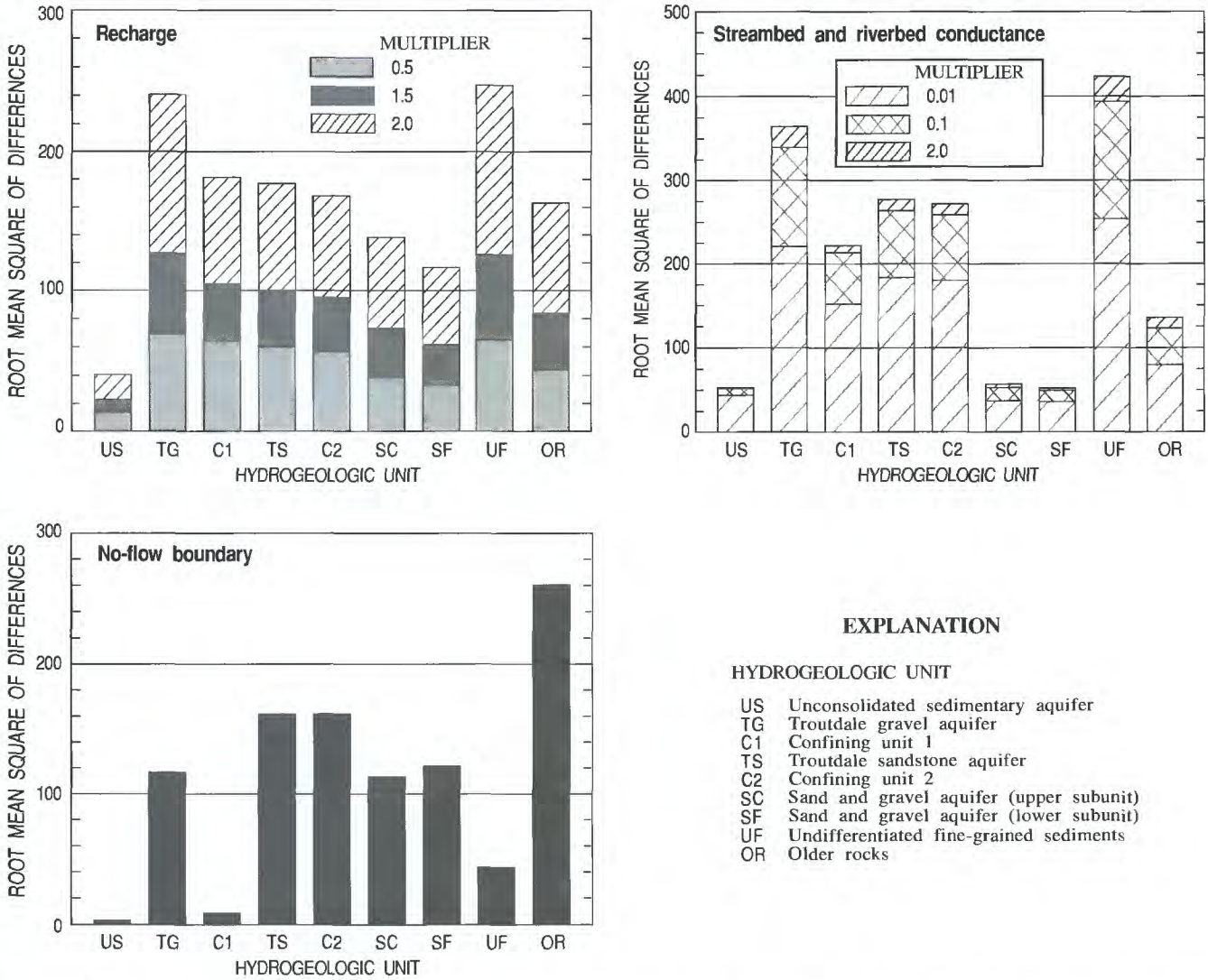

Figure 10. Sensitivity of simulated heads in different hydrogeologic units to variation in recharge from infiltration, variation in streambed and riverbed conductance, and conversion from constant-head to no-flow boundary condition on eastern edge of model.

Simulated heads did show sensitivity to reductions in conductance of one and two orders of magnitude. These conditions forced the model to produce larger head gradients near streams and rivers in order to generate the same discharge to these head-dependent flux boundaries.

Boundary Conditions

Model sensitivity to the boundary condition specified at the eastern edge of the model was evaluated by changing the boundary condition from specified-head to no-flow. Units that had specified-head cells had high RMS differences in this sensitivity simulation (fig. 10). There was much uncertainty in the values of the specified heads because there were few wells in the east boundary area to use for control; thus, large head differences between the specified-head and no-flow simulations do not necessarily indicate that use of a no-flow boundary resulted in a less accurate simulation of the ground-water flow system.

Parameter Adjustment

Initial estimates of hydraulic conductivity were adjusted during calibration in three significant ways: (1) distributions were smoothed within zones to reflect the average cell hydraulic conductivities rather than point values at wells, (2) hydraulic conductivity values of the unconsolidated sedimentary aquifer were

reduced by 85 percent modelwide, and (3) hydraulic conductivity values of the sedimentary units overlying a northwest-southeast trending anticline in Clark County were reduced. The distributions of hydraulic conductivity values obtained by calibration are shown on plates 3–8.

Statistical distributions of the calibrated hydraulic conductivity values in the model were compared with the estimates of hydraulic conductivity values at wells by hydrogeologic unit, as shown in figure 6. The estimates, based on well data, have ranges of three to five orders of magnitude within a hydrogeologic unit. Smoothing of the initial distributions and interpolation of the well data to the model grid resulted in narrowing the ranges of hydraulic conductivity distributions for most units to two to three orders of magnitude. This reduction is reasonable considering (1) that lithologies can vary widely within small areas in natural geologic environments and (2) that the model-cell values must represent the mean value for a very large volume of aquifer material compared to the volume represented by an individual well.

Initial estimates of the hydraulic conductivity of the unconsolidated sedimentary aquifer were biased toward high values by estimating them using well-test data. The aquifer units in the basin consist of heterogeneous sequences of coarse- and fine-grained sediment. Wells typically are screened in the most permeable parts of the unit; therefore, the hydraulic conductivity values estimated from these tests are not accurate estimates of the average hydraulic conductivity of the entire unit. Additionally, many of the wells for which test data were available were near the Columbia River and completed in permeable sands and gravels. The median of initial estimates of hydraulic conductivity in the unconsolidated sedimentary aquifer was 232 ft/d. Reduction of hydraulic conductivity in this unit resulted in more reasonable values with a median of 125 ft/d.

An especially difficult area for the model to simulate was southwestern Clark County. The difficulty stemmed from the sharp change in horizontal hydraulic gradient (fig. 2) that occurs along a northwest-southeast trending line extending from near Ridgefield to Prune Hill (McFarland and Morgan, 1996). Gradients along this trend average 50–100 ft/mi (feet per mile) in contrast to gradients of only 15–25 ft/mi to the northeast and southwest. The trend of this line is coincident with an anticline in the underlying older rocks (pl. 1). Swanson and others (1993) suggested that this deformation in the older rocks might have occurred after deposition of the younger sediments, thus displacing them upward in the section. If the younger sediments were deformed along the axis of this anticline, movement of ground water through this section could be along paths that are not parallel to the bedding planes and the principal axis of horizontal hydraulic conductivity. The effective hydraulic conductivity might lie between the horizontal and vertical values. On the basis of this concept, horizontal hydraulic conductivities of the younger sediments were decreased to one-half their initial values along a zone coincident with the anticlinal structure. This modification produced a much improved representation of the water-level distribution in this area. The effect of this modification on the median hydraulic conductivities of each unit were minor.

The general relations between the initial estimates of hydraulic conductivity values were preserved in the calibrated distributions (fig 6). As discussed above, the median hydraulic conductivity of the unconsolidated sedimentary aquifer unit was reduced from about 230 ft/d to about 125 ft/d. The median values of hydraulic conductivity of the Troutdale gravel aquifer, Troutdale sandstone aquifer, and upper, coarse-grained subunit of the sand and gravel aquifer increased slightly from precalibration values and remained the most permeable units, aside from the unconsolidated sedimentary aquifer. Hydraulic conductivity distributions are typically log-normally distributed (Domenico and Schwartz, 1990); thus, mean and median values can be quite different.

The vertical anisotropy ratio was initially estimated to be 1,000:1 in older rocks and 100:1 in all other units. This parameter was varied during calibration until a best fit was obtained between observed and simulated direction and magnitude of vertical hydraulic gradient. The vertical anisotropy ratios determined from calibration were 1,000:1 in the older rocks and all of the fine-grained units (confining units 1 and 2, the lower fine-grained subunit of the sand and gravel aquifer, and the undifferentiated fine-grained sediments). In the primary aquifer units (unconsolidated sedimentary aquifer, Troutdale gravel aquifer, Troutdale sandstone aquifer, and upper, coarse-grained subunit of the sand and gravel aquifer), which have significant interbedding, the initial ratio of 100:1 yielded the best results.

Boundary conditions on the eastern margin of the model also underwent modification during the calibration process. In the early conceptualization of the ground-water flow system, it was hypothesized that some quantity of subsurface inflow occurs from the older rocks to the sedimentary units along this boundary. The amount of inflow was uncertain, however, because of limited data on the hydraulic gradient in the older rocks and their hydraulic conductivity. A rough estimate of inflow was made using Darcy's law:

$$Q = -KhIA, \qquad (7)$$

where

Q is inflow ($L^3 T^{-1}$);

Kh is horizontal hydraulic conductivity (LT^{-1});

I is hydraulic gradient (dimensionless); and

A is the cross-sectional area of flow (L^2).

Assuming a hydraulic gradient of 100 ft/mi (0.02), a hydraulic conductivity of 1.0 ft/d (1.2×10^{-5} ft/s [feet per second]), and a 2,500-ft-thick flow section 50 miles long (6.6×10^8 ft^2), the inflow across the boundary would be:

$$Q = (1.2\times10^{-5})\ (0.02)\ (6.6\times10^8) = 160 \text{ ft}^3/\text{s}. \qquad (8)$$

This estimate is uncertain and is presented here only to indicate the potential magnitude of inflow.

Heads were initially specified in cells on the eastern boundary so that inflow across the boundary could be estimated using the model. This approach assumed that the values of the specified heads could be estimated accurately and that simulated heads in the interior of the model approximate observed heads. Estimating heads in the boundary cells proved to be very difficult because of the small number of wells in the remote, upland areas; available head data had to extrapolated horizontally to assign heads to all cells on the boundary and vertically to assign heads to cells in the underlying layers of the model.

During parameter adjustment, it was found that the model was insensitive to relatively large changes in some parameters. Numerical experiments by Franke and Reilly (1987) on the effects of boundary conditions on steady-state models show that specified-head boundaries can make models insensitive to the hydraulic characteristics of the ground-water flow system. This can lead to introduction of large errors in the hydraulic characteristics of the aquifer system if they are modified during model calibration when attempting to make simulated heads match observed heads.

A no-flow boundary condition was adopted on the eastern boundary because of the potentially small amount of inflow across the boundary (160 ft^3/s, which is approximately 10 percent of total recharge), the large uncertainty in estimating heads on the boundary, and the potential for introducing errors into the hydraulic characteristics through calibration.

Model Evaluation and Results

The ability of the model to simulate the ground-water flow system was evaluated by comparing simulated water levels and fluxes with measured water levels and fluxes.

Ground-Water Levels

Observed ground-water levels used for comparison with simulated water levels were from 412 wells completed in the four primary aquifer units in the basin (unconsolidated sedimentary aquifer, Troutdale gravel aquifer, Troutdale sandstone aquifer, and coarse-grained upper subunit of the sand and gravel aquifer). Spring 1988 water levels were used as an approximation of the mean water levels for the calibration period. The validity of using spring 1988 water levels for comparison with simulated mean water levels was checked by comparing annual mean water levels (1987–88) and spring 1988 water levels from the 156 observation wells in the basin that were measured bimonthly between spring 1987 and 1988 (McCarthy and Anderson, 1990). It was found that the mean difference between annual mean and spring 1988 water levels was only 0.4 ft. Most observation wells were screened in only one hydrogeologic unit. Because observation wells were rarely located at the center of a model cell (where the simulated water level is most applicable), the model-simulated water level at each observation well was estimated by interpolation from the simulated water levels in the four adjacent model cells. The goodness of fit between observed and simulated water levels was statistically summarized for each calibration run by computing the RMS of the difference between observed and simulated water levels for each of the four primary aquifer units.

The simulated water level at each cell represents the water level at the center of the cell. Some model cells represent thick sequences of the ground-water flow system in which there are vertical hydraulic

gradients. Observation wells are commonly water-supply wells and are open to only a part of the hydrogeologic unit; water levels from these wells do not represent the average water level in the unit. Although vertical interpolation of simulated water levels is possible, it was not done in this analysis because of the small number of wells where it would have been appropriate.

The general directions of ground-water movement and magnitude of horizontal hydraulic gradients simulated within the unconsolidated sedimentary aquifer (pl. 3) agreed well with observed water levels. The most notable exception to this agreement was in a 15 mi^2 area of Clark County south of Salmon Creek and north of Burnt Bridge Creek in the northwest part of T.2N., R.2E. and the northeast part of T.2N., R.1E., where anomalously high heads occur in the unconsolidated sedimentary aquifer (McFarland and Morgan, 1996, pl. 5). Observed water levels in wells in this area are at 200–250 ft above sea level, which is 50–100 ft higher than the regional water table in the area. McFarland and Morgan (1996) suggested that the apparent "mound" in the water table might be caused by high recharge rates from drywells and on-site waste-disposal systems or low permeability sediments within the unconsolidated sedimentary aquifer that impede downward leakage in this area. Snyder and others (1994) estimate recharge from drywells in the area of about 7–9 in/yr, recharge from on-site waste-disposal systems of 1–2 in/yr, and total recharge of about 18–22 in/yr; the total recharge rates are slightly more than in the surrounding area, but are not high enough to explain such a localized anomaly.

Well logs from the area describe beds of "clay" and "sandy clay" within the unconsolidated sedimentary aquifer, and in Mundorff's (1964) description of ground-water occurrences in the area, he reported that these low-permeability beds trap recharge in perched aquifers above the regional water table. It is likely that the water-level anomaly in the area is not a recharge-induced mound, but is a perched aquifer or zone of high downward vertical head gradient caused by low-permeability beds within the unconsolidated sedimentary aquifer. Further evidence that the head anomaly in the unconsolidated sedimentary aquifer does not represent a mound in the regional water table is offered by the fact that there is no similar feature in the underlying Troutdale gravel aquifer.

The heads simulated by the regional model represent the average head within the unconsolidated sedimentary aquifer. The difference between simulated and observed heads in the unconsolidated sedimentary aquifer was less than 30 ft at 86 percent of the 63 observation wells used for comparison (fig. 11). The RMS difference for the unit was 54 ft and the mean error was 11 ft. All of the observation wells used by McFarland and Morgan (1996) to construct head maps for the primary aquifers were used to compute differences of simulated and observed head presented in figures 11. A small group of differences for the unconsolidated sedimentary aquifer shown in figure 11 fall in the 110 to 210 ft range; these differences are for wells in the area where the existence of large vertical gradients or perched zones within the unconsolidated sedimentary aquifer are hypothesized. The observations from these wells were retained in the group used for comparison with model results in order to maintain consistency between this and previous reports (McFarland and Morgan, 1996; Swanson and others, 1993).

Ground-water movement within the Troutdale gravel aquifer, as indicated from the simulated water-level contours on plate 4, is generally from the major recharge areas in the upper Sandy and Clackamas River Basins in the southeast and the western slope of the Cascade Range in Clark County toward the principal discharge areas in the basin. East of the Sandy River, ground water moves to the west and northwest toward the Sandy River canyon and north toward the Columbia River. From upland recharge areas southeast of Sandy, movement is generally to the northwest; however, flowlines diverge as they move downgradient toward the lower Clackamas, Willamette, Columbia, and Sandy Rivers. In Clark County, ground-water movement is strongly influenced by streams and rivers such as Salmon Creek and the East Fork Lewis River. Simulated flow directions and gradients (pl. 4) agree well with those mapped by McFarland and Morgan (1996, pl. 3).

In the Troutdale gravel aquifer, simulated heads were within 30 ft of observed heads at 52 percent of the 243 wells and within 50 ft at 73 percent of the observation wells (fig. 11). The RMS difference for the unit was 63 ft and the mean difference was –3.3 ft. The largest head differences in the Troutdale gravel aquifer were for observation wells located in the southern part of the study area at altitudes above 500 ft. Many of the wells with large differences are completed in the Boring Lava, an intrusive basalt included in the Troutdale gravel aquifer (McFarland and Morgan, 1996).

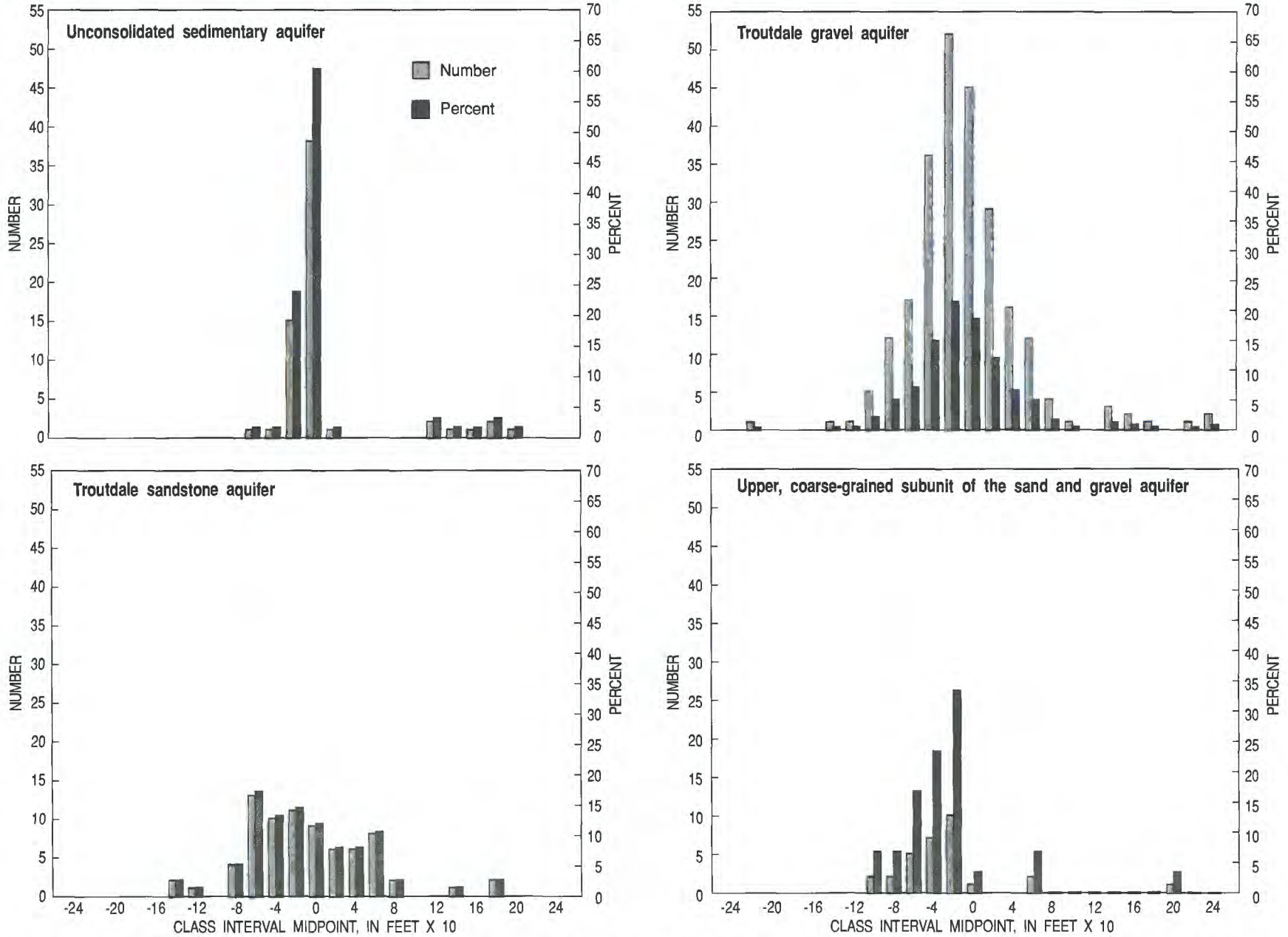

Figure 11. Frequency of the difference between observed and simulated water levels at selected observation wells in the unconsolidated sedimentary aquifer; Troutdale gravel aquifer; Troutdale sandstone aquifer; and upper, coarse-grained subunit of the sand and gravel aquifer.

According to Hogenson and Foxworthy (1965), the regional water table lies below the base of most of the Boring Lava, and any saturated zones within it are perched above old soil horizons or dense, low-permeability flow centers.

The Troutdale sandstone aquifer receives most of its recharge by downward leakage from the Troutdale gravel aquifer through confining unit 1; the principal recharge areas for the Troutdale gravel aquifer are along its updip edge between Camas and Battle Ground in Clark County, in the western Cascade Range east of the Sandy River, and in the upper Sandy and Clackamas River drainages near Sandy. Movement through the unit is northwestward from Sandy, with flow diverging downgradient westward toward the Willamette River and northward toward the Columbia River. Simulated water-level contours on plate 5, from which horizontal directions of flow can be inferred, indicate that much of the discharge from the Troutdale sandstone aquifer is by horizontal flow into the unconsolidated sedimentary aquifer above Blue Lake, where the Columbia River has truncated the Troutdale sandstone aquifer (pl. 1), and by upward flow into the unconsolidated sedimentary aquifer between Blue Lake and Portland International Airport, where the Troutdale sandstone aquifer is continuous beneath the Columbia River. There were 76 wells in the Troutdale sandstone aquifer for which observed heads were available for comparison with simulated heads. Thirty-four percent of the head differences in the Troutdale sandstone aquifer were less than 30 ft, 55 percent were less than 50 ft, and 83 percent were less than 70 ft (fig. 11). The RMS difference for the unit was 74 ft and the mean difference was –2.8 ft.

Observed head data were available from 30 wells in the upper, coarse-grained subunit of the sand and gravel aquifer for comparison with simulated heads (pl. 6). Of the differences between simulated and observed heads, 37 percent were less than 30 ft, 60 percent were less than 50 ft, and 84 percent were less than 70 ft; the RMS difference for the unit was 61 ft and the mean difference was –27 ft (fig. 11).

The RMS and mean differences for the older rocks were 138 and 31 ft for 50 observation wells. The undifferentiated fine-grained sediments had RMS and mean differences of 92 and –46 for 50 observation wells.

Vertical Head Gradients

Vertical gradients in simulated heads showed the presence of local and regional ground-water flow systems in the basin. Local ground-water flow systems generally coincide with small surface-water drainages, where recharge occurs in the upland parts of the drainage, moves through the upper 100–200 ft of the saturated sediments, and is discharged to small streams, seepage faces, or springs at low altitudes in the drainage. The extent of these local ground-water flow systems within the simulated ground-water flow system of the basin was analyzed by computing the vertical water-level gradient between the water-table unit (model layer 1) and the underlying unit (model layer 2). The resulting gradients were used to create a map in which each model cell was shaded according to the direction and magnitude of the simulated vertical head gradient in the shallow part of the system. The relation of ground-water discharge areas to surface-water drainages can readily be seen from the patterns of upward flow (fig. 12).

The extent of the regional ground-water flow systems and the discharge areas for these systems was analyzed by computing the vertical water-level gradient between the water-table unit (model layer 1) and deeper units (model layer 5). The shaded model-cell map in figure 13, which was created using the simulated vertical gradients, shows the location of recharge and discharge areas for the regional ground-water flow system. Comparison of figures 12 and 13 reveals several important features of the ground-water flow system: (1) compared with regional ground-water flow systems, local systems are smaller and more dispersed within the basin, (2) local systems are controlled by local topography and have shorter flow paths from recharge areas to discharge areas than do regional systems, (3) regional systems are broad and the boundaries between their recharge and discharge areas are well defined, and (4) regional discharge areas are controlled by major drainages in the basin, such as the Columbia, Willamette, Lewis, Clackamas, Sandy, and East Fork Lewis Rivers.

Discharge areas for local ground-water flow systems may overlie recharge areas for regional systems, as they do in the upper parts of the Lacamas, Deep, and Tickle Creek Basins (figs. 12 and 13). In the lower parts of the regional ground-water flow system, downward gradients often occur in the shallow part of the system and upward gradients in the deeper system, with gradient reversals occurring in the intermediate zone. In some areas, such as the northern half of T.1N., R.2E. and southern one-half of T.2N., R.2E., high downward gradients exist between the shallow aquifers overlying deeper aquifers that have upward gradients.

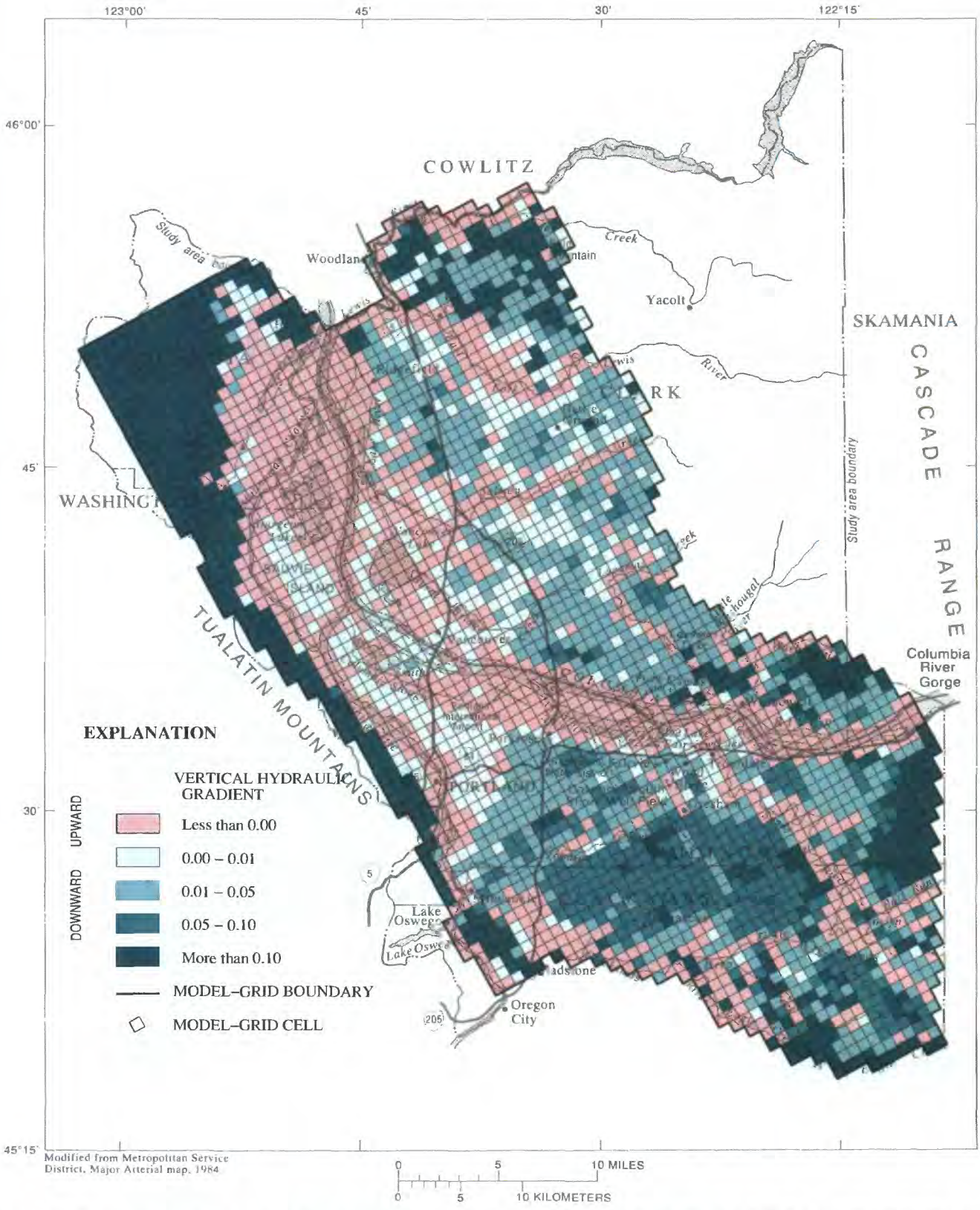

Figure 12. Distribution and extent of shallow, local ground-water flow systems as indicated by simulated vertical head gradients between the water table and underlying unit.

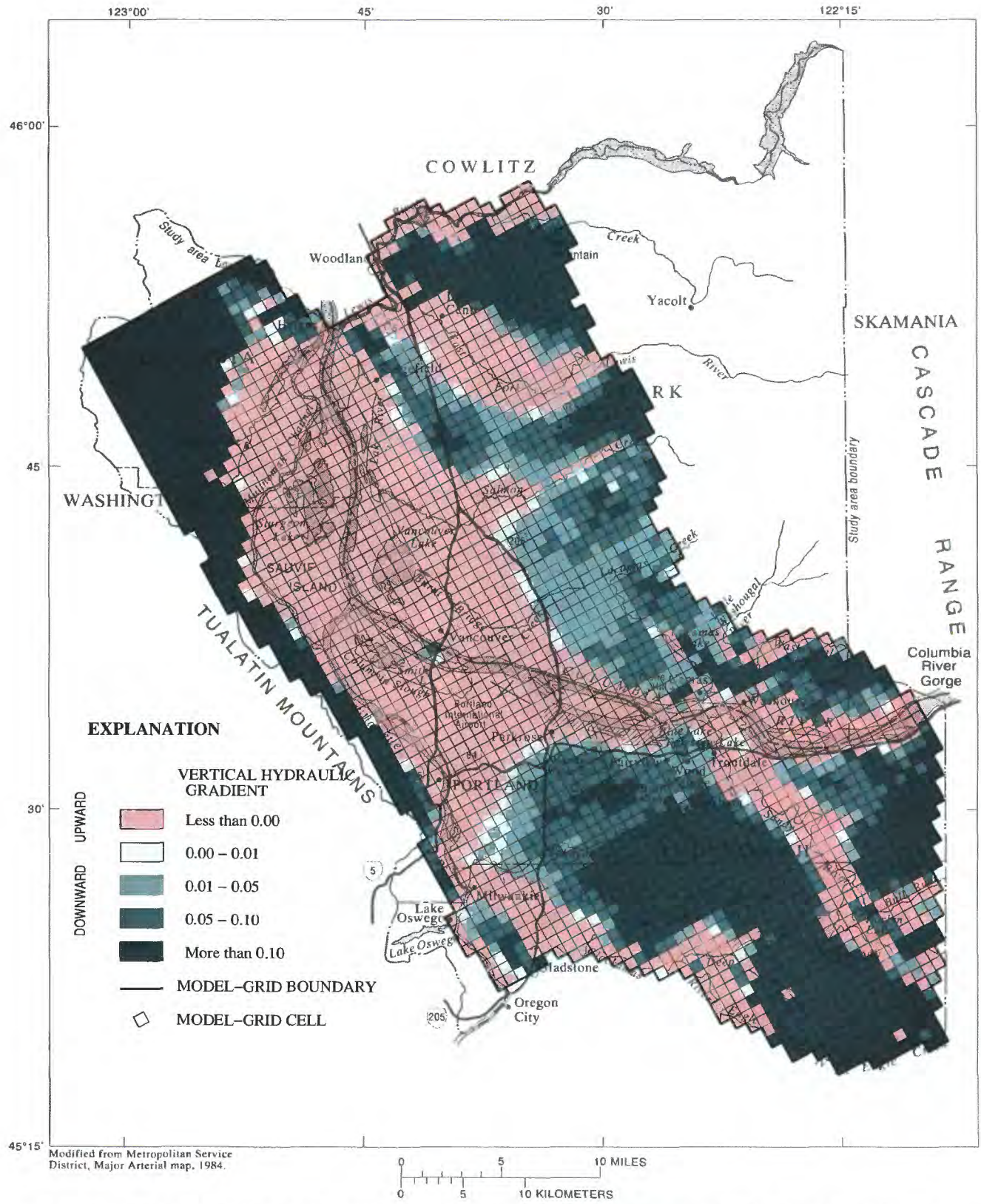

Figure 13. Distribution and extent of deep, regional ground-water flow systems as indicated by simulated vertical head gradients between the water table and deeper units.

These conditions probably result from either high recharge rates to the water table from drywells and on-site waste-disposal systems, or reductions in head in the Troutdale gravel aquifer caused by pumping.

Simulated flux rates from head-dependent flux boundaries (fig. 14) are closely related to the vertical head gradients discussed. Most cells specified as head-dependent flux boundaries, including rivers, streams, and springs, are discharge points in the ground-water system. Independent estimates of ground-water discharge to the Columbia and Willamette Rivers are not available for comparison with simulated ground-water discharge rates to river cells; however, the direction (discharge in most areas) and magnitude (1–2 ft^3/s) of the simulated discharge rates agree with the conceptual model of the system. Recharge to the ground-water system was simulated at head-dependent boundary cells in the headwater areas of some streams and upper reaches of streams that have headwaters outside the model area; although conceptually reasonable, there were few seepage measurements available to verify the simulated flux rates in these areas. Recharge to the shallow aquifers that underlie the Columbia River south of Vancouver Lake also was simulated by the model, indicating that pumping in this area has reversed natural gradients near the river. Additional water-level and chemical data, such as stable isotope concentration, from wells adjacent to the river would be needed to verify this hypothesis.

Discharge to Streams

Estimates of mean stream leakage and discharge rates at selected reaches were used for comparison with simulated leakage and discharge to provide another indicator of the model's ability to simulate the real ground-water flow system. Simulated stream leakage rates represent the mean flux between the stream and the ground-water system during the April 1987 to March 1988 calibration period. Stream discharge simulated by the model represents the mean ground-water contribution to streamflow (base flow) during the 1987–88 calibration period.

Low-flow discharge was measured at 126 sites (pl. 1) on 24 streams and tributaries in September of 1988 (McFarland and Morgan, 1996) and used to estimate mean base flow by assuming a relation between the observed discharge and mean base-flow discharge. Mean base-flow estimates made by hydrograph separation for Cedar and Salmon Creeks in Washington and Johnson Creek in Oregon were compared with low-flow measurements made during September 1988. September 1988 discharges on the three streams equaled 19, 23, and 27 percent of mean base-flow estimates for Johnson, Cedar, and Salmon Creeks, respectively. Despite the wide range of basin characteristics for the three streams, their respective base-flow to low-flow ratios agreed reasonably well. Mean base flow and stream leakage for the 1987–88 period were estimated by assuming the observed low flow was 25 percent of the mean base flow at each of the measurement sites; estimates are listed in Appendix C.

Simulated stream leakage rates were compared with estimated mean leakage rates at 67 sites in the basin (fig. 15; Appendix C). Ground-water discharge occurs at most measurement sites (streams are gaining) and the model simulated this condition well in most parts of the basin. Stream leakage estimates have uncertainties that are proportionate to the discharge of the stream. Leakage estimates on high discharge streams, such as the Sandy River, have large uncertainties because the discharge measurements from which they were estimated have uncertainties of approximately 5 percent. Simulated leakage rates shown in figure 15 lie within the uncertainty range of the estimated leakage rates at 37 (55 percent) of the 67 measurement sites.

Simulated base flow was compared with estimated 1987–88 mean base flow at 126 sites (fig. 16; Appendix C). Low-flow measurements from September 1988 also were used for comparison with model results, but were considered an estimate of the minimum ground-water contribution to streamflow. On streams that have headwaters outside the model boundaries, such as the East Fork Lewis, Sandy, and Bull Run Rivers, the estimated mean base flow was specified at the first stream reach inside the model. Estimated and simulated discharge at all stream reaches where low-flow measurements were made is shown in figure 16. Agreement between the simulated discharge and estimated discharge was generally good. For example, discharge measurements for September 1988 and estimated mean base-flow discharge were compared with simulated base-flow discharge at several sites on Salmon and Tickle Creeks (fig. 17). Simulated base-flow discharge on both creeks closely approximated estimates of 1987–88 base flow.

Water Budgets

The overall 1987–88 water-budget for the model is summarized in table 2. Several components of the budget were specified-flux boundaries to the model.

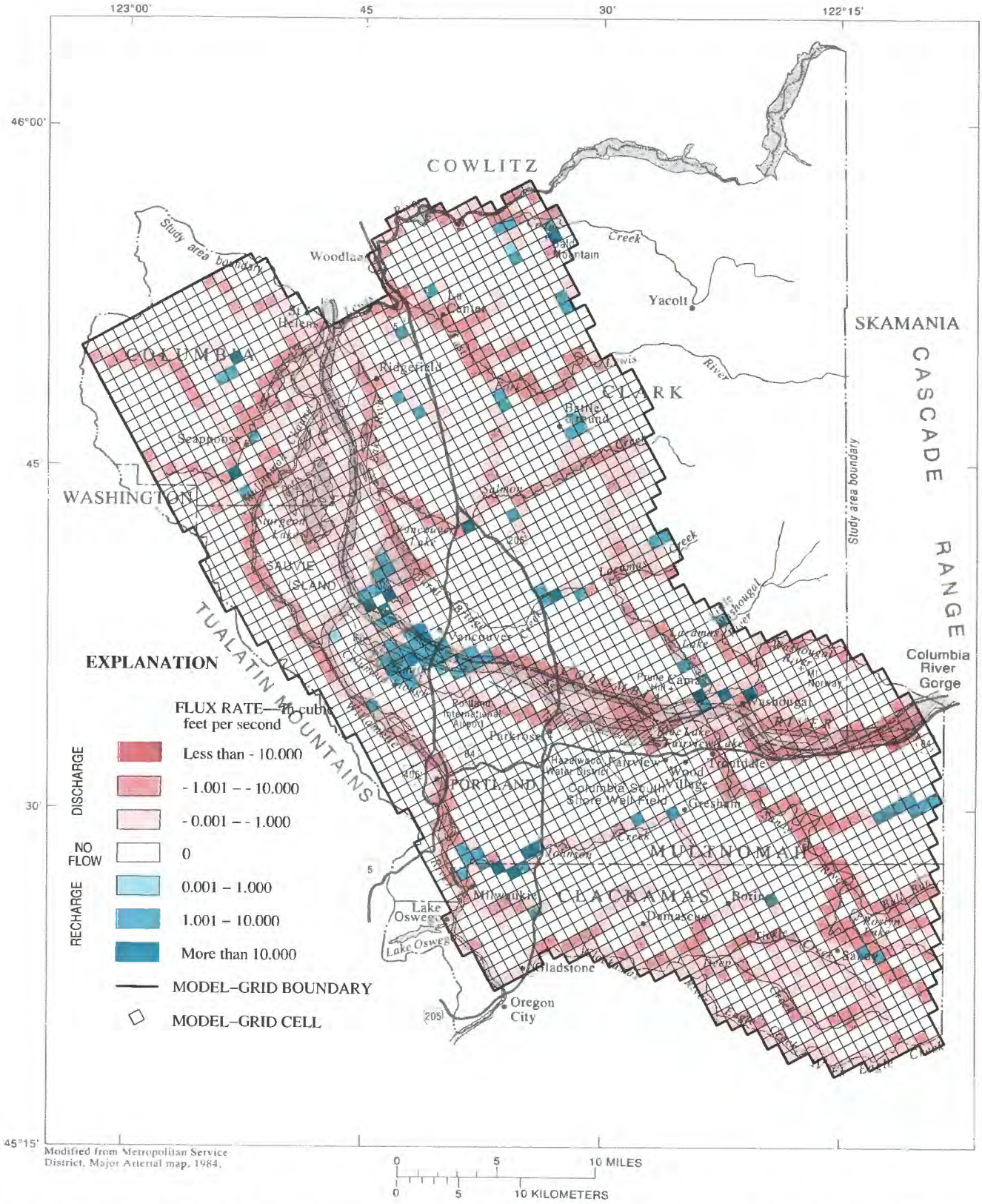

Figure 14. Simulated flux rates at head-dependent flux boundaries (rivers, streams, and springs), 1987–88. (Negative values indicate ground-water discharge.)

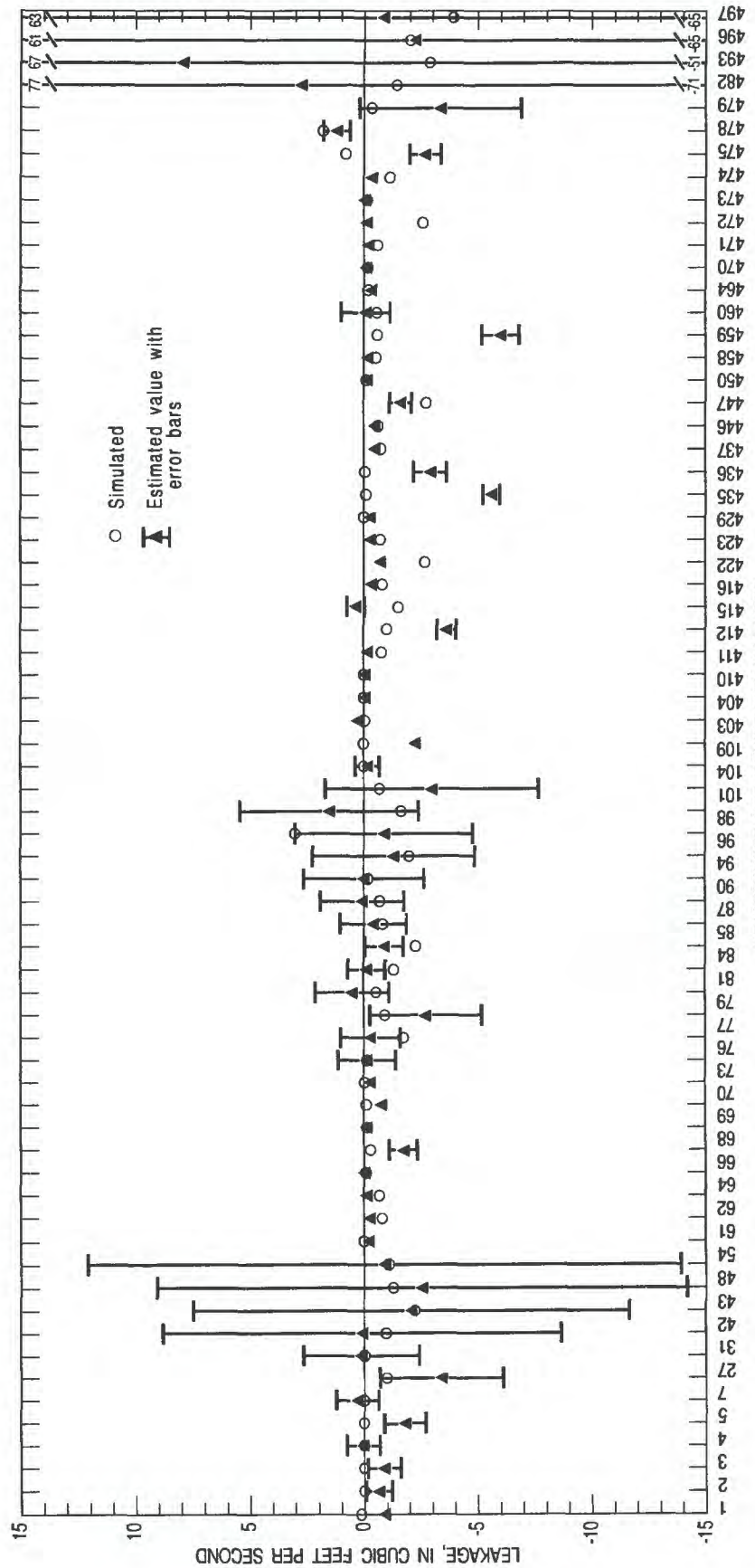

Figure 15. Simulated and estimated stream leakage at measurement sites. (Locations of sites are shown on plate 1.)

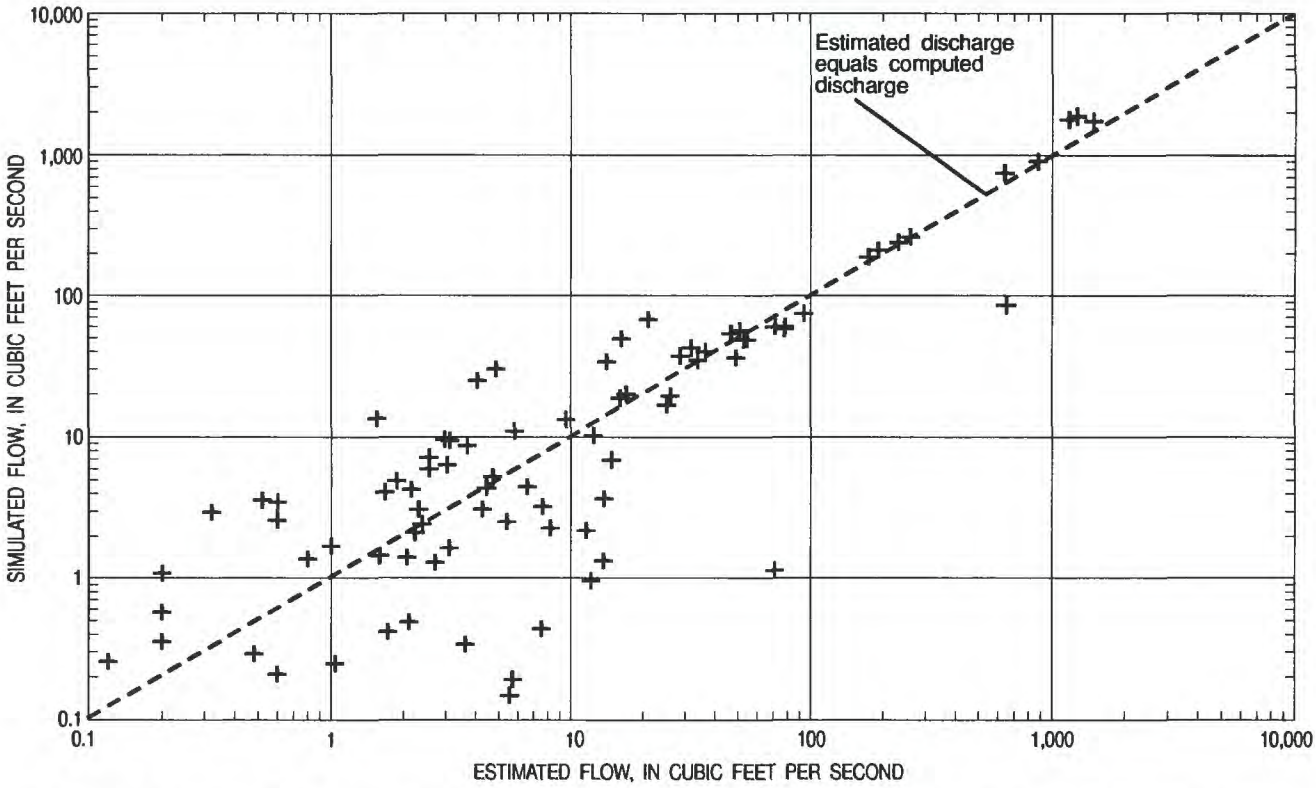

Figure 16. Simulated and estimated mean base flow at measurement sites. (Locations of sites are shown on plate 1.)

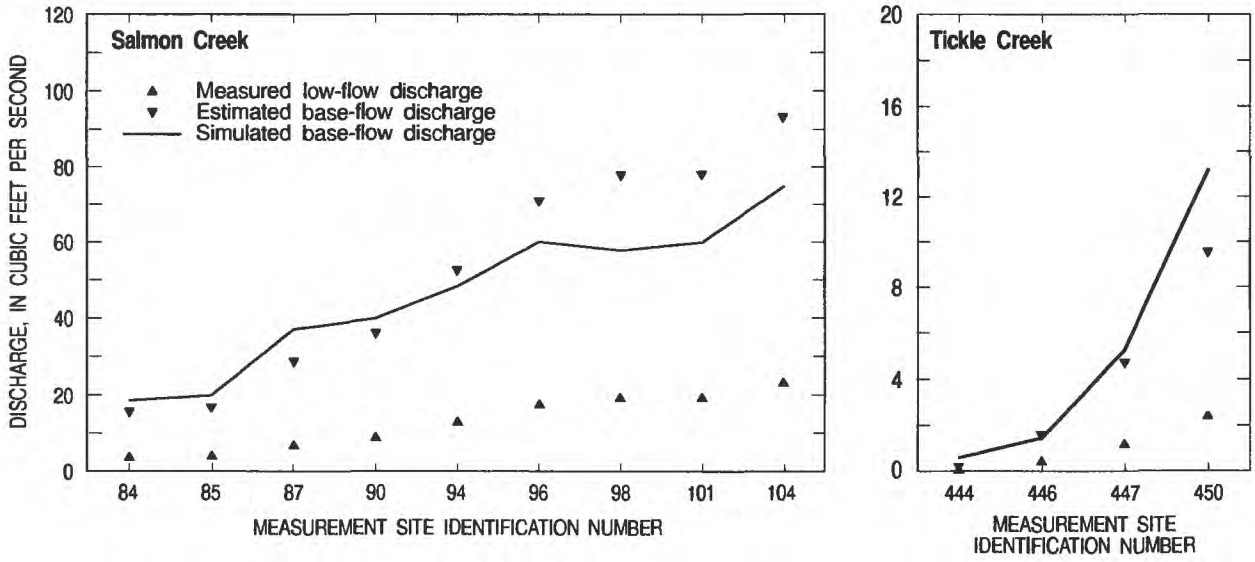

Figure 17. Simulated mean base-flow discharge and estimated discharge at measurement sites on Salmon Creek and Tickle Creek.

Table 2. Ground-water budgets for the Portland Basin, under predevelopment, 1987–88, and hypothetical conditions
[*, budget items simulated by model]

Budget items	Rate (in cubic feet per second)		
	Predevelopment	1987–88	Hypothetical conditions
Inflow			
Infiltration of precipitation	1,710	1,440	1,440
Drywells	0	62	62
On-site waste-disposal systems	0	27	27
*Seepage from rivers	1	36	62
*Seepage from streams	48	88	87
Storage change (decrease)	0	16	0
Total	1,760	1,670	1,679
Outflow			
Well discharge	0	166	258
*Seepage to rivers	606	457	443
*Seepage to streams	1,150	971	972
*Spring discharge	7	6	6
Storage change (increase)	0	70	0
Total	1,760	1,670	1,679

These items included recharge from infiltration of precipitation, drywells, and on-site waste-disposal systems; compensation for estimated changes in storage during the 1987–88 calibration period; and discharge by wells. The components of the budget calculated by the model as head-dependent boundary fluxes included seepage to and from rivers, seepage to and from streams, and spring discharge. Regionally, infiltration of precipitation (1,440 ft^3/s) was by far the most important source of recharge to the system; locally, recharge from drywells (62 ft^3/s) and on-site waste-disposal systems (27 ft^3/s) comprised a large part of recharge to shallow aquifers (Snyder and others, 1994). The storage changes listed as inflow and outflow items in table 2 offset estimated losses and gains in storage in the unconfined aquifers during the calibration period.

The total simulated discharge to streams of 971 ft^3/s (table 2) includes all streams and small rivers simulated with the STREAM package (Prudic, 1989), as described in the section on boundary conditions. The next largest outflow from the system was discharged to rivers (457 ft^3/s); most of this total discharged to the Columbia River; however, seepage to the Willamette River, Multnomah Channel, Vancouver Lake, Sturgeon Lake, and other surface-water bodies also occurred. Well discharge accounted for 166 ft^3/s of total outflow, spring discharge 6 ft^3/s, and storage change about 70 ft^3/s.

In order to develop a more complete understanding of the ground-water flow system represented by the model, information from the model was used to prepare a table of fluxes between hydrogeologic units (table 3) and individual water budgets for each of the units (table 4). The principal components of flux to and from the units are shown diagrammatically in figure 18.

The primary inflows to the unconsolidated sedimentary aquifer (US) are areal recharge (341 ft^3/s) and ground-water flux from the Troutdale gravel aquifer (277 ft^3/s) and older rocks (113 ft^3/s). A large part of the areal recharge to the unconsolidated sedimentary aquifer is from drywells (62 ft^3/s) and on-site waste-disposal systems (27 ft^3/s). Flux from the Troutdale gravel aquifer occurs horizontally along the upgradient contact between the two units and vertically by upward leakage in discharge areas near major rivers and streams. Ground-water movement from the older rocks to the unconsolidated sedimentary aquifer takes place where the younger sediments abut the older rocks at the margins of the basin; much of this flux occurs along the base of the Tualatin Mountains. Outflow from the unconsolidated sedimentary aquifer is chiefly to the Columbia and Willamette Rivers (416 ft^3/s) and to other rivers and streams (290 ft^3/s).

Table 3. Simulated horizontal and vertical fluxes between hydrogeologic units in the Portland Basin, 1987–88

[Values are in units of cubic feet per second. To read fluxes from a unit, read vertically down columns; to read fluxes to a unit, read horizontally along rows. US, unconsolidated sedimentary aquifer; TG, Troutdale gravel aquifer; C1, confining unit 1; TS, Troutdale sandstone aquifer; C2, confining unit 2; UF, undifferentiated fine-grained sediments; SC, sand and gravel aquifer, upper coarse-grained subunit; SF, sand and gravel aquifer, lower fine-grained subunit; OR, older rocks]

		Outflow from unit									
	Hydrogeologic unit	US	TG	C1	TS	C2	UF	SC	SF	OR	Total inflow
Inflow to unit	US	--	277	4	53	7	60	38	0	113	552
	TG	150	--	10	27	0	105	3	0	67	362
	C1	0	66	--	13	0	4	0	0	0	83
	TS	5	129	63	--	19	11	0	0	4	231
	C2	0	1	0	60	--	23	11	0	3	98
	UF	13	158	6	19	25	--	3	1	43	268
	SC	1	10	0	1	17	10	--	23	2	64
	SF	0	0	0	0	10	1	10	--	8	29
	OR	2	15	0	6	18	20	2	3	--	66
Total outflow		171	656	83	179	96	234	67	27	240	1,753
Total inflow minus total outflow		381	–294	0	52	2	34	–3	2	–174	0

Table 4. Simulated water budgets for hydrogeologic units, 1987–88

[All values are in cubic feet per second. Total inflow that does not equal total outflow is because of minor mass balance errors in the model. US, unconsolidated sedimentary aquifer; TG, Troutdale gravel aquifer; C1, confining unit 1; TS, Troutdale sandstone aquifer; C2, confining unit 2; UF, undifferentiated fine-grained sediments; SC, sand and gravel aquifer, upper coarse-grained subunit; SF, sand and gravel aquifer, lower fine-grained subunit; OR, older rocks; GW, ground water (from table 3); RIV, rivers; RCH, areal recharge (includes infiltration of precipitation, drywells, on-site waste-disposal systems, and change in storage); STR, streams; DRN, drains (springs); WEL, well discharge]

Hydrologic unit	Inflow					Outflow						
	GW	RIV	RCH	STR	Total	GW	RIV	RCH	STR	DRN	WEL	Total
US	552	35	341	58	986	171	416	7	290	6	96	986
TG	362	1	743	8	1,114	656	22	0	391	0	44	1,113
C1	83	0	0	0	83	83	0	0	0	0	1	84
TS	231	0	35	0	266	179	6	0	68	0	12	265
C2	98	0	1	0	99	96	0	0	2	0	1	99
UF	268	0	75	0	343	234	0	0	105	0	4	343
SC	64	0	10	0	74	67	0	0	5	0	3	75
SF	29	0	0	0	29	27	0	0	0	0	2	29
OR	66	0	278	0	344	240	13	0	89	0	3	345
Total	1,753	36	1,483	[1]66	3,338	1,753	457	7	[1]950	6	166	3,339

[1] Totals do not equal those in table 2 for seepage to and from streams, because of the method used to compute the budget totals by hydrogeologic unit. See Harbaugh (1990, p. 3) for a detailed discussion. Net flux (inflow minus outflow) is the same in tables 2 and 4.

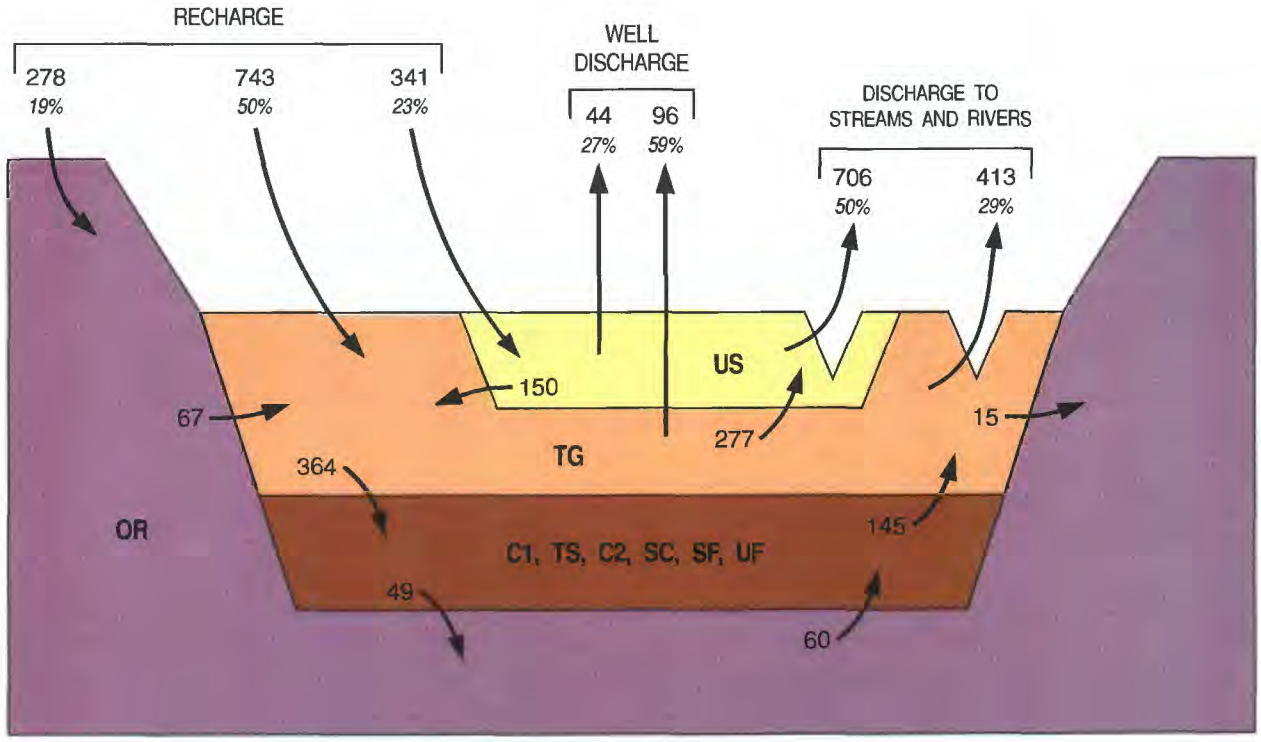

EXPLANATION

Hydrogeologic unit

US	Unconsolidated sedimentary aquifer	**SC**	Sand and gravel aquifer (upper subunit)
TG	Troutdale gravel aquifer	**SF**	Sand and gravel aquifer (lower subunit)
C1	Confining unit 1	**UF**	Undifferentiated fine-grained sediments
TS	Troutdale sandstone aquifer	**OR**	Older rocks
C2	Confining unit 2		

Figure 18. Principal components of the simulated 1987–88 ground-water budget. (Values are from tables 3 and 4 and are in units of cubic feet per second. Numbers in italics are the percentage of each component of the total budget. For example, discharge to streams and rivers from the unconsolidated sedimentary aquifer is 706 ft^3/s, or 50 percent of the total discharge to streams and rivers.

The Troutdale gravel aquifer receives the majority of its inflow from areal recharge (743 ft^3/s), but also receives significant flux from the unconsolidated sedimentary aquifer (150 ft^3/s) and the undifferentiated fine-grained sediments (105 ft^3/s). Direct areal recharge to the unit is principally from infiltration of precipitation where the unit is exposed at land surface (pl. 1) in the upper parts of the Sandy and Clackamas River drainages and in eastern Clark County. Flux from the unconsolidated sedimentary aquifer occurs primarily by downward leakage. Flux from the undifferentiated fine-grained sediments is by upward leakage where the unit underlies the Troutdale gravel aquifer. Discharge to other units (656 ft^3/s) and to streams (391 ft^3/s) comprise the major outflows from the Troutdale gravel aquifer. Most of the discharge to other units is by upward leakage to the unconsolidated sedimentary aquifer (277 ft^3/s) or by downward leakage to the Troutdale sandstone aquifer (129 ft^3/s) and the undifferentiated fine-grained sediments (158 ft^3/s). The importance of the unconsolidated sedimentary aquifer and Troutdale gravel aquifer in the regional flow system is readily apparent from the magnitude of fluxes through them (table 3; fig. 18); 75 percent of recharge to the system and 80 percent of discharge from the system enters and leaves through these units.

The Troutdale sandstone aquifer is not as extensive as the unconsolidated sedimentary aquifer or Troutdale gravel aquifer and, therefore, does not have inflows or outflows of the same magnitude. The Troutdale sandstone aquifer has relatively few exposures in the basin and thus receives only 35 ft^3/s

from areal recharge; most inflow to the unit is by flux from other units (231 ft^3/s), and most of that enters by way of downward leakage from the Troutdale gravel aquifer (129 ft^3/s) where it directly overlies the unit in the upper parts of the Sandy and Clackamas River Basins. Most outflow from the Troutdale sandstone aquifer is by downward leakage to confining unit 1 (60 ft^3/s) and by horizontal flow into the unconsolidated sedimentary aquifer (53 ft^3/s) where the Troutdale sandstone aquifer has been truncated by the Columbia River and abuts the permeable channel sands (see section C-C', pl. 1). Significant outflow also occurs by discharge to streams (68 ft^3/s) such as Deep and Tickle Creeks and the Sandy River.

Inflows to the undifferentiated fine-grained sediments are leakage from other units (268 ft^3/s) and areal recharge (75 ft^3/s). Outflow from the unit is principally by leakage to other units (234 ft^3/s), discharge to streams (105 ft^3/s), and a small amount of well discharge (4 ft^3/s) from lenses of coarser sediments in north-central Clark County.

Virtually all inflow and outflow to and from the confining units 1 and 2 and the lower, fine-grained subunit of the sand and gravel aquifer occurs by leakage to and from adjacent units. A few wells in the basin tap localized permeable strata within the units and withdraw a total of 4 ft^3/s from all three units. In addition, about 2 ft^3/s of discharge is to streams.

Older rocks receive about 19 percent (278 ft^3/s) of the total areal recharge within the modeled area (fig. 18); most of this occurs where older rocks are exposed in the upland areas such as the Tualatin Mountains. Some discharge from the unit is to streams (89 ft^3/s), rivers (13 ft^3/s), and wells (3 ft^3/s), but the primary outflow is by leakage to other units (240 ft^3/s). Most of the leakage is to the unconsolidated sedimentary aquifer (113 ft^3/s), with lesser amounts to the Troutdale gravel aquifer (67 ft^3/s) and the undifferentiated fine-grained sediments (43 ft^3/s) where they overlie older rocks.

Model Usage and Limitations

Many assumptions are necessary to simplify a real hydrogeologic system to the extent that it can be represented by a mathematical model. The assumptions used to construct the model described by this report have been described fully in previous sections. Some of these assumptions, however, limit the scope of application of the model and the hydrologic questions that can reasonably be addressed. The major simplifying assumptions and the limitations they impose are discussed below.

The model developed as part of the Portland Basin study, simulated time-averaged conditions for the period 1987–88. Construction and calibration of a model for simulating transient ground-water flow was prevented by the lack of data documenting historical changes in stress (recharge and pumpage) on the ground-water system and hydrologic response of the system (changes in water levels and discharge to streams). Because the model has not been calibrated to transient conditions, the model cannot be used to predict the transient response of the system. The limitation imposed by this is that intermediate heads and fluxes in the system, between the time a new stress is applied and the time the system reaches a new steady state, cannot be predicted using the model. The model can, however, be used to simulate steady-state conditions for various stress conditions, and the steady-state water levels and fluxes under various ground-water-management conditions can be compared and evaluated on the basis of the eventual effect they would have on the system.

A second limitation on the use of the model is that, as constructed, transmissivities of hydrogeologic units do not change when the saturated thickness of the units change. This is not a serious limitation unless new stresses on the system are great enough to cause significant change to the saturated thickness of any unit. In the most severe case, a model cell, or group of cells, might become completely desaturated; less severe errors might occur if a smaller change in saturated thickness occurs. Model results should be checked for these conditions if large water-level changes are simulated in the uppermost hydrogeologic units.

Finally, boundary conditions involve considerable simplification of the hydrologic system and can have substantial effects on model results; thus, they must be clearly understood to avoid serious errors in model application (Franke and others, 1987). The lateral boundary of the Portland Basin model was specified as a "no-flow" boundary on the basis of assumptions that it coincided with either ground-water flow divides (for example, the Clackamas and Lewis Rivers) or low-permeability rocks (Skamania Volcanics). These assumptions were considered valid for the stress conditions in the basin during the 1987–88 simulation period; however, they should be evaluated carefully when simulating other stress conditions.

An example of a simulation in which model boundary conditions would affect simulated response would be placement of new stresses (such as pumpage from new wells) near a ground-water divide that is simulated as a no-flow boundary. In the real hydrologic system, flux would be induced across that boundary as the location of the divide changed. In the simulated system, the additional flux would not be available and the simulated water-level declines would be greater than those in the real system. Similarly, simulation of addition of pumping stresses near a low-permeability rock contact represented as a no-flow boundary would yield predicted drawdowns greater than actual drawdowns if pumping near the boundary in the real system could induce additional recharge from the lo permeability rocks. For many purposes, these problems do not impose serious limitations on the use of the model as long as the potential effects of the boundary conditions on the results are understood.

SIMULATION OF PREDEVELOPMENT STEADY-STATE CONDITIONS

The calibrated model was used to simulate predevelopment ground-water conditions in the basin to determine if a reasonable match could be obtained between observed and simulated heads for another time period. Predevelopment conditions are defined as those that existed in the basin prior to the drilling of the first well, construction of the first drywell, installation of the first on-site waste-disposal system, first diversion of surface water, and prior to paving of the first street—in other words, conditions that existed before any significant human influence was exerted on the hydrologic system. If this strict definition were imposed, predevelopment conditions have not existed in the basin for over 100 years. Predevelopment conditions are usually assumed to represent true steady-state (equilibrium) conditions, in which recharge and discharge are balanced and the volume of ground water in storage is nearly constant except for changes caused by normal fluctuations in precipitation and evapotranspiration.

The predevelopment period was chosen to test the model because, by definition, human-caused stresses that are difficult to estimate, such as well discharge and drywell recharge, did not exist. The disadvantage of using the predevelopment period was that there is little information on which to base a quantitative comparison of simulated and real changes in the ground-water system. Under ideal circumstances, long-term records of water-level change would be available for wells in the major aquifers in various parts of the basin; in reality, only about 15 wells in the basin have water-level records prior to 1970 and the oldest records in the basin only date back to the early 1950's. Data from these wells were used to make qualitative comparisons of simulated and real water-level changes since predevelopment, by assuming that water-level changes in these wells represented the minimum water-level changes since predevelopment.

Stresses on the system were modified by eliminating all well discharge and recharge from drywell and on-site waste-disposal systems and by modifying the average annual rate of infiltration by precipitation to reflect the absence of impervious surfaces. Eliminating well discharge reduced total discharge by 166 ft^3/s (table 2). Snyder and others (1994) showed that rates of infiltration by precipitation in the basin were closely related to average annual rainfall, altitude, and the percentage of impervious area. Their regression equation (see equation 3) showed the importance of impervious area to recharge in the basin; for example, recharge in an area where 25 percent of the surface is impervious would be nearly 9 in/yr less than in the same area with no impervious surface. Recharge from infiltration of precipitation during the predevelopment period was estimated by using equation 3 with the same values of mean annual precipitation (1968–82) and land surface altitude as was used by Snyder and others (1994); however, the percentage of impervious area was assumed to be zero for each model cell for predevelopment conditions.

Estimates made using these assumptions show that annual recharge from infiltration of precipitation decreased by 270 ft^3/s (16 percent) from 1,710 ft^3/s to 1,440 ft^3/s between the predevelopment period and 1987–88. Most of this decrease occurred in high density residential, commercial, and industrial areas of Portland and Vancouver (fig. 19), where recharge from infiltration of precipitation has been reduced by up to 25 in/yr. In spite of increases in impervious surfaces, areas such as east Multnomah County and the Burnt Bridge Creek area of Clark County, where drywells and on-site waste-disposal systems are used extensively, received more recharge in 1987–88 than under predevelopment conditions (fig. 19).

Water-level changes in the basin since predevelopment were calculated as the difference between simulated predevelopment and 1987–88 water levels.

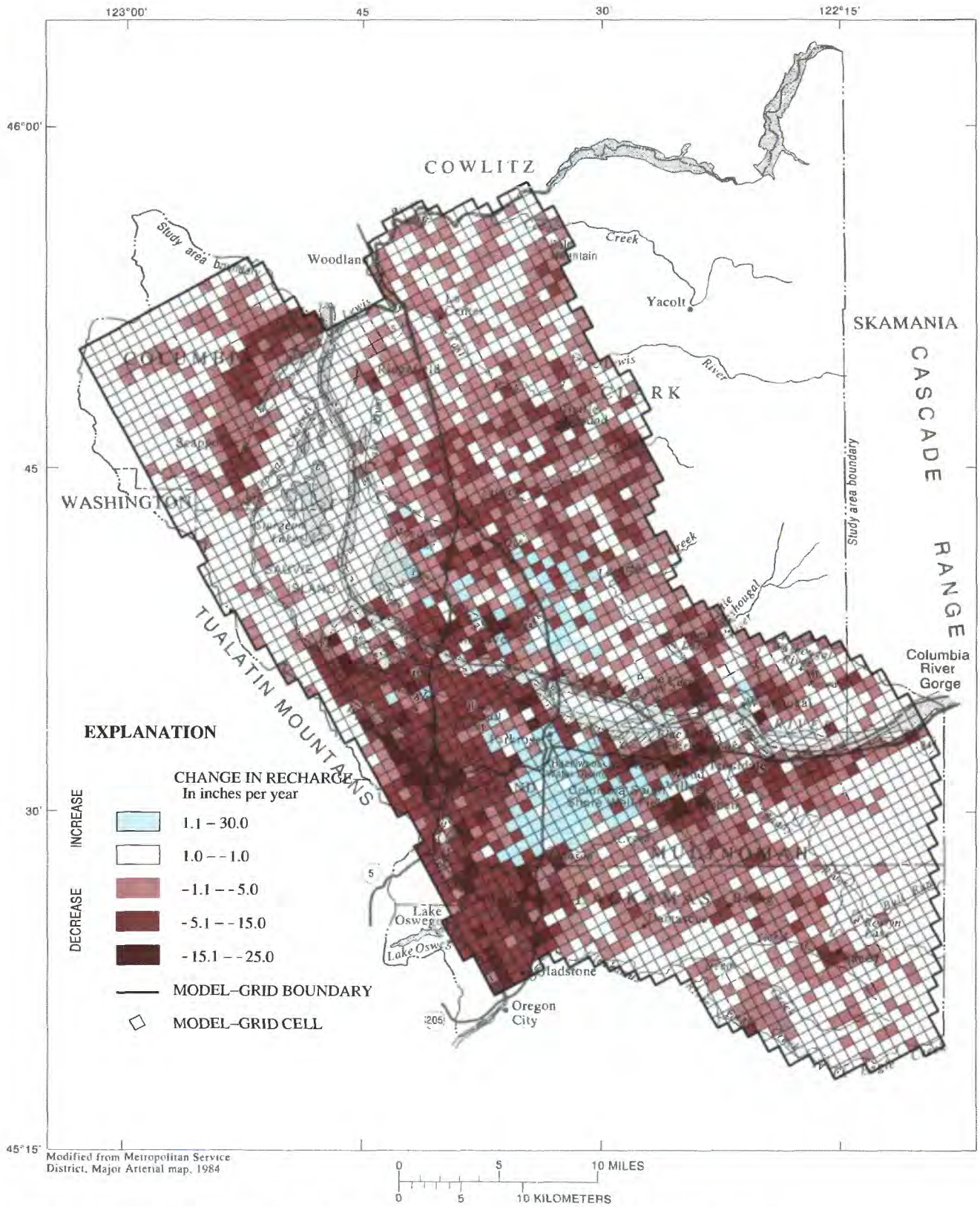

Figure 19. Estimated change in recharge distribution from predevelopment to 1987–88 conditions.

These changes were compared to estimates of water-level changes in selected long-term observation wells in the basin. Changes in simulated water levels reflect only the changes in recharge and well discharge from predevelopment to 1987–88; no other model parameters or boundary conditions were modified. Maps of simulated water-level change for the unconsolidated sedimentary aquifer, Troutdale gravel aquifer, Troutdale sandstone aquifer, and undifferentiated fine-grained sediments are shown in figures 20, 21, 22, and 23, respectively.

Results indicate that water levels have declined moderately (less than 10 ft) throughout most of the basin, primarily in response to reduced recharge in urban areas. Larger declines occurred where pumping is concentrated for public-supply and industrial use in southern Clark County and for agricultural use in the Sandy-Boring area of Oregon. Simulated declines in Clark County were most extensive in the Troutdale gravel aquifer, with a maximum of 40–50 ft and a minimum of 20–30 ft over a broad area within T.2E. bounded by the Columbia River on the south and by Salmon Creek on the north (fig. 21). These simulated declines result from both pumping and reduction in recharge due to urbanization. Concentrated pumping for agricultural use in the area surrounding Sandy and Boring resulted in simulated declines of as much as 40–50 ft in both the Troutdale gravel aquifer (fig. 21) and the Troutdale sandstone aquifer (fig. 22).

Increases in ground-water level were simulated in localized areas of the unconsolidated sedimentary aquifer and Troutdale gravel aquifer in the northeastern part of T.1S., R.2E., where drywell and on-site waste-disposal systems provide large quantities of secondary recharge (figs. 20 and 21).

One long-term observation well in Clackamas County, locally known as the "Issacs" well (T.2S., R.3E., section 6), is completed in the Troutdale gravel aquifer and has been monitored since 1962. During the period 1962–88, water levels in the well declined approximately 25 ft (McCarthy and Anderson, 1990). It is not known how much additional change occurred between predevelopment conditions and 1962; however, 25 ft could be assumed to be the minimum amount of change for the aquifer in this area. Simulated water-level change in the Troutdale gravel aquifer in this area was 20–30 ft (fig. 21). The "Meirs" well, located approximately 7 miles east (T.2S., R.4E., section 5) and completed in the same unit, has been monitored since 1958 and shows a decline of about 20 ft (McCarthy and Anderson, 1990). Simulated declines in this area were 30–40 ft (fig. 21). A well in T.1N., R.2E., section 23 has been monitored since 1967 and shows no long-term trend of decline or rise; simulated water-level changes within the unconsolidated sedimentary aquifer and Troutdale gravel aquifer in this area were 0 to 10 ft.

Two observation wells in Clark County also gave indications of the minimum water-level changes in the Troutdale gravel aquifer since predevelopment. The first well, located in T.2N., R.2E., section 30, showed a 5 ft decline between 1955 and 1988; declines of 10–20 ft were simulated by the model in this area. The second well indicated that declines of at least 12 ft have occurred in T.3N., R.1E., section 21; declines of 0–10 ft were simulated in this area (fig. 21).

Greater recharge from infiltration of precipitation and the absence of pumping left more ground water available to discharge to rivers and streams during predevelopment conditions. Discharge to rivers was 33 percent greater and discharge to streams was 18 percent greater than under 1987–88 conditions (table 2). Less recharge as a result of more impervious surfaces has decreased the flow rate through the shallow aquifers and decreased discharge to rivers and streams. The addition of pumpage near rivers and streams has increased the quantity of seepage from rivers (from 1 to 36 ft^3/s) and streams (from 48 to 88 ft^3/s) to the ground-water system. Streams and rivers throughout the basin received less ground-water discharge in 1987–88 than during predevelopment conditions. In some areas where the simulation shows that pumping has lowered the water table, streams may have stopped receiving discharge completely, or if they have sufficient flow, have come a source of recharge to the shallow aquifers (pl. 9). Some river and stream reaches that contributed recharge to the ground-water system under predevelopment conditions also contributed more recharge after the water table was lowered by nearby pumping.

SIMULATION OF HYPOTHETICAL PUMPING CONDITIONS

The most important use of the model described in this report, beyond the present study, will be to simulate the response of the ground-water system to hypothetical management plans or conditions. Therefore, a set of conditions typical of those that could be simulated was defined and used to test the response of the model to pumping stresses greater than those in effect during the 1987–88 calibration period.

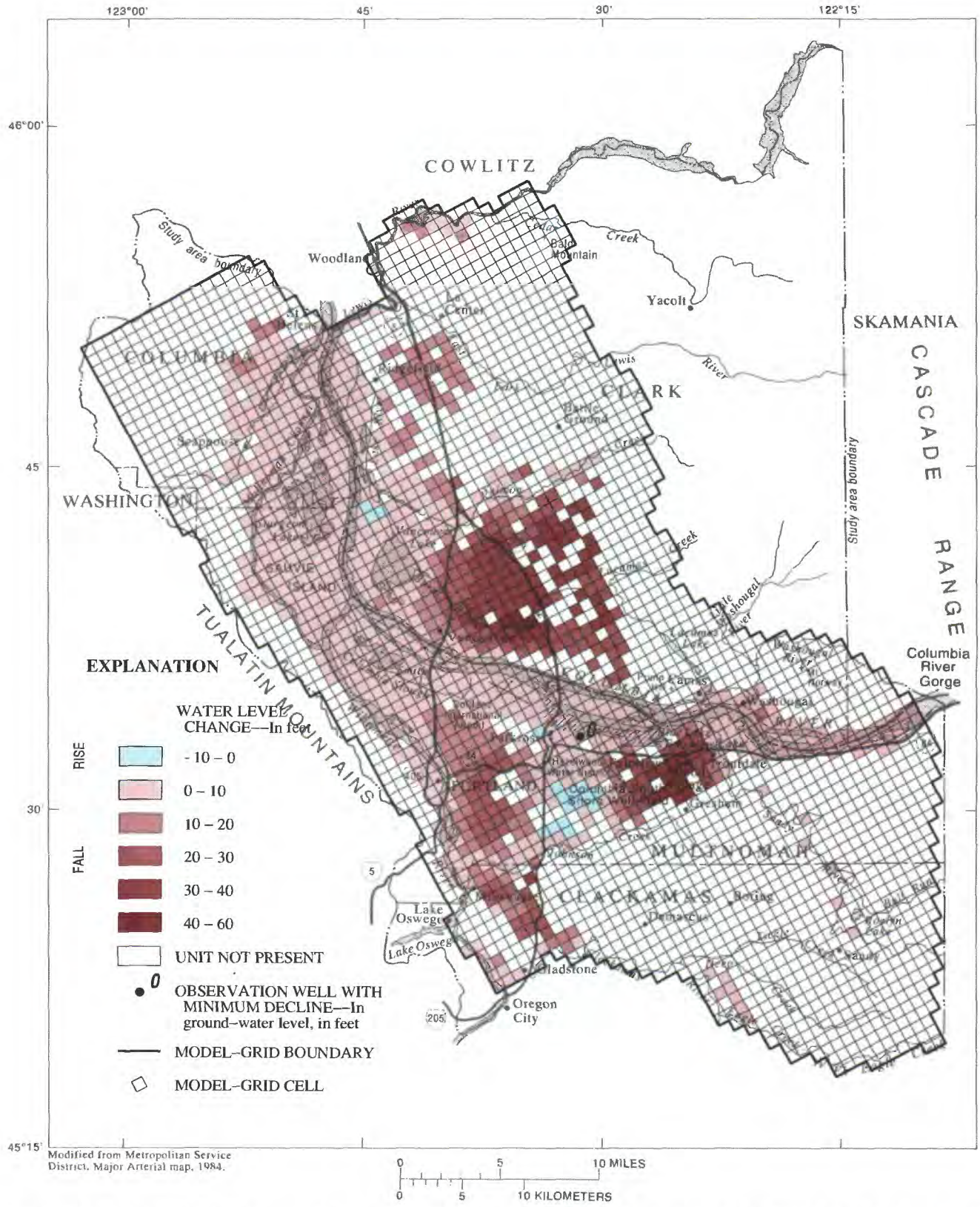

Figure 20. Simulated water-level change between predevelopment and 1987–88 conditions in the unconsolidated sedimentary aquifer. (A negative change indicates rising water level.)

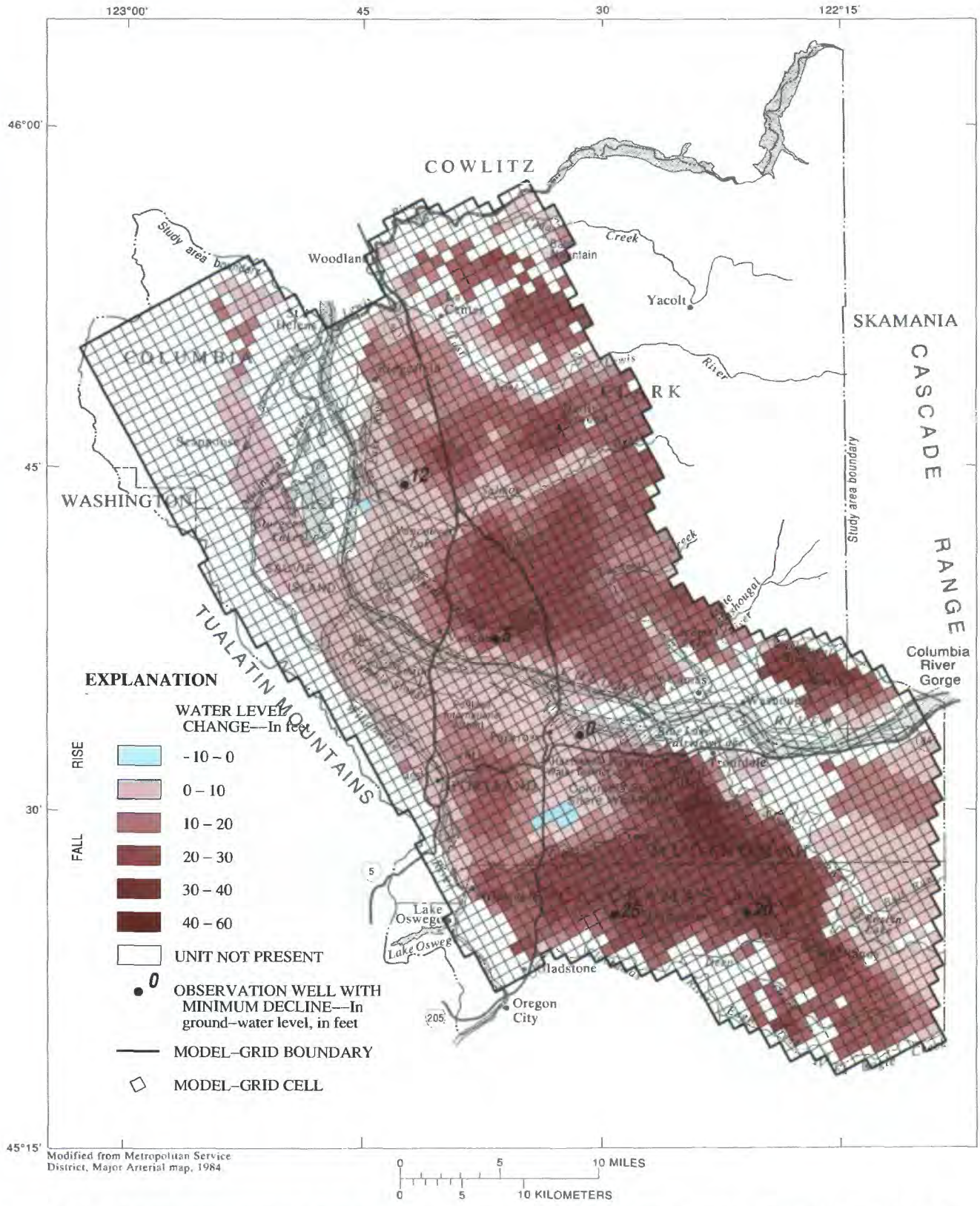

Figure 21. Simulated water-level change between predevelopment and 1987–88 conditions in the Troutdale gravel aquifer. (A negative change indicates rising water level.)

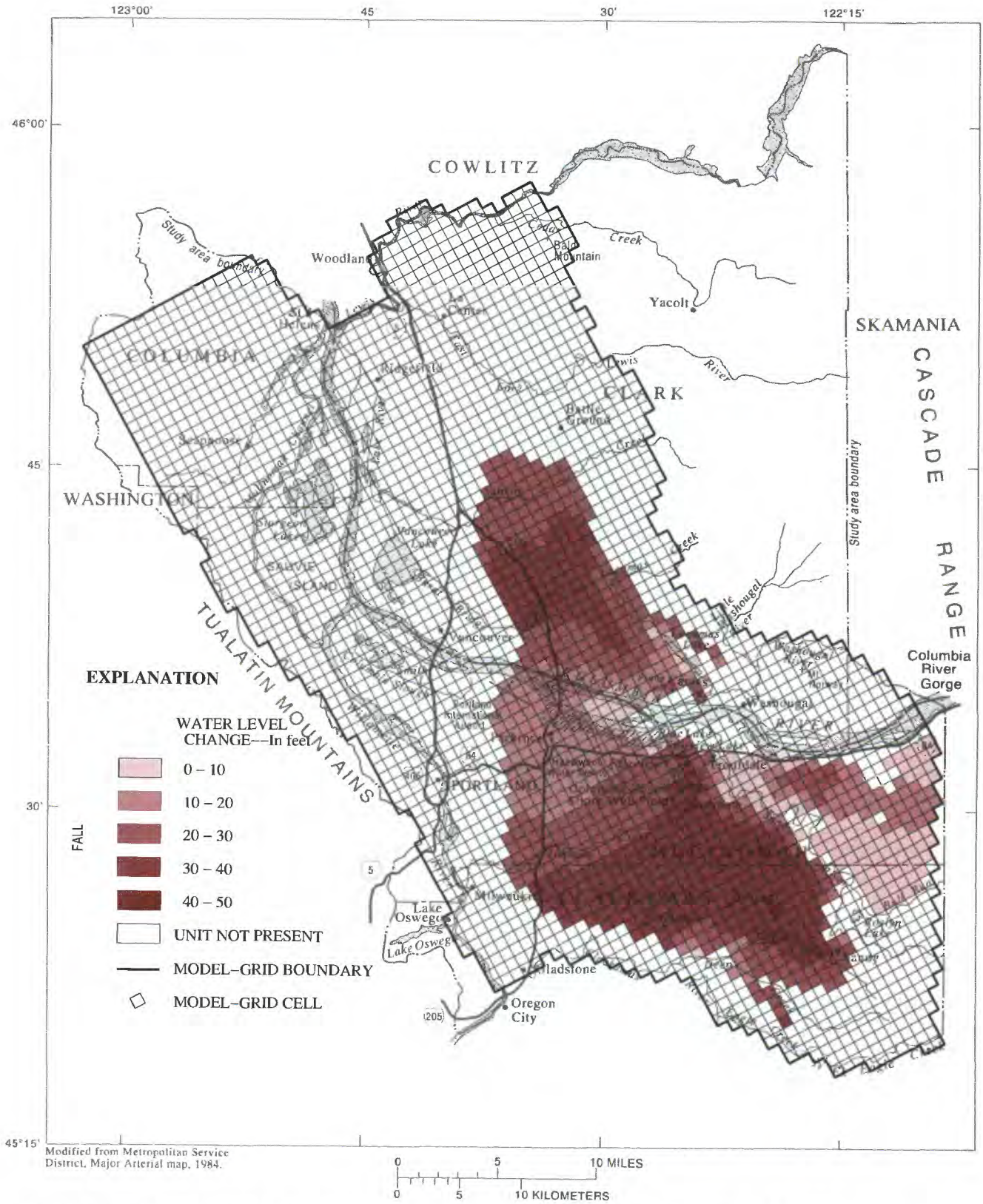

Figure 22. Simulated water-level change between predevelopment and 1987–88 conditions in the Troutdale sandstone aquifer. (A negative change indicates rising water level.)

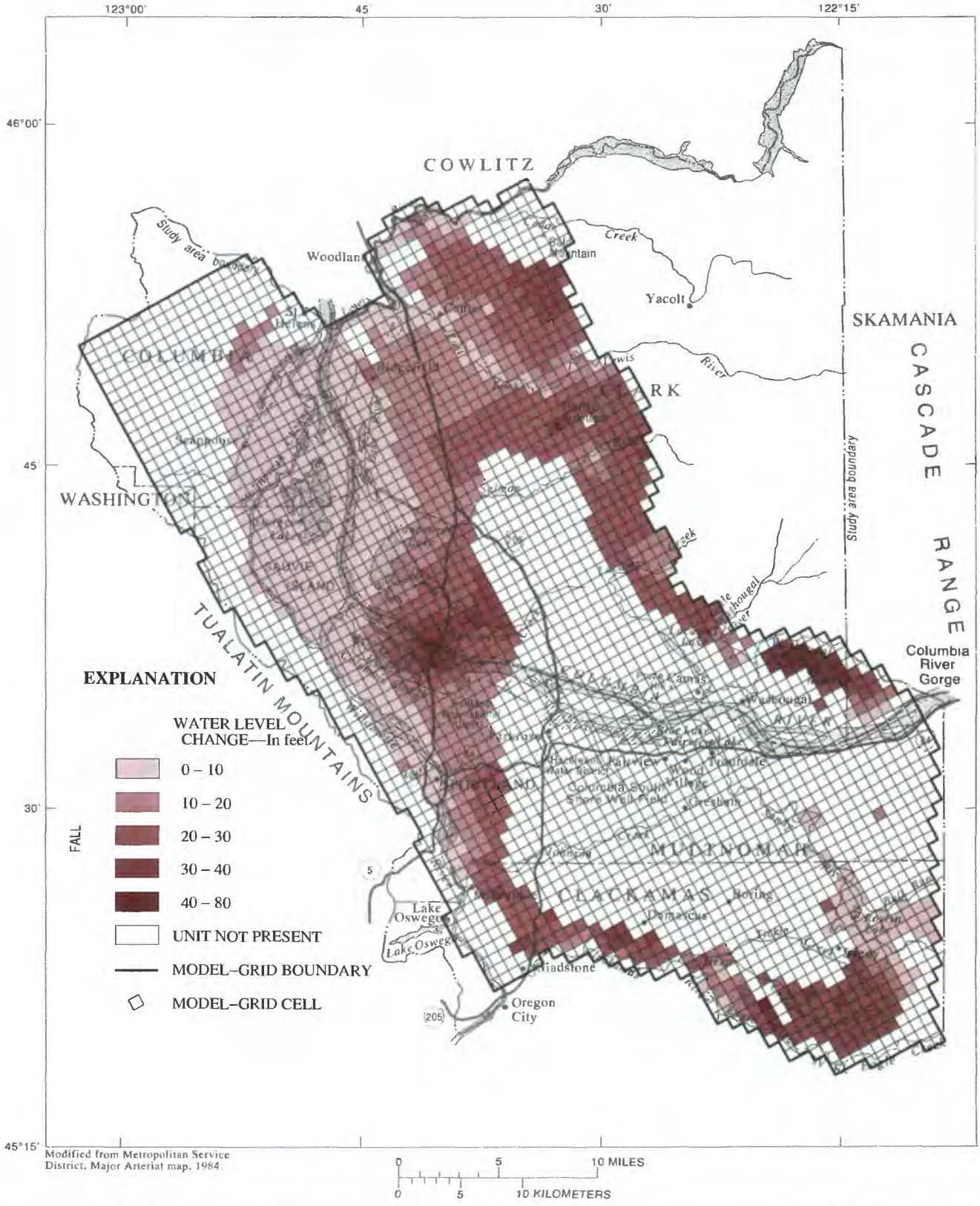

Figure 23. Simulated water-level change between predevelopment and 1987–88 conditions in the undifferentiated fine-grained sediments. (A negative change indicates rising water level.)

The hypothetical management condition defined for this simulation was one in which increased demands for public water supply in Clark County and the city of Portland are met by increasing ground-water withdrawals. The projected ithdrawals in Clark County were based on estimates of increased water needs for the year 2010 (R.D. Swanson, Intergovernmental Resource Center, Clark County, Washington, oral commun., April 1991); withdrawals by the city of Portland were based on the assumption that the Columbia South Shore well field, presently used only rarely, would be operated at 25 percent of its 150 ft^3/s capacity. The condition under which the well field would be operated at 25 percent of capacity would be when the wells are used to meet late summer and peak demand during a 3-month period each year. As a result, total withdrawals in Clark County were increased by 54 ft^3/s and in the Columbia South Shore well field by 38 ft^3/s (fig. 24); the total, 92 ft^3/s, represented a 55 percent increase from 1987–88. About 48 percent (44 ft^3/s) of the increase in pumping was from the unconsolidated sedimentary aquifer, 11 percent (10 ft^3/s) from the Troutdale gravel aquifer, 13 percent (12 ft^3/s) from the Troutdale sandstone aquifer, and 17 percent (16 ft^3/s) from the upper, coarse-grained subunit of the sand and gravel aquifer. In Clark County, most of the new pumpage was from the Troutdale gravel aquifer and Troutdale sandstone aquifer, whereas in the Columbia South Shore well field, most of the increased withdrawals were from the unconsolidated sedimentary aquifer near Blue Lake and Troutdale sandstone aquifer and upper, coarse-grained subunit of the sand and gravel aquifer. Recharge was maintained at the same rates used in the 1987–88 simulation.

Changes in simulated water levels in the unconsolidated sedimentary aquifer, Troutdale gravel aquifer, Troutdale sandstone aquifer, and undifferentiated fine-grained sediments are shown in figures 25, 26, 27, and 28, respectively. Declines in simulated water levels in the unconsolidated sedimentary aquifer were less than 5 ft throughout most of the basin except in Clark County, where declines were as much as 20 ft (fig. 25). The large declines in Clark County probably were caused by increased downward leakage from the unconsolidated sedimentary aquifer that was induced by the increased pumping in the underlying Troutdale gravel aquifer. Declines of 20–40 ft were simulated in the Troutdale gravel aquifer in response to increased pumping from that unit south of Salmon Creek and near Camas (fig. 26). A small area of decline in the Troutdale gravel aquifer also was simulated near Battle Ground. The broadest area of large water-level declines was within the Troutdale sandstone aquifer (fig. 27); simulated declines of 20–40 ft accompanied withdrawals in the Portland well field area and similar declines were simulated near Camas. Declines in the Troutdale sandstone aquifer affected the undifferentiated fine-grained sediments where the two units are in contact and resulted in declines of 10–20 ft within a small area north of Vancouver (fig. 28).

The simulated water budget for the hypothetical conditions (table 2) indicates that, at equilibrium, much of the additional 92 ft^3/s of pumpage is supplied by increased recharge from, and decreased discharge to, the Columbia River. Placement of new pumping near the Columbia River, such as that in the Columbia South Shore well field near Blue Lake and near Camas, induced an additional 26 ft^3/s of recharge from the river (pl. 9). A multiwell aquifer test conducted on wells in the unconsolidated sedimentary aquifer near Blue Lake and subsequent analysis of stable isotope concentrations (oxygen-18 and deuterium) in the well discharge indicates that substantial quantities of river water recharge the aquifer under pumping stress (McCarthy and others, 1992). Areas adjacent to the Columbia River near Vancouver and northeast Portland (southeast T.2W., R.1E.), where flux between the river and the aquifer reversed from discharge to recharge between predevelopment and 1987–88, supplied even more recharge under the hypothetical conditions (pl. 9). Another source of ground water to the new pumping stress was the simulated reduction, or capture, of an additional 14 ft^3/s that discharged from the aquifer to rivers in 1987–88.

The total recharge from streams and discharge to streams listed in table 2 indicates that the hypothetical pumping conditions had little effect on simulated stream leakage from the small streams. Comparison of simulated base-flow discharge at selected sites on Salmon Creek for 1987–88 and under hypothetical pumping conditions shows, however, that within the area of increased pumpage, the ground-water discharge to Salmon Creek would be reduced under these pumping conditions (fig. 29). Mean base-flow discharge at the lower end of Salmon Creek would be reduced by approximately 8 percent. In contrast, Tickle Creek is located outside the area influenced by additional pumpage under these conditions, and simulated base flow was virtually unaffected (fig. 29).

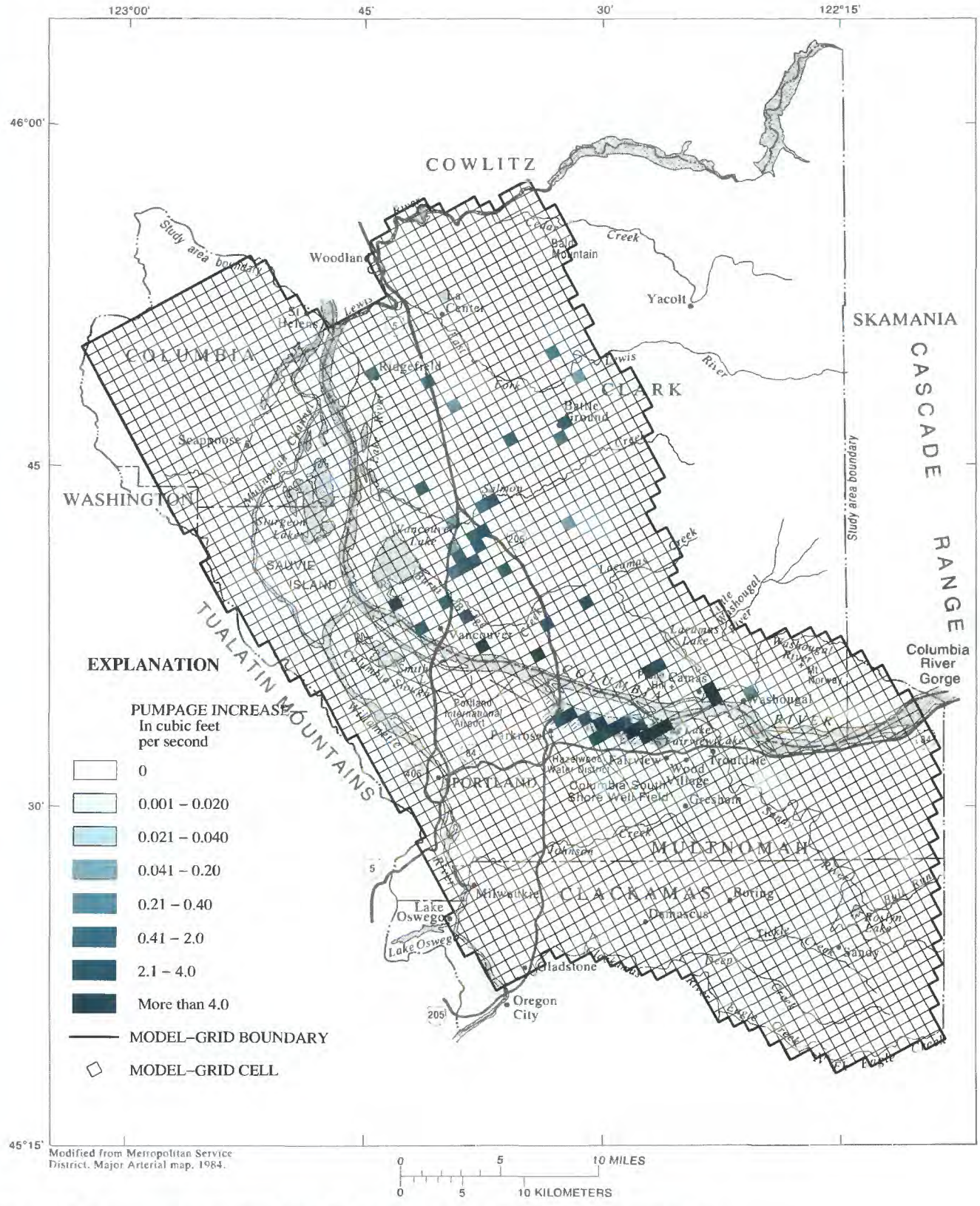

Figure 24. Pumpage increase from 1987–88 conditions to hypothetical pumping conditions.

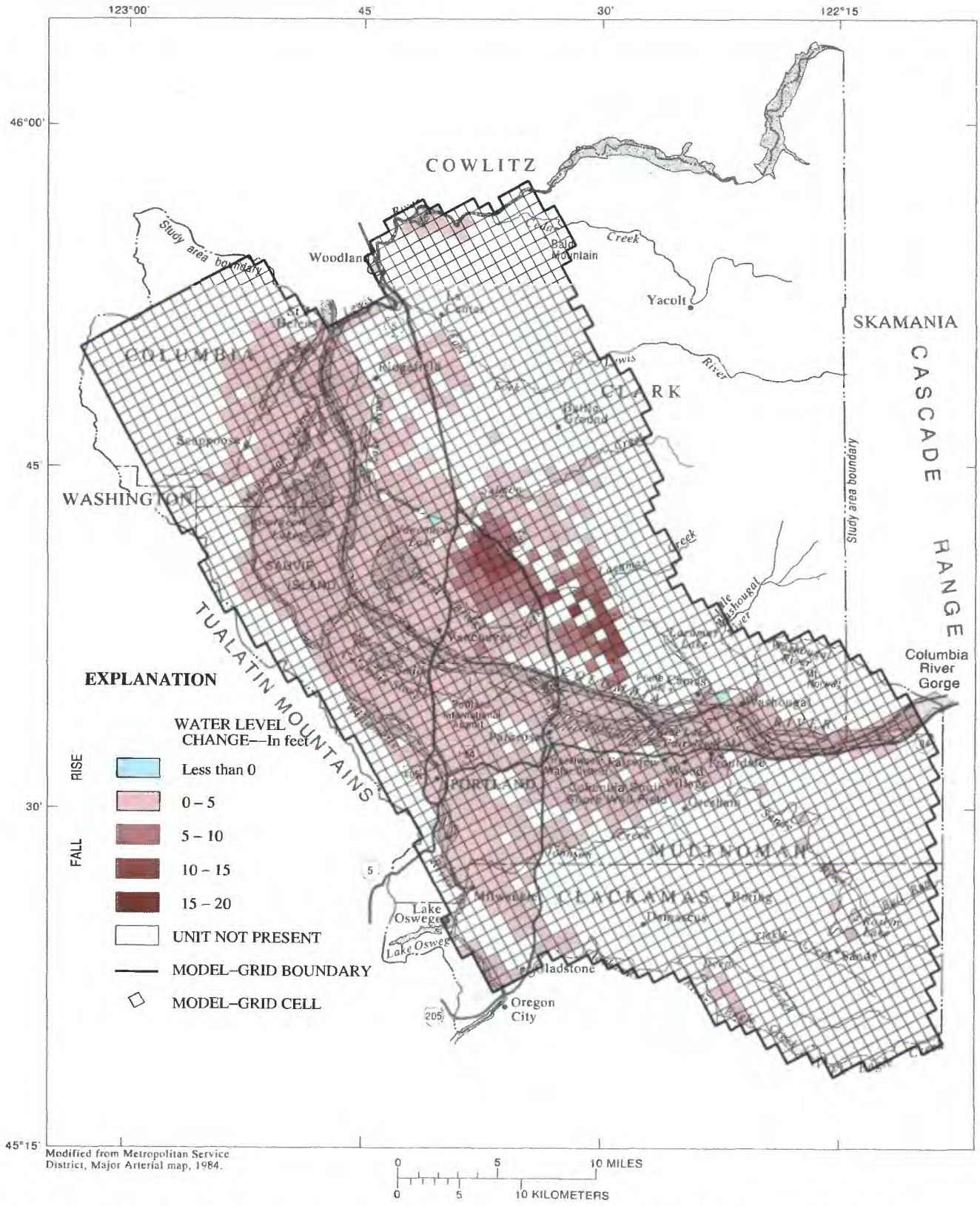

Figure 25. Simulated water-level change from 1987–88 to steady state under hypothetical pumping conditions in the unconsolidated sedimentary aquifer.

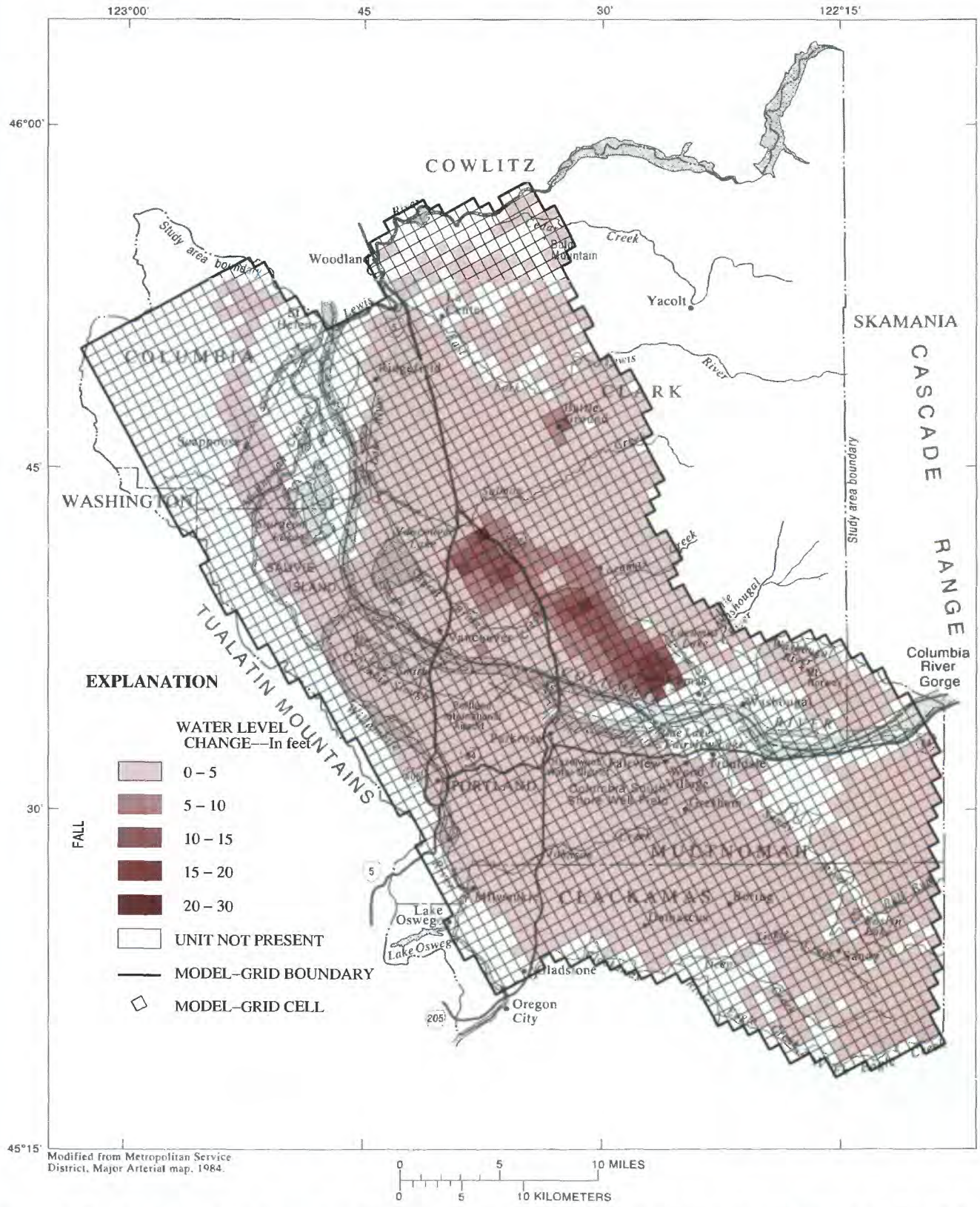

Figure 26. Simulated water-level change from 1987–88 to steady state under hypothetical pumping conditions in the Troutdale gravel aquifer.

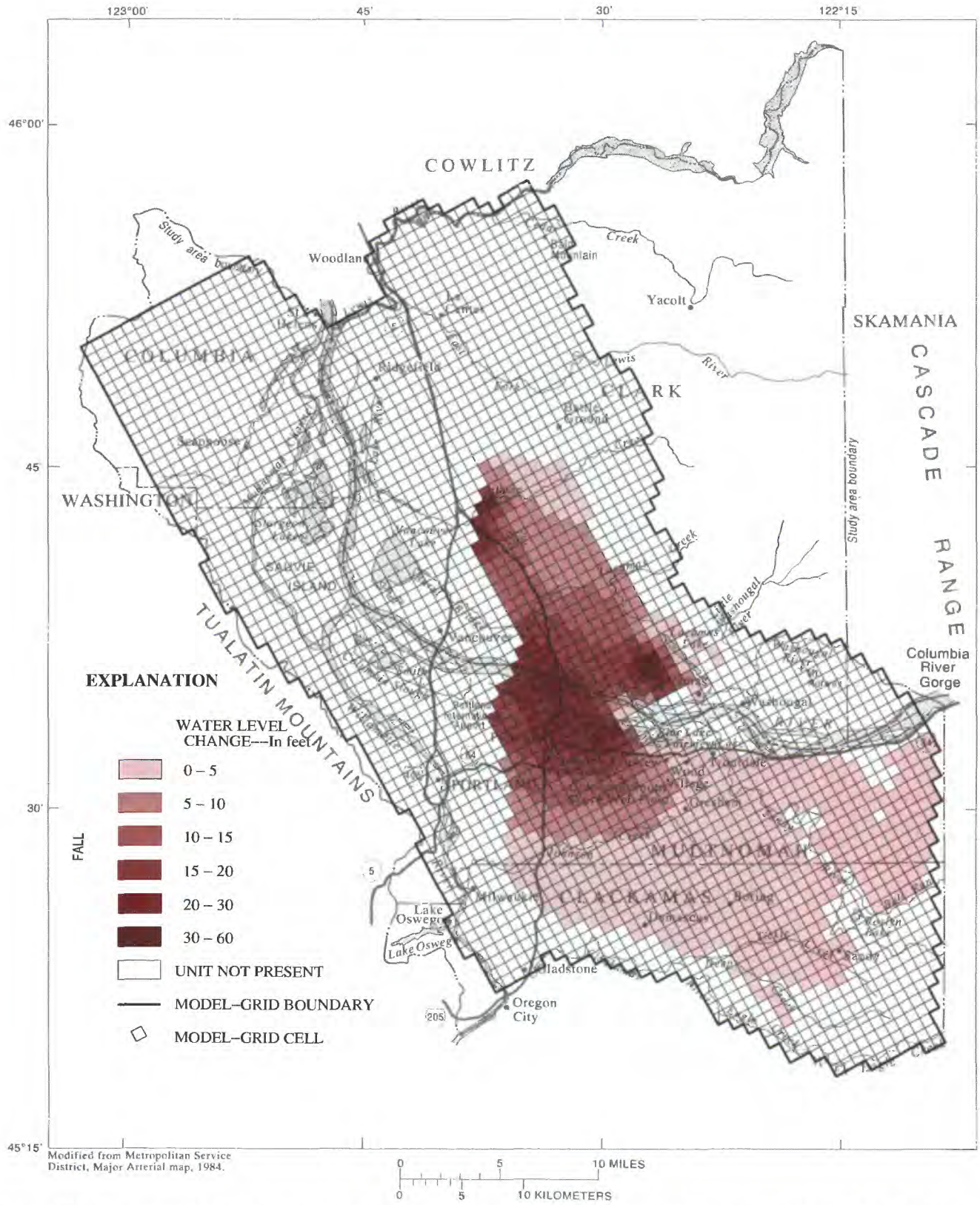

Figure 27. Simulated water-level change from 1987–88 to steady state under hypothetical pumping conditions in the Troutdale sandstone aquifer.

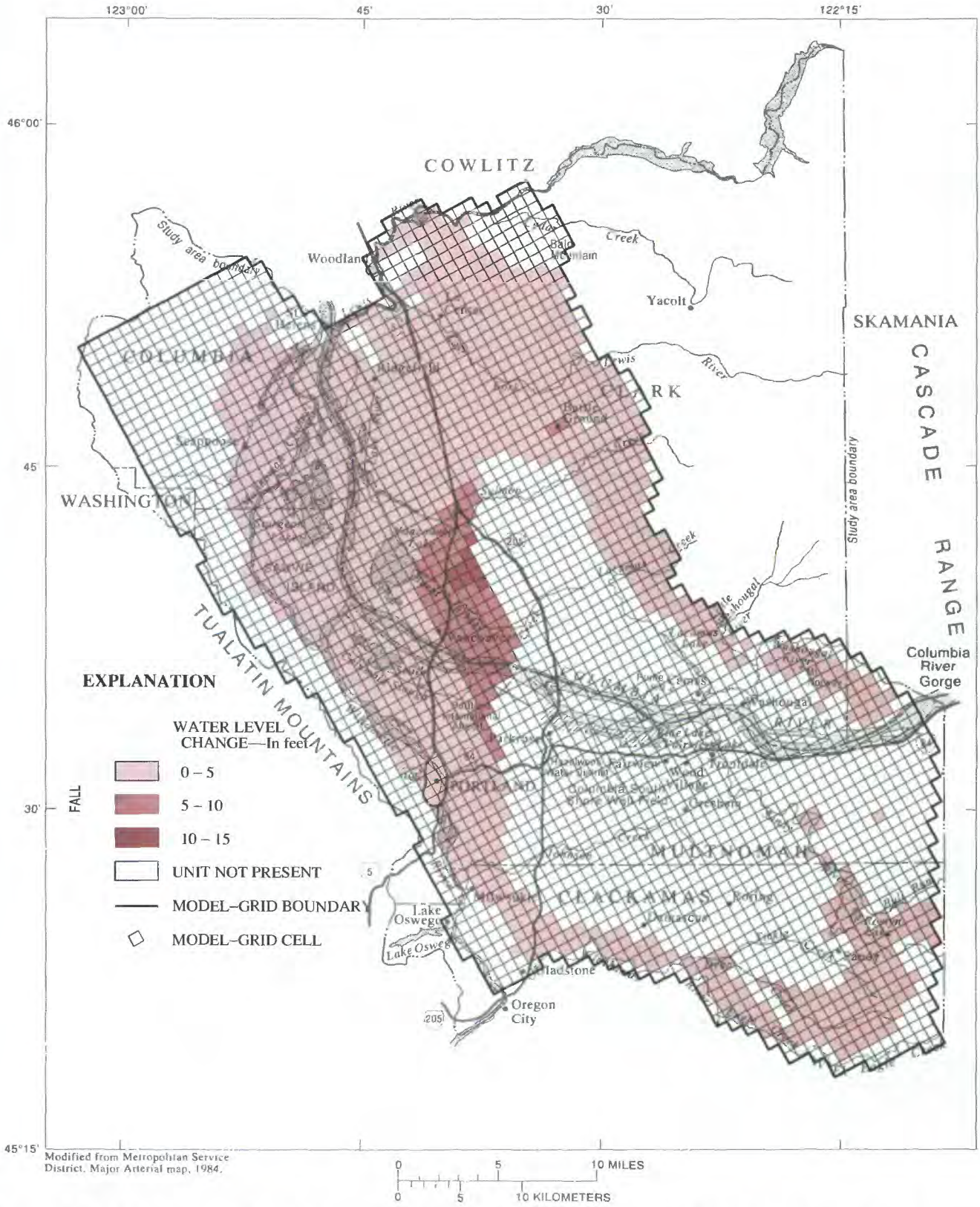

Figure 28. Simulated water-level change from 1987–88 to steady state under hypothetical pumping conditions in the undifferentiated fine-grained sediments.

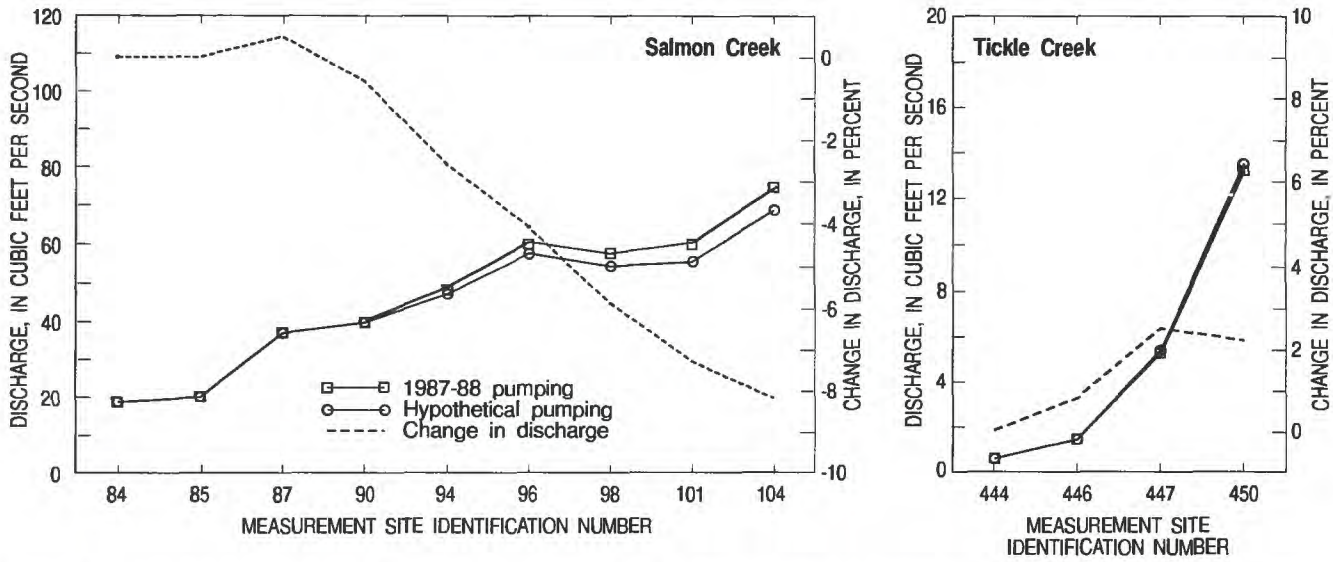

Figure 29. Simulated mean base-flow discharge for 1987–88 and hypothetical pumping conditions on Salmon Creek and Tickle Creek. (Simulated change in base-flow discharge between 1987–88 and hypothetical pumping conditions is shown as percentage of 1987–88 base-flow discharge.)

PRIORITIES FOR FUTURE DATA COLLECTION

A program of data collection and further model calibration would improve the understanding of the hydrologic system and aid in development of a model that could be used to simulate changes in the system over time. A data-collection program for the Portland Basin that would allow calibration of a transient model would include at least the following:

(1) Monitoring of long-term ground-water levels: Many of the monitoring wells established for this study could be retained in a long-term monitoring network. Wells could be selected that would give good areal coverage in each of the major aquifer units. Higher density coverage near pumping centers and, if possible, the capability to measure water level at different depths at the same locations would help to define the vertical hydraulic gradients.

(2) Inventory of ground-water withdrawals: Most withdrawals in the basin are for public-supply and industrial uses. These withdrawals would be inventoried each year; for highly seasonal uses, monthly or weekly withdrawals would be inventoried.

(3) Periodic updating of recharge rates: The distribution and rate of recharge will continue to change as urbanization decreases pervious areas where infiltration can occur and sanitary-sewer installation reduces on-site waste-disposal systems. Elimination of combined sanitary and storm sewers might increase the number of drywells in the basin. To accommodate these changes in the model, recharge rates would be updated on the basis of current land-use and sewering practices.

This model was constructed to simulate the ground-water system at a regional scale. Many situations in the basin occur at scales that do not allow them to be addressed directly with the "regional" model. For example, determination of the effects of pumping a single well on flow in a stream 500 ft from the well is not a reasonable application of a regional-scale model in which the minimum cell dimension is 3,000 ft per side. This type of problem would be best addressed with a more detailed local analysis, possibly a "subregional" model that included only the area immediately surrounding the stream and well and used smaller model cells.

The boundaries of a subregional model could be arbitrarily located because the fluxes across them would be calculated by the regional model described in this report. This approach has been used to allow more detailed modeling of local areas within a regional ground-water flow system; examples include a study of the ground-water system on Long Island, New York (Buxton and Reilly, 1986) and a study of the Owens

Valley in California (W.R. Danskin, U.S. Geological Survey, oral commun., December 1991). Development of subregional models in the basin will require data-collection programs designed to specifically address the problems for which each subregional model is developed.

SUMMARY AND CONCLUSIONS

In order to provide an improved understanding of the regional hydrogeologic framework of the Portland Basin, the U.S. Geological Survey conducted a 3-year cooperative study of the basin with the Oregon Water Resources Department, the city of Portland Bureau of Water Works, and the Intergovernmental Resource Center located in Clark County, Washington. This report, the seventh completed as part of the cooperative study, describes a numerical model of the regional ground-water flow system and the analysis that was made using the model.

The numerical model of the ground-water flow system in the Portland Basin, Oregon and Washington, was used to (1) test and refine the conceptual understanding of the flow system, (2) estimate the effects of past and future human-caused changes to ground-water recharge and discharge on ground-water levels and streamflow, and (3) determine priorities for ground-water monitoring and data collection that would facilitate improvements in the utility and accuracy of the model. The model covered an area of 981 square miles and included most of Multnomah County, Oregon, and Clark County, Washington, as well as parts of Clackamas, Washington, and Columbia Counties in Oregon and Skamania County in Washington.

Volcanic and marine sedimentary rocks form a structural basin that has been filled with up to 1,800 ft of fluvial and lacustrine sediments. Nine hydrogeologic units have been defined on the basis of their regional hydraulic characteristics. The primary aquifers in the basin are the unconsolidated sedimentary aquifer and the Troutdale gravel aquifer; secondary aquifers include the Troutdale sandstone aquifer, the upper, coarse-grained subunit of the sand and gravel aquifer, and the older rocks where they consist of Columbia River basalts. The four remaining units function primarily as confining beds, but might locally contain coarse-grained beds used as aquifers.

Principal components of recharge to the system include infiltration of precipitation, effluent from on-site waste-disposal systems, and runoff to drywells. Recharge from direct infiltration of precipitation was estimated using a regression model relating mean annual recharge to mean annual precipitation, altitude, and impervious area. Recharge rates within the model area ranged from zero where impervious area was near 100 percent to 49 in/yr in the higher altitude, forested parts of the basin. Recharge from on-site waste-disposal systems and drywells was a significant source (as much as 26 in/yr) in unsewered areas of east Multnomah County, Oregon, and southern Clark County, Washington.

Natural discharge from the ground-water system is by seepage to rivers, streams, and, to a lesser extent, springs. Discharge also occurs from wells, and in 1988 the mean withdrawal rate was 166 ft^3/s. Ninety percent of the ground water pumped in 1988 was used for public-supply and industrial needs. Agricultural needs accounted for only 10 percent of pumpage. Eighty-five percent of the total withdrawals were from the unconsolidated sedimentary aquifer (58 percent) and the Troutdale gravel aquifer (27 percent).

A three-dimensional finite-difference model of the basin was constructed by dividing the nine hydrogeologic units into eight model layers, each having 3,040 square cells with dimensions of 3,000 ft per side. The sensitivity of simulated water levels and fluxes to uncertainty in input data, such as hydraulic conductivity and recharge, was assessed by observing the variation of simulated heads and fluxes in response to changes in hydraulic characteristics and boundary conditions. Model results were found to be most sensitive to horizontal hydraulic conductivity. A steady-state model was calibrated using time-averaged data for the 1987–88 period. Horizontal hydraulic conductivities, streambed and riverbed conductances, and vertical anisotropy ratios were the principal parameters changed during calibration. Median horizontal hydraulic conductivity ranged from 130 ft/d in the unconsolidated sedimentary aquifer to about 1 ft/d in the older rocks. Vertical anisotropy ratios ranged from 1,000:1 in the older rocks and fine-grained units to 100:1 in the primary aquifer units.

Simulated heads were compared to measured heads in 417 observation wells, and parameter adjustment proceeded until close agreement between the observed and simulated heads was obtained. Simulated stream leakage and base-flow discharge also were

compared with observed data during the calibration process. The root-mean square of the difference of observed and simulated heads in the primary aquifers (unconsolidated sedimentary, Troutdale gravel, Troutdale sandstone, and sand and gravel) was used to measure the goodness of fit of the model; root-mean-square values ranged from 54 ft (mean error 11 ft) in the unconsolidated sedimentary aquifer to 74 ft (mean error –2.8 ft) in the Troutdale sandstone aquifer. Many of the larger differences in the unconsolidated sedimentary aquifer and the Troutdale gravel aquifer were in an area where wells are believed to be completed in perched water zones.

The regional-scale flow systems within the basin have their recharge areas in the upland exposures of older rocks and the Troutdale gravel aquifer and are characterized by long ground-water flow paths, which ultimately discharge to one of the basin's large rivers, such as the Columbia, Willamette, Lewis, or Clackamas. Superimposed on these regional-scale flow systems are many local-scale systems in which ground-water flow is controlled by local topographic features and discharge is to smaller rivers and streams. Most ground water in the basin moves through these local flow systems within the unconsolidated sedimentary aquifer and the Troutdale gravel aquifer before being discharged by seepage to streams or rivers. Fifty-eight percent of ground-water discharge in the basin is to smaller rivers and streams, 27 percent is to the Columbia and Willamette Rivers, and 10 percent is to wells and springs.

As a semiquantitative check on the validity of model-predicted response under another set of stresses on the system, the model was used to simulate predevelopment (no human-caused influences) steady-state conditions in the basin. A predevelopment recharge distribution was simulated, in which areas that now have drywells and on-site waste-disposal systems had reduced recharge and areas now covered by impervious surfaces had increased recharge. Recharge under predevelopment conditions was estimated to be 180 ft^3/s greater than under 1987–88 conditions. Ground-water discharge by wells was assumed to be zero. In Clark County, model-simulated predevelopment water levels in the Troutdale gravel aquifer were as much as 50 ft higher than 1987–88 water levels in areas where the aquifer has been used most heavily for public supply. Similar declines were simulated in the Troutdale sandstone aquifer near Sandy, where agricultural pumpage is concentrated. Data from long-term observation wells in the basin indicate that simulated changes in water level between predevelopment and present conditions were reasonable.

Another simulation was made to estimate the steady-state response of the ground-water flow system to a hypothetical future condition in which increased pumpage was used to meet the public-supply requirements within the basin in 2010. Total pumpage in the hypothetical condition was 55 percent greater than the 1987–88 pumpage of 166 ft^3/s. The additional pumpage was allocated within Clark County (54 ft^3/s) and in the area of the Portland well field (38 ft^3/s). Simulated water-level declines under this condition were greatest in the Troutdale sandstone aquifer on both sides of the Columbia River. Most of the additional 92 ft^3/s of pumpage was supplied by increased recharge from, and decreased discharge to, the Columbia River. Simulated base-flow discharge to Salmon Creek was decreased by as much as 8 percent in the lowermost reaches of the stream.

REFERENCES CITED

Buxton, H.T., and Reilly, T.E., 1986, A technique for analysis of ground-water systems at regional and subregional scales applied on Long Island, New York: U.S. Geological Survey Water-Supply Paper 2310, p. 129–142.

Collins, C.A., and Broad, T.M., 1993, Estimated average annual ground-water pumpage in the Portland Basin, Oregon and Washington: U.S. Geological Survey Water-Resources Investigations Report 91–4018, 26 p., 4 pls.

Cooley, R.L., and Naff, R.L., 1990, Regression modeling of ground-water flow: U.S. Geological Survey Techniques of Water-Resources Investigations, book 3, chap. B4, 232 p.

Domenico, P.A., and Schwartz, F.W., 1990, Physical and chemical hydrogeology: New York, John Wiley and Sons, 824 p.

Franke, O.L., Reilly, T.E., and Bennett, G.D., 1987, Definition of boundary and initial conditions in the analysis of saturated ground-water flow systems—an introduction: U.S. Geological Survey Techniques of Water-Resources Investigations, book 3, chap. B5, 15 p.

Franke, O.L., Reilly, T.E., 1987, The effects of boundary conditions on steady-state response of three hypothetical ground-water flow systems—Results and implications of numerical experiments: U.S. Geological Survey Water-Supply Paper 2315, 12 p.

Hansen, A.J., Jr., 1993, Modifications to the modular three-dimensional finite-difference ground-water flow model used for the Columbia Plateau Regional Aquifer System Analysis, Washington, Oregon and Idaho: U.S. Geological Survey Open-File Report 91–532, 162 p.

Harbaugh, A.W., 1990, A computer program for calculating subregional water budgets using results from the U.S. Geological Survey modular three-dimensional finite-difference ground-water flow model: U.S. Geological Survey Open-File Report 90–392, 46 p.

Hartford, S.V., and McFarland, W.D., 1989, Lithology, thickness, and extent of hydrogeologic units underlying the east Portland area, Oregon: U.S. Geological Survey Water-Resources Investigations Report 88–4110, 23 p., 6 pls.

Hogenson, G.M., and Foxworthy, B.L., 1965, Ground water in the east Portland area, Oregon: U.S. Geological Survey Water-Supply Paper 1793, 78 p., 2 pls.

Johnson, A.I., 1967, Specific yield—Compilation of specific yields for various materials: U.S. Geological Survey Water-Supply Paper 1662–D, 74 p.

McCarthy, K.A., and Anderson, D.B., 1990, Ground-water data for the Portland Basin, Oregon and Washington: U.S. Geological Survey Open-File Report 90–126.

McCarthy, K.A., McFarland, W.D., Wilkinson, J.M., and White, L.D., 1992, The dynamic relationship between ground water and the Columbia River—Using deuterium and oxygen-18 as tracers: Journal of Hydrology, v. 135, no. 1/4, p. 1–12.

McDonald, M.G., and Harbaugh, A.W., 1988, A modular three-dimensional finite-difference ground-water flow model: U.S. Geological Survey Techniques of Water-Resources Investigations, book 6, chap. A1, 576 p.

McFarland, W.D., and Morgan, D.S., 1996, Description of the ground-water flow system in the Portland Basin, Oregon and Washington: U.S. Geological Survey Water-Supply Paper 2470–A, 58 p., 7 pls.

Morgan, D.S., and Dettinger, M.D., 1994, Ground-water flow conditions in Las Vegas Valley, Nevada, Part II—Simulation analysis: U.S. Geological Survey Open-File Report 90–179, 151 p.

Mundorff, M.J., 1964, Geology and ground-water conditions of Clark County, Washington, with a description of a major alluvial aquifer along the Columbia River: U.S. Geological Survey Water-Supply Paper 1600, 268 p., 3 pls.

Orzol, L.L., and McGrath, T.S., 1992, Documentation of a software interface between a modular, finite-difference, ground-water flow model and a geographic information system data base: U.S. Geological Survey Water-Resources Investigations Report 92–50, 202 p.

Prudic, D.E., 1989, Documentation of a computer program to simulate stream-aquifer relations using a modular, finite-difference, ground-water flow model: U.S. Geological Survey Open-File Report 88–729, 113 p.

Prych, E.A., 1983, Numerical simulation of ground-water flow in Lower Satus Creek Basin, Yakima Indian Reservation, Washington: U.S. Geological Survey Water-Resources Investigations Report 82–4065, 78 p.

Snyder, D.T., Morgan, D.S., and McGrath, T., 1994, Estimates of recharge from infiltration of precipitation, on-site sewage-disposal systems, and dry wells in the Portland Basin, Oregon and Washington: U.S. Geological Survey Water-Resources Investigations Report 92–4010, 34 p.

Swanson, R.D., McFarland, W.D., Gonthier, J.B., and Wilkinson, J.W., 1993, A description of hydrogeologic units in the Portland Basin, Oregon and Washington: U.S. Geological Survey Water-Resources Investigations Report 91–4196, 56 p.

Trimble, D.E., 1963, Geology of Portland, Oregon and adjacent areas: U.S. Geological Survey Bulletin 1119, 119 p., 1 pl.

Willis, R.F., 1977, Ground water exploratory program: Portland, Oregon, Bureau of Water Works, 284 p., 17 pls.

———1978, Pilot well study: Portland, Oregon, Bureau of Water Works, 150 p., 23 pls.

APPENDIX A

Maps showing saturated thickness of hydrogeologic units

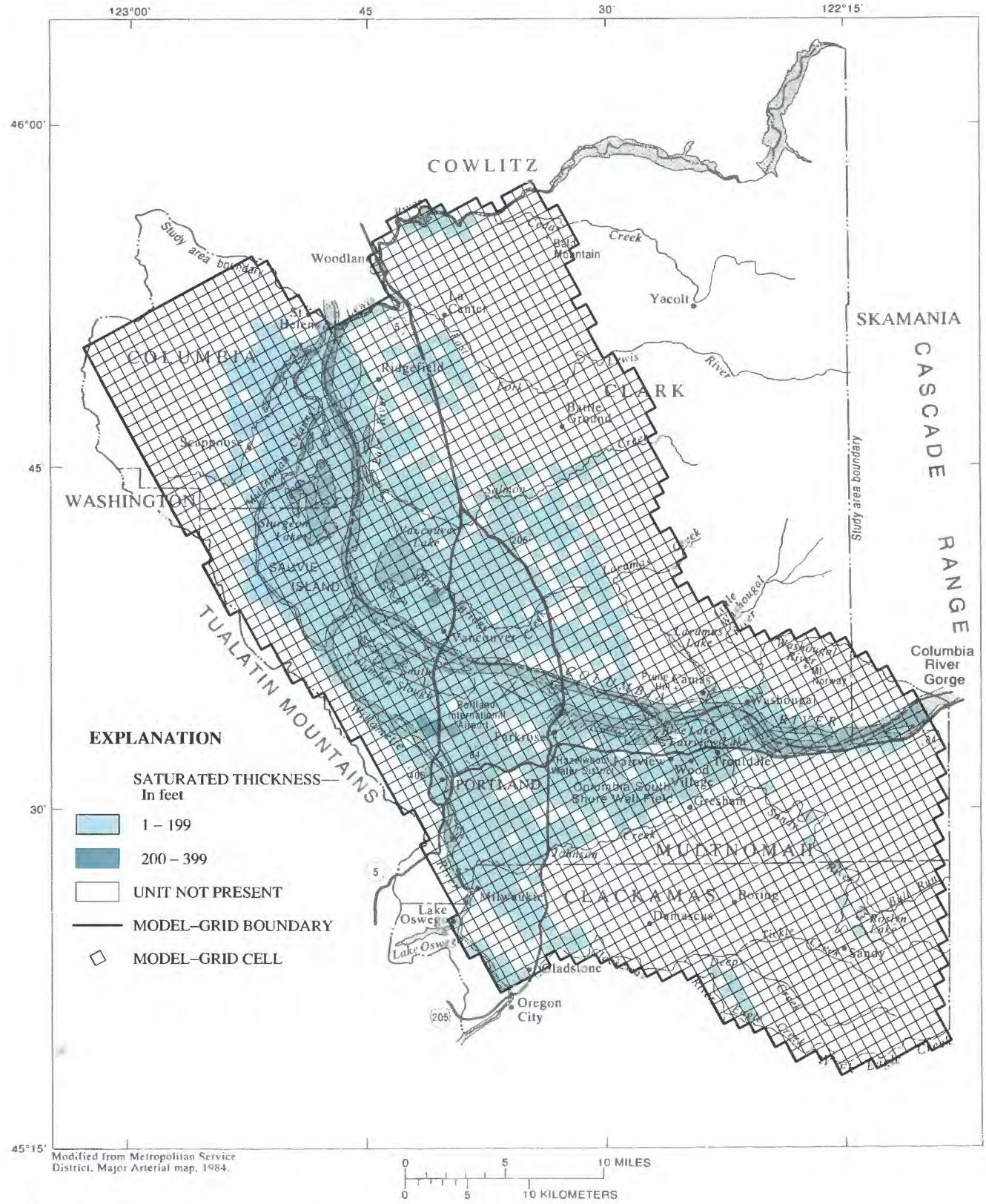

Figure A–1. Saturated thickness of unconsolidated sedimentary aquifer.

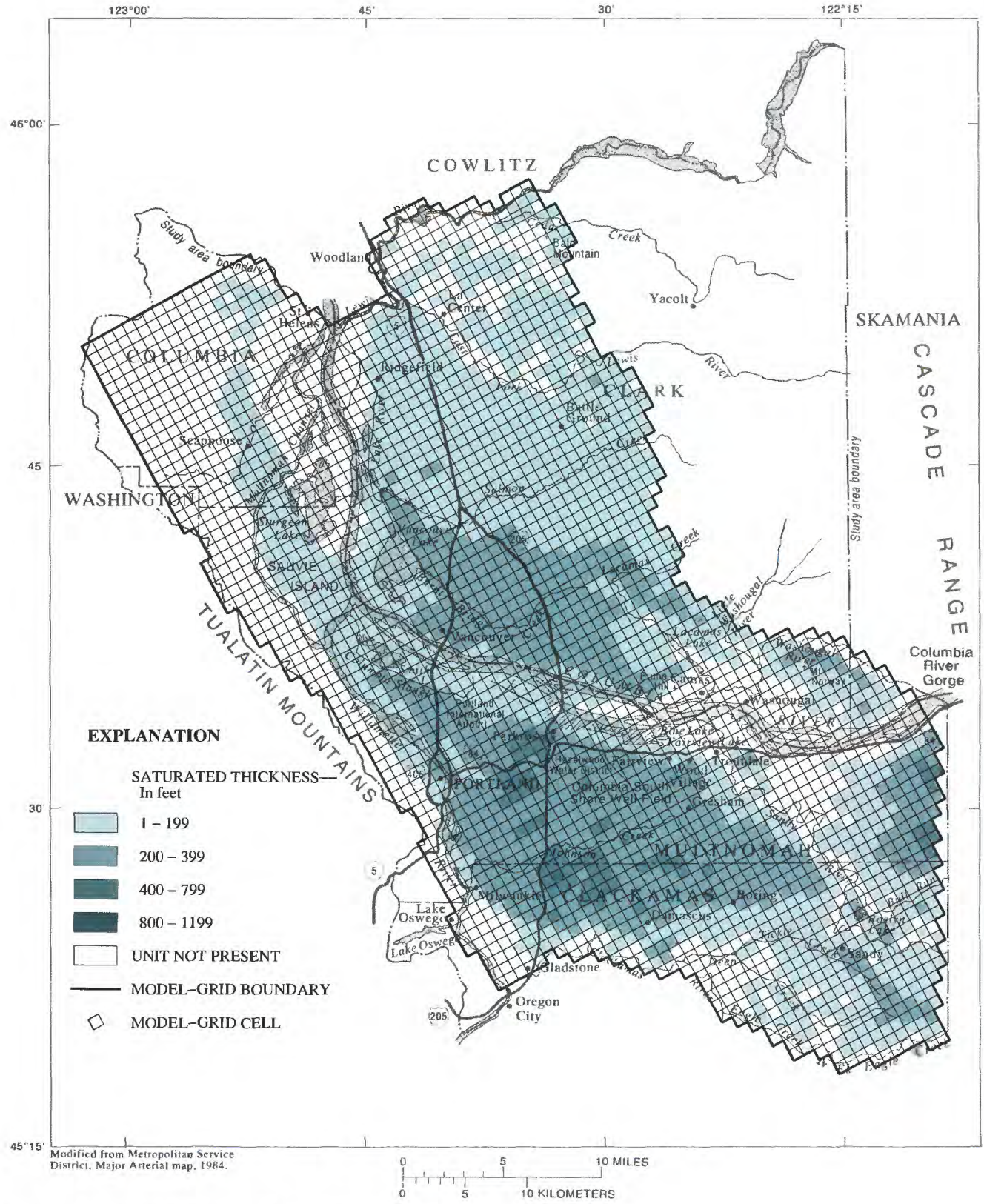

Figure A–2. Saturated thickness of Troutdale gravel aquifer.

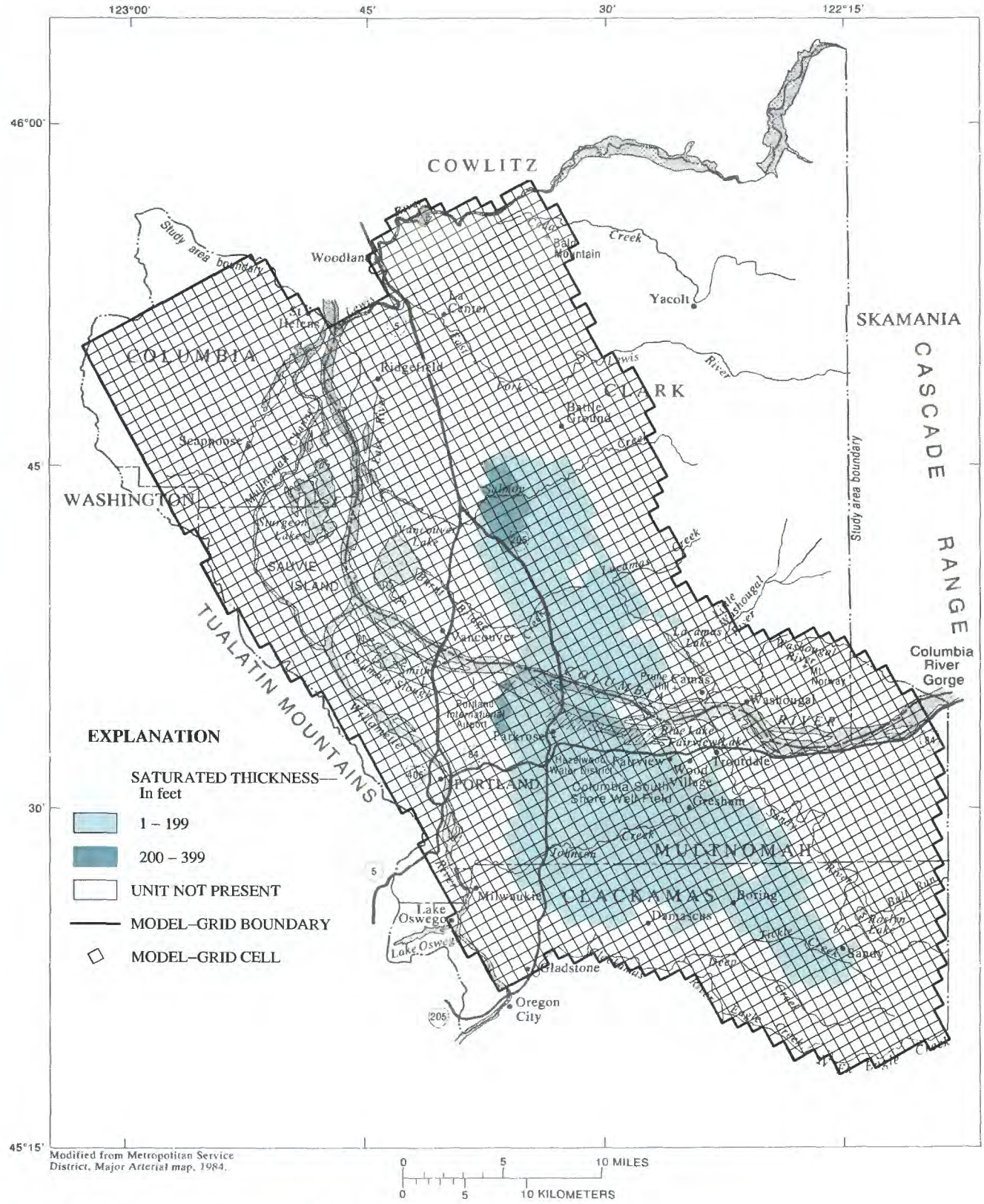

Figure A–3. Saturated thickness of confining unit 1.

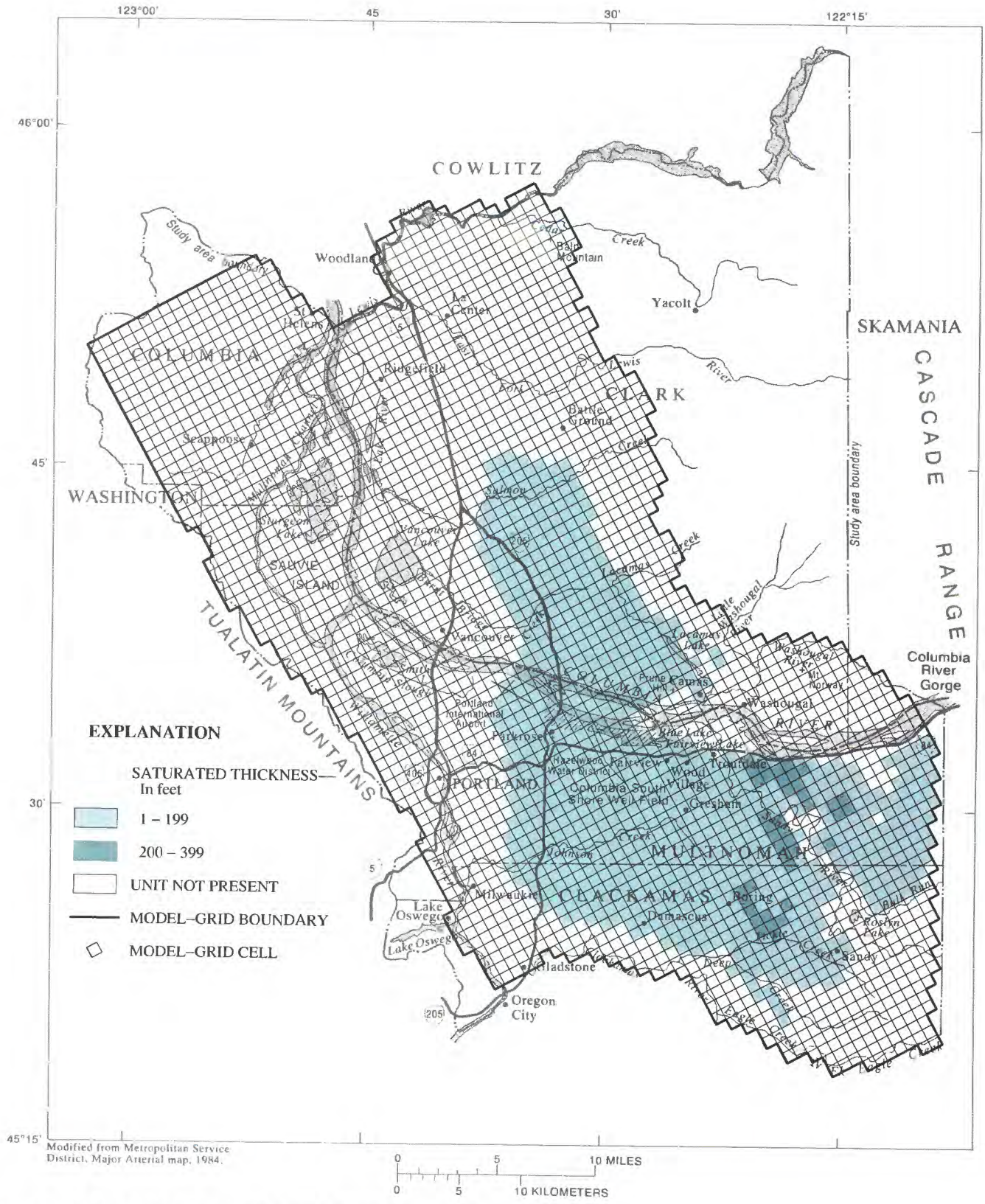

Figure A–4. Saturated thickness of Troutdale sandstone aquifer.

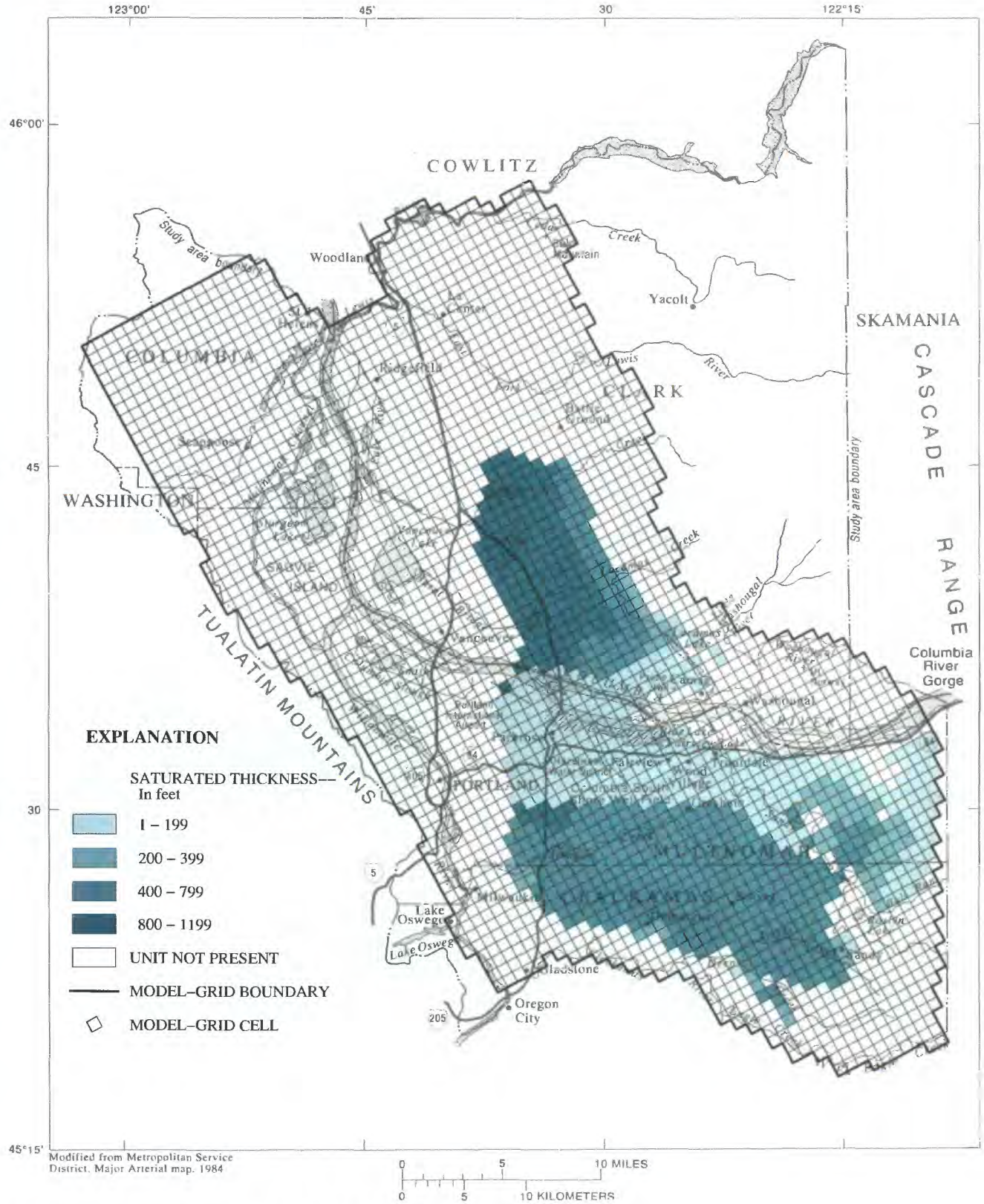

Figure A–5. Saturated thickness of confining unit 2.

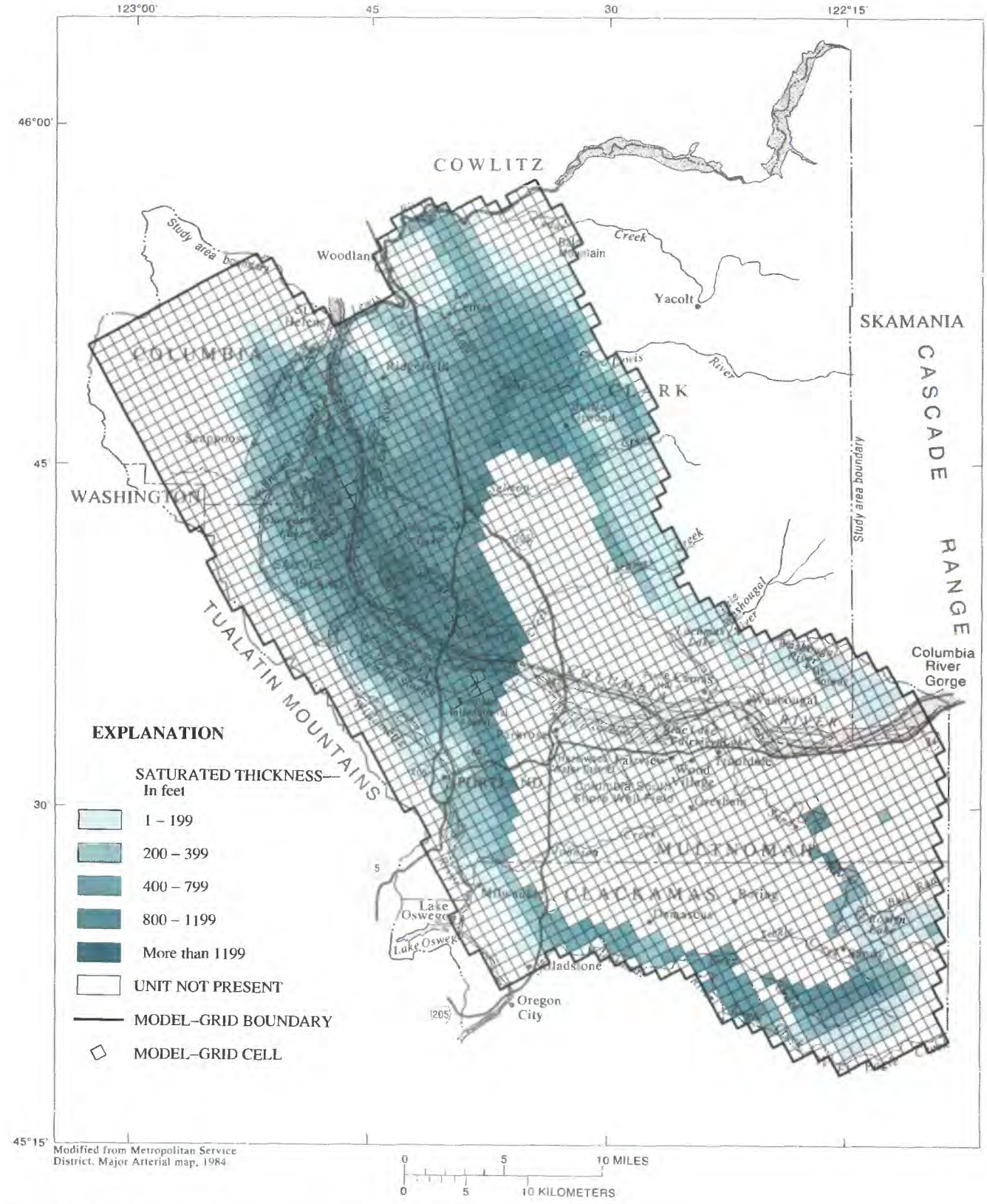

Figure A–8. Saturated thickness of the undifferentiated fine-grained sediments.

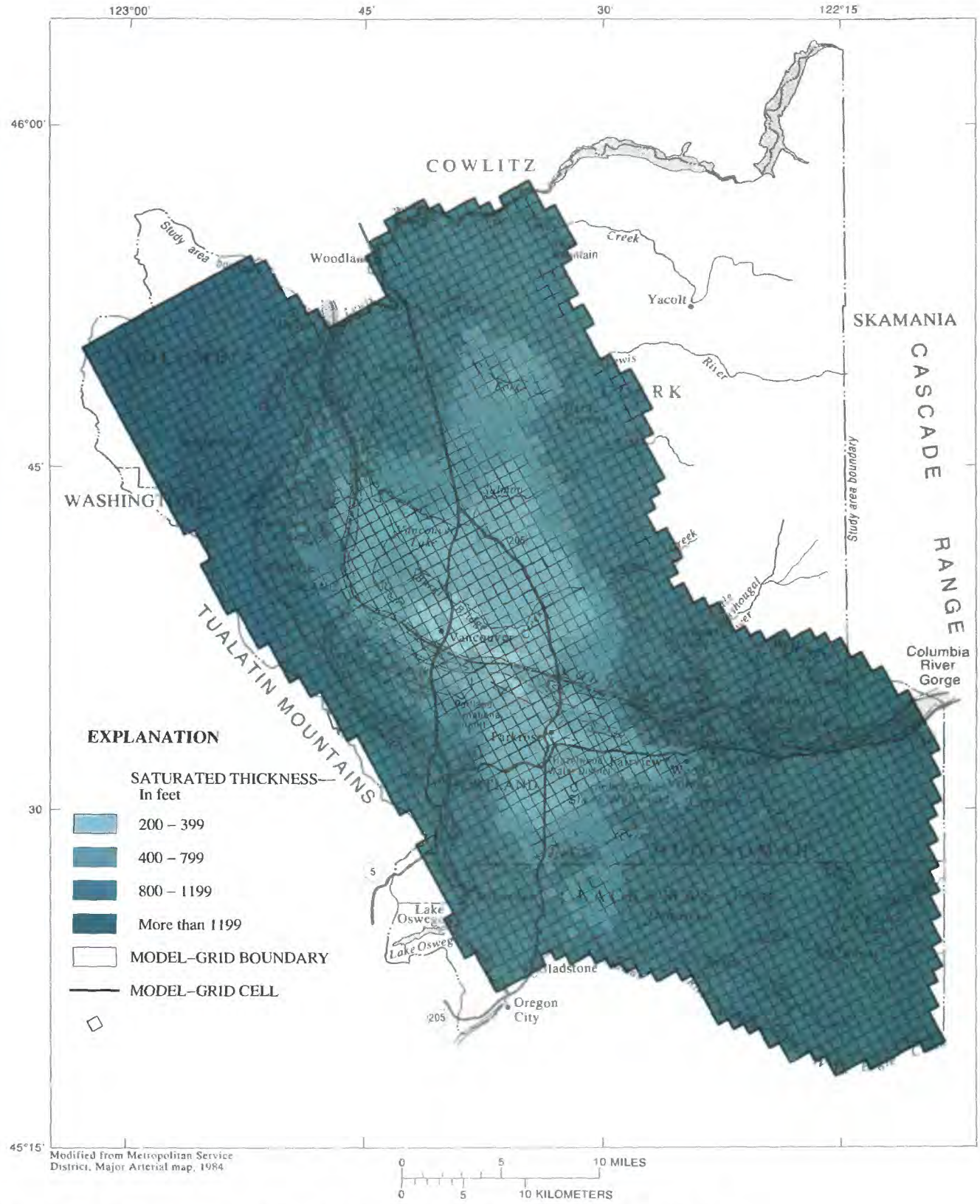

Figure A–9. Saturated thickness of older rocks above altitude of 2,000 feet below sea level.

APPENDIX C

Selected streamflow and leakage characteristics at sites in the Portland Basin, 1987–88

Appendix C

Selected streamflow and leakage characteristics at sites in the Portland Basin, 1987–88

[(A) measured low-flow discharge, September 1988; (B) estimated mean annual base flow; (C) simulated mean base flow, April 1987–March 1988; (D) measured leakage, September 1988; (E) estimated mean annual leakage; and (F) simulated mean leakage, April 1987–March 1988 at selected sites in the Portland Basin. All values are in units of cubic feet per second (ft^3/s). Segment and reach numbers were used to identify the stream in the ground-water flow model. The measurement site numbers are shown on plate 1]

Measurement location	Number		Site ID NO.	Discharge			Leakage		
	Segment	Reach		(A)	(B)	(C)	(D)	(E)	(F)
Burnt Bridge Creek at 112th Ave.	170	7	1	1.39	5.56	0.148	-0.22	-0.88	0.148
Burnt Bridge Creek at Burbon Rd.	170	11	2	2.82	11.28	.000	-.16	-.64	.000
Burnt Bridge Creek at Evergreen St.	170	17	3	3.67	14.68	.000	-.22	-.88	.000
Burnt Bridge Creek at St. Johns Blvd.	170	19	4	3.62	14.48	.000	.01	.04	.000
Burnt Bridge Creek at Leverich Park	170	23	5	4.55	18.20	.000	-.45	-1.80	.000
Cold Canyon Creek at Hazel Dell Dr. by Burnt Bridge Creek	171	3	6	.45	1.80	.000	--	--	.000
Burnt Bridge Creek	172	1	7	4.61	18.44	.000	.08	.32	5
Cedar Creek Tributary	82	5	23	.53	2.12	.495	--	--	-.023
Pup Creek at Spurrel Rd. near Cedar Creek	84	1	24	1.11	4.44	4.400	--	--	-.337
Cedar Creek at Grist Mill	85	4	27	13.60	54.40	48.641	-.85	-3.40	-.983
Cedar Creek Tributary	86	2	29	--	--	.057	--	--	.057
Cedar Creek Tributary	88	2	30	--	--	.041	--	--	.041
Cedar Creek at confluence	89	2	31	12.70	50.80	56.261	.03	.12	-.019
East Fork Lewis River Tributary	92	3	41	.10	.40	.000	--	--	.000
East Fork Lewis River at Lewisville Park	94	9	42	43.70	174.80	189.087	.02	.08	-.965
East Fork Lewis River at Daybreak Park	94	18	43	47.80	191.20	211.734	-.52	-2.08	-2.238
Mill Creek near East Fork Lewis River	96	5	44	.15	.60	.211	--	--	-.057
East Fork Lewis River Tributary	95	6	45	.52	2.08	1.423	--	--	-.037
East Fork Lewis River above Mason Creek	97	10	48	58.10	232.40	240.816	-.64	-2.56	-1.267
Mason Creek at confluence near East Fork Lewis River	98	19	51	1.45	5.80	11.012	--	--	-.022
East Fork Lewis River Tributary	100	9	52	.14	.56	.000	--	--	.000
East Fork Lewis River Tributary	102	5	53	--	--	.000	--	--	.000
East Fork Lewis River above Lockwood Creek	103	2	54	65.00	260.00	262.567	-.23	-.92	-1.088
Lockwood Creek near East Fork Lewis River	104	14	55	1.07	4.28	3.120	--	--	-2.575
Brezee Creek near East Fork Lewis River	106	7	56	.68	2.72	1.308	--	--	-.341
East Fork Lewis River Tributary	108	3	57	.10	.40	.000	--	--	.000
McCormick Creek near East Fork Lewis River	110	8	58	.16	.64	.000	--	--	-.557
Jenny Creek near East Fork Lewis River	112	6	59	.29	1.16	.000	--	--	-.037
Jenny Creek Tributary near East Fork Lewis River	112	7	60	--	--	.037	--	--	.002
Fifth Plain Creek NE 212th Ave.	176	1	61	.09	.36	.000	-.05	-.20	.000
Fifth Plain Creek at NE Davis Rd.	176	6	62	.26	1.04	.248	-.06	-.24	-.789
Shanghai Creek at 222nd Ave. near Fifth Plain Creek	177	3	63	.56	2.24	2.110	--	--	-.319
Shanghai Creek at NE 212 Ave. near Fifth Plain Creek	177	4	64	.60	2.40	2.429	-.03	-.12	-.671
Shanghai Creek at Fifth Plain Creek	177	8	65	.54	2.16	4.320	--	--	-.595
Fifth Plain Creek at Ward Rd.	178	2	66	.76	3.04	6.408	.00	.00	-.076
China Ditch at Ward Rd. near Fifth Plain Creek	175	6	67	.15	.60	2.597	--	--	-.116
Fifth Plain Creek at Hwy 500	179	4	68	3.10	12.40	10.267	-.43	-1.72	-.279
Gee Creek at Park	127	5	69	.12	.48	.293	-.03	-.12	-.140
Gee Creek at NW Royle Rd.	127	7	70	.43	1.72	.421	-.19	-.76	-.111
Gee Creek Tributary	128	4	71	.10	.40	.000	--	--	.000
Gee Creek at Hwy 501	129	1	72	--	--	1.689	--	--	.061
Gee Creek at Abrams Park	129	3	73	.78	3.12	1.643	-.07	-.28	-.044

Appendix C

Measurement location	Number Segment	Number Reach	Site ID NO.	Discharge (A)	Discharge (B)	Discharge (C)	Leakage (D)	Leakage (E)	Leakage (F)
Matney Creek at NE 68th St. near Lacamas Creek	181	2	75	1.06	4.24	0.000	--	--	-0.615
Lacamas Creek at NE 217th Ave.	182	2	76	6.32	25.28	16.732	-0.03	-0.12	-.130
Lacamas Creek at Hwy 500	182	6	77	6.54	26.16	19.402	-.07	-.28	-1.726
Lacamas Creek at Lacamas Park	183	7	79	12.30	49.20	36.606	-.68	-2.72	-.909
Little Washougal River at SE Blair Rd.	190	3	80	8.49	33.96	34.755	--	--	-2.581
Little Washougal River at Blair (Gage Site)	190	6	81	7.98	31.92	42.310	.13	.52	-.528
Salmon Creek at 182nd Ave.	138	8	84	4.04	16.16	18.650	-.03	-.12	-1.308
Salmon Creek at 167th Ave.	138	9	85	4.27	17.08	19.958	-.22	-.88	-2.263
Morgan Creek at NE 167th Ave. near Salmon Creek	137	2	86	1.64	6.56	4.513	--	--	-.309
Salmon Creek at Hwy 503	139	9	87	7.20	28.80	37.111	-.10	-.40	-.820
Weaver Creek near Hwy 503 near Salmon Creek	140	11	88	1.43	5.72	.192	--	--	-.320
Salmon Creek Tributary at end of 112th Ave.	142	6	89	.52	2.08	.000	--	--	-.061
Salmon Creek at 112th Ave.	143	1	90	9.13	36.52	39.999	.02	.08	-.696
Curtin Creek at 139th St. near Salmon Creek	144	11	93	3.43	13.72	1.342	--	--	-.748
Salmon Creek at 72nd Ave.	145	1	94	13.20	52.80	48.417	.00	.00	-.182
Mill Creek at Salmon Creek Rd. near Salmon Creek	148	15	95	.64	2.56	5.990	--	--	-.073
Salmon Creek at I-205 Overpass	149	5	96	17.80	71.20	60.089	-.33	-1.32	-2.002
Salmon Creek Tributary at 119th St.	150	4	97	.80	3.20	.000	--	--	.000
Salmon Creek at Hwy 99	151	3	98	19.50	78.00	57.858	-.22	-.88	3.026
Salmon Creek Tributary 200 feet east of Interstate-5	152	7	99	.38	1.52	.000	--	--	.000
Salmon Creek below Klineline Pond	153	2	101	19.60	78.40	60.028	.38	1.52	-1.625
Cougar Canyon Creek at 119th St. near Salmon Creek	154	6	103	.77	3.08	.000	--	--	.000
Salmon Creek above 36th Ave.	155	3	104	23.40	93.60	74.896	-.75	-3.00	-.684
Whipple Creek at Union Rd.	158	5	105	--	--	.000	--	--	.000
Whipple Creek at 11th Ave.	158	8	106	.42	1.68	.000	--	--	.000
Packard Creek at 179th St. near Whipple Creek	159	6	108	.16	.64	.000	--	--	.000
Whipple Creek at 179th St.	160	1	109	2.65	10.60	.000	-.04	-.16	.000
Whipple Creek Tributary at end of 189th St.	161	4	110	.18	.72	.000	--	--	-.231
Beaver Creek at Cochran Rd.	15	12	401	.04	.16	.000	--	--	.000
Kelly Creek at Mt. Hood Community College near Beaver Creek	14	11	402	.64	2.56	.000	--	--	.000
Beaver Creek at Troutdale Rd.	16	3	403	1.44	5.76	.000	-.57	-2.28	.000
Beaver Creek at Columbia Rd.–Troutdale	16	6	404	.91	3.64	.344	.07	.28	-.026
Mt. Scott Creek at Mt. Scott Creek Rd.	51	4	409	--	--	.000	--	--	.000
Mt. Scott Creek at Sunnyside	51	5	410	.02	.08	.000	-.01	-.04	.000
Mt. Scott Creek at SE 97th	51	7	411	.04	.16	.000	-.01	-.04	-.011
Mt. Scott Creek behind COSTCO	51	9	412	.15	.60	.000	-.04	-.16	-.776
Mt. Scott Creek at Rusk Rd.	51	12	415	2.05	8.20	2.275	-.91	-3.64	-1.019
Mt. Scott Creek near Kellogg Creek	51	13	416	1.91	7.64	3.294	.09	.36	-1.508
Rock Creek at Troge Rd.	40	8	421	.05	.20	.361	--	--	-.301
Rock Creek at Sunnyside Rd.	40	12	422	.20	.80	1.390	-.08	-.32	-.800
Rock Creek at Hwy 224	40	15	423	.58	2.32	3.094	-.18	-.72	-2.701

Appendix C

Meesurement location	Number Segment	Number Reach	Site ID NO.	Discharge (A)	Discharge (B)	Discharge (C)	Leakage (D)	Leakage (E)	Leakage (F)
Richardson Creek at Royer Rd.	38	3	428	0.02	0.08	0.000	--	--	0.000
Richardson Creek at Hwy 224	38	8	429	.25	1.00	1.703	-0.07	-0.28	-.726
Kellogg Creek at Webster Rd.	52	2	434	--	--	.000	--	--	.000
Kellogg Creek at Theisen Rd.	52	4	435	.13	.52	.009	-.07	-.28	-.015
Kellogg Creek at Rusk Rd.	52	7	436	1.89	7.56	.444	-1.40	-5.60	-.085
Kellogg Creek at Oatfield Rd.	53	3	437	3.70	14.80	6.937	-.73	-2.92	-.041
Tributary to Kellogg Creek at McLoughlin Blvd.	54	2	439	.15	.60	.000	--	--	.000
Tickle Creek at Hwy 211	25	10	444	.05	.20	.576	--	--	-.063
Tickle Creek at 362nd	25	14	446	.40	1.60	1.451	-.12	-.48	-.742
Tickle Creek at Colorado Rd.	25	18	447	1.18	4.72	5.276	-.12	-.48	-.625
Tickle Creek Tributary at Colorado Rd.	26	6	448	.15	.60	3.486	--	--	-.825
Tickle Creek at Deep Creek Rd.	27	4	450	2.39	9.56	13.224	-.40	-1.60	-2.758
Deep Creek at Crane Rd.	22	14	455	.39	1.56	13.561	--	--	-1.614
Deep Creek Tributary near Hwy 211	23	11	457	.13	.52	3.601	--	--	.10
Deep Creek at Hwy 211	24	1	458	1.02	4.08	25.049	-.03	-.12	-.103
Deep Creek at Hoist Rd.	24	8	459	1.22	4.88	30.340	-.04	-.16	-.523
Deep Creek at Aemisegger Rd.	28	2	460	4.07	16.28	49.866	-1.50	-6.00	-.593
Deep Creek Tributary at Aemisegger Rd.	29	4	461	.05	.20	1.083	--	--	-.195
North Fork Deep Creek at confluence near Deep Creek	33	17	462	.78	3.12	9.475	--	--	-.081
Noyer Creek at Deep Creek Rd. near Deep Creek	35	7	463	.03	.12	.257	--	--	-2.591
Deep Creek at Hwy 224	36	1	464	5.28	21.12	67.512	-.02	-.08	-.567
Johnson Creek at Palmblad Rd.	47	6	469	.08	.32	3.001	--	--	-.537
Johnson Creek at Walters Rd.	47	10	470	.42	1.68	4.120	-.08	-.32	-.192
Johnson Creek at SE 190th Ave.	47	14	471	.47	1.88	4.933	-.02	-.08	-.159
Johnson Creek at Gaging Station near Foster Rd.	47	17	472	.64	2.56	7.199	-.05	-.20	-.593
Johnson Creek at SE 112th & Brookside	47	21	473	.74	2.96	9.600	-.03	-.12	-2.604
Johnson Creek at 82nd Ave.	47	26	474	.92	3.68	8.712	-.01	-.04	-.145
Johnson Creek at SE 45th and Johnson Creek Blvd.	47	31	475	1.35	5.40	2.558	-.09	-.36	-1.147
Johnson Creek at Tidemar Johnson Park	47	32	478	3.45	13.80	3.705	-.67	-2.68	.811
Johnson Creek above Crystal Springs Creek	47	34	479	2.91	11.64	2.190	.30	1.20	1.792
Crystal Springs Creek at Sherrett St. by Johnson Creek	48	6	480	10.50	42.00	.000	--	--	-.708
Johnson Creek at SE River Rd.	49	4	482	17.70	70.80	1.142	-.84	-3.36	-.343
Sandy River near Sandy	2	10	483	219.00	876.00	904.238	--	--	-7.481
Cedar Creek at Fish Hatchery near Sandy River	1	13	484	3.55	14.20	34.006	--	--	-2.209
Bull Run River above Sandy River at Dodge Park	6	7	485	160.00	640.00	755.737	--	--	-.392
Sandy River at Gaging Station near Bull Run, Oregon	7	1	486	370.00	1,480.00	1,730.455	.68	2.72	-1.437
Walker Creek at confluence near Sandy River	8	6	487	3.03	12.12	.956	--	--	.014
Sandy River at Oxbow Park	9	10	493	294.00	1,176.00	1,769.988	1.98	7.92	-2.890
Trout Creek at Gordon Creek Rd. near Sandy River	10	14	494	4.35	17.40	.000	--	--	-.000
Gordon Creek at Gordon Creek Rd. near Sandy River	12	14	495	11.70	46.80	53.724	--	--	-.076
Sandy River at Stark St.	13	18	496	317.00	1,268.00	1,866.029	-.56	-2.24	-2.002
Sandy River at Troutdale	13	23	497	318.00	1,272.00	1,881.473	-.21	-.84	-3.907

☆ U.S. GOVERNMENT PRINTING OFFICE: 1997-547-442